Multi-Scale, Multi-Proxy Investigation of Late Holocene Tropical Cyclone Activity in the Western North Atlantic Basin

François Oliva

Thesis submitted to
the Faculty of Graduate and Postdoctoral Studies
in partial fulfillment of the requirements for the
Doctorate of Philosophy in Geography

Department of Geography, Environment and Geomatics
Faculty of Arts
University of Ottawa

Supervisors:
Dr. André E. Viau
Dr. Matthew C. Peros

Thesis Committee:
Dr. Luke Copland
Dr. Denis Lacelle
Dr. Michael Sawada
Dr. Francine McCarthy

Abstract

Paleotempestology, the study of past tropical cyclones (TCs) using geological proxy techniques, is a growing discipline that utilizes data from a broad range of sources. Most paleotempestological studies have been conducted using “established proxies”, such as grain-size analysis, loss-on-ignition, and micropaleontological indicators. More recently researchers have been applying more advanced geochemical analyses, such as X-ray fluorescence (XRF) core scanning and stable isotopic geochemistry to generate new paleotempestological records. This is presented as a four article-type thesis that investigates how changing climate conditions have impacted the frequency and paths of tropical cyclones in the western North Atlantic basin on different spatial and temporal scales.

The first article (Chapter 2; Oliva et al., 2017, Prog Phys Geog) provides an in-depth and up-to-date literature review of the current state of paleotempestological studies in the western North Atlantic basin. The assumptions, strengths and limitations of paleotempestological studies are discussed. Moreover, this article discusses innovative venues for paleotempestological research that will lead to a better understanding of TC dynamics under future climate change scenarios.

The second article (Chapter 3; Oliva et al., submitted, The Holocene) presents the development of the first database summarizing the most up-to-date paleotempestological proxy data available for TC reconstructions for the western North Atlantic basin. Subsets of this new database are then used to reconstruct TC variability in the western North Atlantic basin. Using our new developed subsets, we investigate a key hypothesis, the Bermuda High Hypothesis that has been proposed to have influenced TC paths over centennial to millennial timescales. Results show an oscillation in the distribution of TC landfalls along the North American coast, suggesting a centennial oscillation in the mean summer position of the high pressure system. We suggest that a more serious, millennial scale shift in the Bermuda High to a northeastern (NE position) may have occurred at ~3000 and ~1000 cal yr BP.

The third article (Chapter 4; Oliva et al., under review, Marine Geology) presents a local multi-proxy reconstruction of TC activity during the past 800 years from Robinson Lake, Chezzetcook

Inlet in Nova Scotia, Canada. Here, we are testing the more recent use of the XRF scanning approach to paleotempestology at a local scale. Two sediment cores were extracted from Robinson Lake that were dated by ^{210}Pb and ^{14}C, analyzed for organic matter content, benthic foraminifera and thecamoebians, sediment grain size, and a range of elements and elemental ratios determined by XRF core scanning. Results show two periods of low TC activity based on multiple proxies including XRF technology: one from ~1150 to 1475 CE (800 – 475 cal yr BP) and the other from 1670 CE (280 cal yr BP) to the present, with the intervening period from ~1475 to 1670 CE (475 – 280 cal yr BP) as a time of more frequent and possibly higher magnitude TC activity.

The fourth article (Chapter 5. Oliva et al., in preparation, Canadian Journal of Earth Sciences) explores the potential use of stable oxygen isotopes in tree ring α-cellulose to reconstruct past local TC activity surrounding areas of known TC strikes. Cores of 12 *Picea mariana* trees were extracted adjacent to Robinson Lake, Chezzetcook Inlet, Nova Scotia in order to test more contemporary and historically documented records of TC activity in this region as per Chapter 4. TCs precipitate ^{18}O-depleted rain, leaving a unique signature in the source water that trees use to form cellulose. Using an autoregressive integrated moving average (ARIMA AR-1) model to detrend the data, local and regional time series were reconstructed. Local reconstructions led to most (> 95%) hurricanes and all major hurricane (± 1 year) being recorded in the isotope record, whereas the regional reconstruction shows no major hurricane, only a few hurricanes (< 40%) and one signal with a higher error (> 1 year).

This thesis contributes to advancing our knowledge in paleotempestology of the western North Atlantic basin by: 1) bringing an up-to-date current status on paleotempestology, 2) the development and ongoing use of a new paleotempestology database for the western North Atlantic basin publicly available, 3) a local scale study using new XRF core elemental technology and 4) the exploratory use of tree-ring α-cellulose oxygen isotopic analysis based on contemporary and historical documents at local sites.

Table of Contents

List of Figures

List of Tables

Acknowledgements

First, I want to thank Dr. André Viau and Dr. Matthew Peros and the National Sciences and Engineering Research Council (NSERC) Discovery Grant for funding this research. I also want to express my gratitude to Drs. Viau and Peros for agreeing to undertake this project, thus giving me the opportunity to follow my passion for the field. My heartfelt gratitude to my thesis committee, Dr. Luke Copland, Dr. Denis Lacelle, Dr. Michael Sawada and Dr. Francine McCarthy for their guidance and expertise. A special acknowledgment to M. Jean Bjornson for his dedication to this project and his invaluable guidance and friendship. I would like to thank Marielle Fontaine and Dr. Chantel Nixon for their assistance in the field and Dr. Eduard Reinhardt and Shawn Kovacs from McMaster University for their help with the XRF laboratory analyses. I gratefully acknowledge my co-authors on Chapter 3: Marc Bouchard; Chapter 4: Drs. Eduard Reinhardt and Chantel Nixon, as well as Alexandre Morin; and on Chapter 5: Dr. Trevor Porter and Benoit Faucher. I would also like to thank Dr. Konrad Gajewski, Michelle Chaput, Karen Neil, Robert Way and the other members of the Laboratory for Paleoclimatology and Climatology (LPC) for their advice, friendships and support all along my graduate studies, as well as Dr. Marie-Claude Fortin for her unwavering support throughout the final stages of my thesis. A special mention to Dr. Eric Crighton, Chantal Arcand, Nathalie Maras and Jim McGrath from the Department of Geography, Environment and Geomatics for their administrative, technical and overall support. Thank you to Mik, Isabelle, Marie-Ange, Etienne, Steve, Françoise, Les Campeau and to so many other close friends and family who have always encouraged and supported me throughout my studies. I am grateful to my siblings Mathias, Marie-Laure and Alexandra for their life-long support. I would also like to thank Serge Labine for his encouragement throughout my studies.

A very special thank you to my mother Catherine, her love, support, dedication, pride and enthusiasm have driven me to succeed and never give up; and my late father, Bohumil, for passing on his love of science and knowledge to me. His memory and example will never cease to guide me. Finally, I would like to dedicate my thesis to the two loves of my life: my wonderful wife, Tess Campeau who has always to loved, encouraged and supported me as well as endured my long hours of studying and writing over the entire course of my studies; and to our adorable and loving daughter Clara. No matter how tired or discouraged I may be, you always know how to make me smile and happy again. I love you.

Chapter 1 – Introduction

1.1 Background

Tropical cyclones (TCs) are organized storms, with low-pressure centers that form in environments with four very specific attributes: 1) enhanced vorticity; 2) moisture and deep convection; 3) weak vertical wind shear and; 4) a deep layer of sea surface temperatures > 26°C (Tory & Frank, 2010). Different names are attributed to TCs depending on their strength (wind speed) and location on Earth. When TCs in the Atlantic reach sustained winds of 119 km /h, they are called hurricanes. Hurricanes are then defined by category as per the Saffir-Simpson scale (Table 1.1) (Schott et al., 2012). TCs originating in the Atlantic basin can have devastating consequences to the eastern North American seaboard and along the interior coast of the Gulf of Mexico. It is not only the atmospheric effects of the storms but the resulting storm surges that bear a major impact on the population and can impact the economy by billions of dollars. Damage to roads, buildings, communication systems and ports lead to homelessness, disruption in manufacturing, transport and an increase in insurance premiums (Romero-Lankao et al., 2014). Tropical cyclones do not impact just low-latitude coastlines; eastern Canada is also affected by these events. For example, two of the top 5 most costly natural disasters to affect the Canadian Maritimes since 1900 CE were TCs. Tropical storms Irene and Hurricane Juan together cost Canadians an estimated $169 000 000 (Table 1.2)(Canadian Disaster Database, 2015). Non-tropical flood events are twice as frequent as tropical storms and hurricanes, but the total estimated cost to the state is lower than costs associated with tropical storms and hurricanes (CDD, 2015).

According to the National Hurricane Centre at the National Oceanic and Atmospheric Administration (NOAA), a total of 83 tropical cyclones have impacted Nova Scotia since 1851, with 21 of them being hurricanes (NOAA, 2015). Efforts are being made to reduce the risk of damage from major storms, such as the revisions to building codes (Romero-Lankao et al., 2014). Although some studies suggest that extreme Atlantic cyclones have increased in frequency and intensity over the last 100 years (Paciorek et al., 2002; Lehmann et al., 2011), others have argued that there have been no significant trends over this time period (Weinkle et al., 2012).

Liu (2010) defines paleotempestology as the "field of science that studies past hurricane activities". It is important to study past hurricane activity in the context of present and future climate change. Historical and observational records of tropical storms date only back to the last century, making any long-term trend difficult to observe. This is especially true for category 4 and 5 hurricanes which are extremely rare (Liu, 2013). Long-term trends also increase the signal-to-noise ratio and help hydroclimate scientists understand how large scale mechanisms such as sea-surface temperatures and ocean-atmospheric teleconnections (e.g. El Nino Southern Oscillation, North Atlantic Oscillation) influence tropical cyclones (Liu, 2010). The two main types of archives used in paleotempestology are geological and historical data (Liu, 2013). A commonly used geological indicator is overwash sediment generated by the storm surge. Marine deposits can be brought inland by storm surges from various sources such as nearshore, offshore or the barrier itself. This creates layers of coarse marine sediments amongst layers of finer, more organic rich lacustrine sediments in coastal waterbodies. Other marine indicators such as shells, corals or marine foraminifera have also been used to identify storm overwash events (Liu, 2013; Williams, 2010; Liu et al., 2008; Hippensteel & Martin, 1999). Oxygen isotopes from tree rings, corals and speleothems have also been successfully used because rain resulting from a hurricane is often strongly depleted in ^{18}O (Lawrence & Gedzelman, 1996, Frappier et al., 2007; Miller et al. 2006). Historical archives comprise of observational records from ship logs, newspapers, diaries and colonial records (Liu, 2013; Chenoweth, 2006; Landsea et al., 2004; Mock, 2004).

1.2 Scope and Objectives

Although there are no significant trends in tropical storm frequency in the North Atlantic basin over the last century (Chan & Xu, 2009; Kubota & Chan, 2009; Mohapatra et al., 2011; Weinkle et al., 2012), with rising sea-surface temperatures the IPCC AR5 (2013) reports with some confidence that there will be an increase in storm intensity and an increase in major storm frequency in the North Atlantic basin (Christensen et al., 2014; Elsner et al., 2008; Paciorek et al., 2002; Lehmann et al., 2011).

There are several advantages to researching paleotempestology in Nova Scotia. Nova Scotia is located at the typical northern margin of modern hurricane paths which allows us to test certain hypotheses, such as the Bermuda High hypothesis (Liu, 2004) and whether hurricane paths may shift in time (Liu and Fearn, 2000; Peros et al., 2015). Very limited paleotempestology research is being conducted north of 30°N and none north of New England. Here, we studied the Chezzetcook Inlet area for its location within the modern tropical storm paths, accessibility and previous available research for background information on this area (Scott and Collins, 1996; Gehrels et al., 2005).

The main objectives of this thesis are to:

1) Compile, synthesize and analyze the available information in paleotempestology of the western Atlantic basin and create tools for researchers in the discipline to use and,
2) Contribute data by pushing known geochemical limits of proxy analysis.

The objectives of the thesis were attained by synthesizing and analyzing the available research and by creating new data for the northern margin of tropical cyclones to better understand the underlying dynamics of storm activity under different climate conditions of the past. The results contribute to advancing our knowledge of TC activity in the western Atlantic basin can be used to test hypotheses for future climate change scenarios.

1.3 Thesis Format

The thesis follows a manuscript-style format in which four articles are developed. An introductory chapter (Chapter 1) presents background on the field of paleotempestology, the scope and objectives of the thesis and introduces the study location. Chapters 2 to 5 open with the abstract and current status in the publishing process. Chapters 2, *A review of the spatial distribution of and analytical techniques used in paleotempestological studies in the western North Atlantic Basin* (2017) synthesizes the scientific literature in the field of paleotempestology. Chapter 3, *Testing the Bermuda High Hypothesis through Tropical Cyclone Activity in the Western North Atlantic Basin* develops on future work suggested in Chapter 2 by introducing a database of reconstructed TC strikes and active periods with some preliminary analysis. Chapter 4 *A high-resolution multi-proxy reconstruction of tropical cyclone variability during the past 800 years from Nova Scotia, Canada* is a high-resolution reconstruction of tropical cyclone activity in the Chezzetcook Inlet, Nova Scotia. Chapter 5 *On the use of oxygen isotopes from tree ring α-cellulose to reconstruct past tropical cyclones in the Canadian Maritime region* is a more modern TC reconstruction testing a method never used at this latitude. Chapter 6 highlights the findings and scientific contributions from these articles. The references from the entire thesis are found following Chapter 6.

1.4 Co-Author Contributions

For all chapters, I led the writing, analysis, field and laboratory work while Dr. Viau and Dr. Peros contributed by reviewing and editing the manuscripts. In Chapter 3, M. Bouchard assisted in the creation of the database and analysis. In Chapter 4, Dr. Peros and Dr. Nixon assisted in the field work, Dr. Reinhardt assisted with XRF scanning and data interpretation, A. Morin assisted with other laboratory work. All authors contributed in the revision of the manuscript. In Chapter 5, B. Faucher assisted with the laboratory work and Dr. Porter assisted in providing guidance for lab methods and with the interpretation of the data.

Table 1.1 Saffir-Simpson hurricane wind scale.

Category	Wind Speed
1	119 – 153 km/h
2	154 – 177 hm/h
3	178 – 208 km/h
4	209 – 251 km/h
5	> 252 km/h

Table 1.2 Top 5 costly natural disasters affecting the Canadian Maritimes since 1900 CE (CDD, 2015).

Type of Natural Disaster	Event	Geographic Reach	Year	Estimated Cost (in millions CDN$)
Winter Storm	Ice Storm	Ontario to NB	1998	4635.72
Tropical Storm	Tropical Storm Irene	Quebec and Maritimes	2011	137.8
Flood	Saint John & Miramichi Rivers	NB and St. Lawrence Region QC	1994	57.02
Tropical Storm	Hurricane Juan	Nova Scotia and PEI	2003	30.9
Epidemic	Infectious Salmon Virus	Bay of Fundy, NB	1997	25.88

Chapter 2 – A review of the spatial distribution of and analytical techniques used in paleotempestological studies in the western North Atlantic Basin

2.1 Abstract

Paleotempestology, the study of past tropical cyclones (TCs) using geological proxy techniques, is a growing discipline that utilizes data from a broad range of sources. Most paleotempestological studies have been conducted using "established proxies", such as grain-size analysis, loss-on-ignition, and micropaleontological indicators. More recently, however, researchers have been applying more advanced geochemical analyses, such as XRF core scanning and stable isotopic geochemistry, to generate new paleotempestological records. In this paper we begin by providing a list of paleotempestological studies for the western North Atlantic basin and illustrate the spatial coverage of these studies. We then review the premises behind both established and new proxies and discuss their strengths and limitations at resolving past hurricane activity. Lastly, we suggest future directions for paleotempestological research based on our review of the literature that we argue will ultimately lead to a better understanding of tropical cyclone dynamics under future climate change scenarios.

This chapter has been published as: *Oliva F., Peros M., Viau A. (2017) A review of the spatial distribution of and analytical techniques used in paleotempestological studies in the western North Atlantic Basin. Progress in Physical Geography. DOI: 10.1177/0309133316683899*

2.2 Introduction

Tropical cyclones (TCs) have devastating consequences for the Eastern North American seaboard, the Caribbean, and the interior coast of the Gulf of Mexico. The wind, precipitation and storm surges associated with TCs can cause major impacts on local and regional landscapes and ecosystems (e.g. Hurricane Katrina in 2005; Burton and Hicks, 2005). Moreover, the effects of TCs on humans and infrastructure are also closely intertwined; for example, damage to roads, buildings and ports can lead to homelessness, disruptions in manufacturing and transport, and an increase in insurance premiums, as seen in New Orleans and many other locations (Romero-Lankao et al., 2014).

Paleotempestology, a term first coined by Dr. Kerry Emanuel of the Massachusetts Institute of Technology (MIT), is the field of science that studies past tropical cyclone activities using a wide range of proxy techniques conducted in a number of different environments (Liu, 2004). Despite paleotempestology being an active area of research for several decades, we still know relatively little about past TC frequencies and intensities in the Atlantic Basin (which we define as including adjacent regions such as the Gulf of Mexico and Caribbean). Given increasing North Atlantic coastal populations (Hippensteel, 2010), it is critical to study past TC activity in this area to better understand how TC activity will change under current climate warming scenarios.

Reliable and continuous historical and observational records of TCs date back only to the last century in many regions (Liu, 2013), making long-term trends difficult to identify. This is especially true for category 4 and 5 hurricanes, which are rare. Reconstructions showing long-term trends aid in better identifying the underlying signal from noise in the data series. These types of analyses help hydroclimatologists better understand how large scale mechanisms such as sea-surface temperatures and ocean-atmospheric teleconnections influence TCs through the comparison of paleotempestological reconstructions to other proxy data and climate models (Liu, 2013). Extending historical records into the past through the use of geological proxies will help us understand how these extreme storms may change in the future (Liu and Fearn, 1993).

The purpose of this paper is to: 1) describe the various proxy techniques and dating methods used in paleotempestological research in the western Atlantic Basin; and 2), discuss their utility and limitations in paleotempestological research, with a view to help guide future research efforts. To meet these objectives, we begin this review by presenting a detailed list of paleotempestological studies from the western North Atlantic Basin and identify where these studies were undertaken geographically and what proxy and dating methods they employed. We then briefly discuss "established" methods, which we define as being sedimentology-based proxies of past TC events, and then review newer geochemical-based techniques (including XRF core scanning and stable isotope geochemistry). In addition, we discuss the advantages and limitations of each technique in order to suggest approaches for future research in this rapidly growing field. It is our hope that this review will be helpful to future researchers as a guide to help them better understand how various proxies are used in paleotempestology, and will complement other recent reviews that examine paleotempestology more generally (Liu, 2013; Wallace et al., 2014).

2.3 Data sources and the spatial distribution of paleotempestological studies

Observations of past TC activities arise from two main sources. First, instrumental data from satellites covering the last 50 years provide considerable detail and spatial coverage (Vecchi and Knutson, 2008). Prior to this, the pre-satellite monitoring era can be divided into two periods: before 1944 where the only recordings were from ships at sea or storm landfalls, and the period 1944-1965 when planes went on reconnaissance flights to validate ship sightings (Vecchi and Knutson, 2008). Second, historical archives are based on observational records from sources such as ship logs, newspapers, diaries and colonial records, and extend back in time several hundred years, although are sometimes characterized by incomplete or ambiguous information on past TC activities (Liu, 2013; Chenoweth, 2006; Landsea et al., 1999; Mock, 2004).

Over the last several decades, a number of researchers including Dr. Kam-Biu Liu (Louisiana State University) and Dr. Jeffrey Donnelly (Woods Hole Oceanographic Institution) and their students have dedicated much of their time to advancing the field of paleotempestology over centennial to millennial time-scales. In addition to their efforts, a number of other research groups have undertaken paleotempestological investigations. A comprehensive (but not necessarily exhaustive) list of peer-reviewed papers for the western North Atlantic Basin is provided in Table 2.1 (note this list does not include summary papers [e.g., Frappier et al., 2007a or Wallace et al., 2014] or rebuttals of published studies [e.g., Otvos, 2011]).

This list shows that fifty-nine peer-reviewed papers presenting original data have been published on the paleotempestology of the western North Atlantic. Table 2.1 also identifies the specific proxy indicators and dating methods used in those studies. A majority of TC reconstructions (n=47, or 80%) use grain size analysis and/or the organic content of sediment cores (defined here as established proxies), while comparatively fewer studies have used other indicators, such as elemental composition as determined by X-ray fluorescence (XRF) (n=9, or 15%), geochemical (n=7, or 12%), and micropaleontological evidence (n=15, or 25%).

A map of the spatial distribution of study sites (Figure 2.1) shows that they tend to cluster along the north coast of the Gulf of Mexico, the Carolinas, the north-eastern United States, and Belize, and that noticeable gaps are present along the Atlantic and Gulf of Mexico coasts of Florida, the islands of Cuba and Hispaniola, the Lesser Antilles and the Caribbean coast of Honduras (Figure 2.1). This distribution may reflect a combination of factors, such as the presence of suitable sampling locations, the likelihood of TC landfall, and even proximity to research institutions with staff focused on paleotempestological research (e.g., Louisiana State University, Baton Rouge, LA and the Woods Hole Oceanographic Institution, Cape Cod, MA). Moreover, no paleotempestology studies have been published along the North American coast north of Maine (Figure 2.1)(Buynevich et al., 2007) apart from federal government research inferring past hurricane activity based on soil profiles and forests (Ponomaranko, 2009).

2.4 Established proxies

2.4.1 Grain-size analysis

Grain-size analysis along a core can reveal much about past environmental changes, particularly as they relate to energy transport conditions (Liu, 2013; Donnelly and Woodruff, 2007). Normally-deposited material in low-energy environments such as coastal lakes and marshes is typically fine, organic-rich sediment. Coarser sediment layers are commonly used as evidence of an energy shift in the environment, such as sediment overwashing a barrier due to a storm surge coupled with intense wave activity (Figure 2.2) (Donnelly and Webb, 2004; Donnelly et al., 2001a; Donnelly et al., 2001b; Donnelly et al., 2004; Liu, 2013).

Researchers have used several techniques to generate grain-size data. Some have used a more qualitative approach which includes describing the presence of visible sand layers which are then attributed to past hurricane strikes, often based on a comparison of the timing of these sand layers with historically documented TCs (Donnelly et al., 2001a; Donnelly et al., 2001b; Donnelly et al., 2004; Hansom and Hall, 2009; Liu and Fearn, 2000; Liu et al., 2008; Liu et al., 2011; Scott et al., 2003). On a quantitative level, the sieving method, which works to separate particles into size fractions (often greater or less than 63µm), is widely used (Brandon et al., 2014; Donnelly et al., 2015; Hippensteel and Martin, 1999; Kiage et al., 2011; Lane et al., 2011; Mattheus and Fowler, 2015; McCloskey and Keller, 2009; McCloskey and Liu, 2012a; Reese et al., 2008; Williams, 2009; 2010; 2013) and can be an efficient way of determining key grain-size fractions, such as percent sand, in a sample. Laser particle size analyzers (LPSA) are a newer, more costly, yet more precise method for grain-size analysis and their advantage lies in their ability to generate a complete grain size distribution from a small sample in fractions much finer than what is possible with mechanical sieving (Boldt et al., 2010; Brown et al., 2014; Donnelly and Woodruff, 2007; Hawkes and Horton, 2012; Horton et al., 2009; Malaizé et al., 2011;

McCloskey and Liu, 2012b; Naquin et al, 2014; Nikitina et al., 2014; Peros et al., 2015; Toomey et al., 2013; van Hengstum et al., 2014). When sieving or using a LPSA, most researchers have attempted to isolate the mineral (carbonate and siliciclastic) components so as to not bias a sample with organic particles which may not be related to the energy level.

One point that emerges from a review of the literature is that there is no standardized approach for the removal of organic matter; Boldt et al. (2010), for example, combusted their samples at 550°C in a furnace to remove organic matter before undertaking grain size analysis, whereas Malaizé et al. (2011) used hydrogen-peroxide (H_2O_2) to digest organic matter. There are no known studies assessing the effects of the use of different methods for the removal of organic matter on particle size distributions in paleotempestological research, and a comparative study examining the potential effects would be worthwhile. For example, the combustion of samples in a furnace is often used (e.g., Boldt et al., 2010), but it is unclear to what extent this may fuse fine particles together, especially in samples containing clay, potentially skewing grain size distribution results toward coarser particles (Vaasma, 2008).

2.4.2 Organic matter analysis

Loss-on-ignition (LOI), used to quantify the organic matter, total carbonate, and siliclastic content (as a function of sediment dry weight), is another common method that has been used to provide information on past storm events based on the premise that a storm overwash layer will have less organic content than lagoon sediments deposited during periods of normal, low-energy sedimentation (McCloskey and Liu, 2012a; 2012b). All of the studies which analyzed organic content by LOI used a similar method laid out by Ball (1964), Dean (1974) or more recently by Heiri et al (2001), which involves combustion in a high-temperature furnace followed by weighing the residue with a high-precision balance to estimate the mass lost in the sample. The only exception was Malaizé et al. (2011) who removed organic matter from their samples by pyrolysis (oxygen-less combustion).

2.4.3 Micropaleontological analysis

The most commonly used micropaleontological proxy in paleotempestology is benthic foraminifera (Hippensteel and Martin, 1999; Lane et al., 2011; Liu et al., 2008; Peros et al., 2007). Foraminifera are small (usually <1mm) shelled amoeba, that include both benthic (bottom dwelling) and planktonic (water-column dwelling) species (Scott et al., 2001). Many benthic species are known to live in marginal marine habitats such as coastal marshes, mangroves, estuaries and lagoons. Storm surges transport and deposit offshore foraminifera into normally freshwater or brackish coastal settings such as lagoons and marshes where they are often preserved (Adomat and Gischler, 2016; Hippensteel and Martin, 1999; Murray, 2006) and it is the presence of these species that are used as indicators of past hurricane strikes (Collins et al., 1999; Hawkes and Horton, 2012; Hippensteel and Garcia, 2014; Hippensteel et al., 2013; Hippensteel and Martin, 1999; Horton et al., 2009; Lane et al., 2011; Scott et al., 2003; Williams 2009; 2010; 2013). The only species known in freshwater environments is *Allogromiida*, but many thrive in brackish marginal environments, so it is important to understand the salinity of the environment to differentiate allochthonous marine species from those that may form naturally in the wetland (Gupta, 1999). Some have also argued for the use of samples from unaffected sections of marshes as control markers for differentiating TC-deposited species to autochthonous species (Hippensteel et al., 2013, Hippensteel and Martin, 1999). A potential limitation in the use of foraminifera (and other micropaleontological indicators, see below) is based on salinity change in coastal wetlands—which results in a shift in species assemblages—unrelated to TC activity (Peros et al., 2015). For example, short-duration droughts or marine incursions related to the breaching of the barrier may result in an increase in lagoon salinity and a shift to species whose ecological tolerance is more typical or high salinity conditions (Peros et al., 2015). Such changes can be common in coastal environments and the interpretation of paleotempestological records can be facilitated through the use of multiple proxies.

Dinoflagellate cysts (a type of eukaryote marine phytoplankton) are another micropaleontological indicator that have been used to identify marine inputs into fresh- to brackish coastal wetlands based on their presence in lagoon deposits (Liu et al., 2011; Liu et al., 2008). In addition, the salinity at the time of deposition in a sediment core can be reconstructed using dinoflagellates as species inhabit environments with differing salinities, which can be useful to help reconstruct the evolution of the lagoon or wetland system in response to long-term changes in sea level and climate (Liu and Fearn, 2000). An understanding of how such systems change is critical to the interpretation of proxy indicators as the detectability of a TC may vary as the depositional environment changes (Hippensteel et al., 2013). Finally, in addition to dinoflagellates, other studies have also relied upon diatoms (Hansom and Hall, 2009; Liu and Fearn, 1993; 2000; Liu et al., 2008; McCloskey and Keller, 2009; McCloskey and Liu, 2012b), pollen (Liu et al., 2008; 2011; McCloskey and Liu, 2012b), ostracods (Malaizé et al., 2011) or bivalves (van Hengstum et al., 2014) to identify or validate storm-surge-generated overwash layers.

2.4.4 Chronology building

According to the list of studies (Table 2.1), the three main absolute dating methods used in paleotempestological research are carbon-14 (^{14}C), cesium-137 (^{137}Cs) and lead-210 (^{210}Pb). In many cases, ^{14}C is used in conjunction with either ^{137}Cs or ^{210}Pb (or both) to establish a reliable core-chronology. Most studies which used ^{137}Cs and ^{210}Pb also relied upon ^{14}C (Boldt et al., 2010; Brandon et al., 2014; Brown et al., 2014; Denommee et al., 2014; Donnelly and Woodruff, 2007; Donnelly et al., 2004; 2015; Liu and Fearn, 1993; Nikitina et al., 2014; Peros et al., 2015; Toomey et al., 2013; Williams, 2013; Woodruff et al., 2008). One paper solely used ^{210}Pb dating (Collins et al., 1999) and one paper only used ^{137}Cs (along with layer counting; Frappier et al., 2007b). Three studies utilized all three dating methods (Brandon et al., 2013; Lane et al., 2011; van Hengstum et al., 2014).

Donnelly et al. (2001; 2015) and Nikitina et al. (2015) showed that bulk lead pollution can also be used to validate chronological findings for the historic period, without needing to use the specific ^{210}Pb isotope. Others studies have used other independent means for validating their chronologies, for example the use of marine microfossils (Williams, 2013), pollen (Donnelly et al., 2001a; 2001b; 2015), and other elemental concentrations (Ti) (Woodruff et al., 2008). Brandon et al. (2014) and Williams (2013) have shown that ^{137}Cs can also be used effectively to date individual TC events near the 1963 bomb pulse. Modern radiometric dating can also bring more insight into the depositional environment, as Denommée et al. (2014) used varying ^{210}Pb activities to validate non-linear sediment accumulation rates, which is what would be expected in a sediment core preserving high magnitude depositional events, such as TC-induced sedimentation.

These radiometric techniques come with potential limitations as well. For example, in radiocarbon dating, one fundamental limitation is the reservoir effect, or old-carbon error. The reservoir effect happens when the sample has less ^{14}C relative to the abundance of the isotope in the environment leading to an older radiocarbon age (Yu et al., 2007). In coastal settings in particular, where paleotempestological records are most likely to be generated, it is also essential to take into consideration the marine radiocarbon reservoir effect, which is the offset in radiocarbon age between terrestrial organisms and those who have marine derived carbon (e.g. molluscs) (Ascough et al., 2005). Limitations in ^{210}Pb dating include, but are not limited to, the choice of model with which to calculate ages based on ^{210}Pb activities. The two main models are the constant initial concentration (CIC) and constant rate of supply (CRS) models. The CIC model is used for sites with constant sedimentation rates and the CRS model is used when there are changes in the rates of modern sedimentation. Using the CIC model will yield erroneous results for cores with varying sedimentation rates (Ghaleb, 2009), which, as discussed, may be common in paleotempestological studies (Ghaleb, 2009).

2.5 Geochemical methods

2.5.1 X-ray fluorescence (XRF) core scanning

In addition to the established proxies outlined above, the past decade has seen the introduction of a number of geochemical-based proxies in paleotempestological research. One of the analytical procedures used to generate such data is the use of XRF core scanning, which is essentially the use of a well-established analytical technique (X-ray fluorescence) arranged in a manner to enable sediment cores (and other materials, like speleothems) to be scanned at high precision (Kylander et al., 2011). One of the most widely used XRF core scanning systems is the Swedish built Cox Analytical Systems ITRAX (Boldt et al., 2010; Donnelly and Woodruff, 2007; Donnelly et al., 2015; Toomey et al., 2013). These machines typically provide sub-mm scale resolution of up to 62 elements in the range of aluminum to uranium, in addition to core x-radiography (Kylander et al. 2011). The high cost and infrastructure requirements of these units have also meant that smaller, faster, portable XRF systems (pXRF; such as the Olympus Delta Mining and Geochemistry handheld XRF Analyzer; McCloskey and Liu, 2012a) have been used in the field (Weindorf et al., 2014) for paleotempestological research. These devices produce data at much lower spatial resolution (usually mm- to cm-scale) but have the advantage of being considerably cheaper and can be easily used in the field for exploratory work (Naquin et al., 2014).

The use of XRF technology has been applied to paleotempestological studies in three primary ways: 1) to develop an X-ray of the core to differentiate denser from less dense sections, with the former generally reflecting higher mineral-content and therefore TC-overwash material (Boldt et al., 2010; Brandon et al., 2014); 2), to generate very high-resolution elemental data with which to identify TC overwash events directly (Woodruff et al., 2009; Naquin et al., 2014); and 3), to date sections of the core (usually near the core top) based on the identification of increases in elements related to human activities such as mercury, or lead, which itself can be dated using the historical record (e.g., Brandon et al., 2014; Donnelly et al., 2015).

Core X-radiography has been shown to be a useful aid to help support grain-size based data, especially in cores where visual evidence of TC overwash events are not discernible (Toomey et al., 2013). However, this technique by itself is not fool-proof, as some cores show no evidence of either changes in grain size or density (e.g., Toomey et al., 2013), requiring the use of other techniques to detect hurricane-induced events. Thus, it is usually used as supporting proxy data, but is automatically generated by most XRF core scanning systems so it requires little time to be invested in data generation.

The use of elemental geochemical data to identify storm overwash layers rests on the assumption that hurricane storm surges transport and deposit allochthonous material with a different elemental signature than that contained in the low-energy autochthonous sediments. Research using this technique appears to be better developed in other basins (e.g., Pacific, Mediterranean). For example, Woodruff et al., (2009) showed that Sr (normally abundant in marine shells and other materials) was a good indicator of marine overwash in two coastal lakes in southern Japan. In addition, Sabatier et al. (2012) used ratios of Si/Al and Zr/Al to identify storm events in cores on the south coast of France, and showed that increases in these ratios were highly correlated with increases in sediment grain size. In the Atlantic Basin, Naquin et al. (2014) interpreted decreases in terrestrial indicators such as Ti, Fe, and Zn as evidence of TC overwash, although this data was only used to support LOI and grain size data already available for the core. In addition, McCloskey and Liu (2012a) argued that increases in Fe, Ti, and Zn (again, identified as having a terrestrial origin) were associated with hurricane overwash in organic-rich peat sediments, possibly due to the reworking of terrestrial sediments by hurricane storm surges.

Finally, the use of XRF core scanning as a dating technique relies on the detection of a change in an element which can be linked to past human landuse or industrial activities (much the same way as the "*Ambrosia* rise" is used in pollen analysis [McAndrews, 1988]). This approach has been successfully applied to cores from locations such as in the northeastern United States (Boldt et al., 2010; Donnelly et al., 2015) where human impacts have been large and the timing of their initiation is well known. However, while this approach may be effective in some areas (e.g. Donnelly and Woodruff, 2007), it is not clear to what extent it would be applicable in more remote areas where the landuse history is not well established or where human impacts have been gradual, rather than more abrupt, making the attribution of an increase in a certain element difficult to establish (Han et al., 2002). Nevertheless, this is a useful application of XRF technology to help refine historic-scale chronologies where Pb-210 data is unavailable.

Thus, at this stage, the use of very high resolution XRF data as an indicator of hurricane activity is still relatively uncommon. The reasons for this are unclear, but they may be due to: a) the effectiveness of established methods (e.g., grain size) in paleotempestolgical study; b), the lack of a clear understanding of which elements or element ratios best detect overwash; or c), the lack of access to an XRF core scanning unit. It should also be emphasized that XRF elemental results have the potential to be used as a proxy of grain size itself; research such as Sabatier et al. (2012) and Cuven et al. (2010) has shown that sediment grain size is often correlated with certain elements (e.g., K, Fe, and Ti) and XRF core scanning may be a fast technique to estimate grain size without the effort of LPSA and potential problems associated with the removal of organic material (see above). XRF-generated grain size estimates would also be available at considerably higher resolution that most LPSA results, which are usually generated at 0.5 or 1 cm resolution, making the detection of much finer or shorter duration events possible (and thus it may enable cores of lower sedimentation rate to yield more data). The disadvantage of this approach is that at present, the use of XRF core scanning as a proxy for grain size is mostly qualitative and does not provide the full distribution of grain sizes possible with LPSA, which might be informative about past energy conditions and sediment source areas (Cuven et al., 2010).

Other limitations with XRF core scanning lie in the composition of the core. Cores composed of highly variable organic content (Löwemark et al. 2011) or inhomogeneous water content (Weindorf et al., 2014) or grain size (Weltje and Tjallingii, 2008) will change the composition of material that can be measured and cause the measured elemental data to vary, which may call for the data to be normalized (Löwemark et al. 2011) or calibrated (Weltje and Tjallingii, 2008). The effect of gaps, cracks and uneven sample surfaces in the core can also cause erroneous results and affect the overall quality of the data (Löwemark et al. 2011).

2.5.2 Stable isotopic geochemical indicators

Tropical cyclones tend to have a unique isotopic signature, with hurricane rainwater being depleted of heavier oxygen isotopes by up to 10‰ compared to normal rainwater (Figure 2.2; Lawrence and Gedzelman, 1996), making the use of stable isotope chemistry an important technique in paleotempestological research (Frappier et al., 2007b; Kilbourne et al., 2011; Kolodny et al., 2009; Lawrence et al., 2008; Li et al., 2011). Some researchers have also analyzed isotopes of carbon, nitrogen, or a combination of these elements (Das et al., 2013; Frappier et al., 2007b; Lambert et al., 2008; Li et al., 2011, Malaizé et al., 2011). The materials typically analyzed for isotope geochemistry include calcareous microfossils (such as ostracodes) in sediment cores (Lawrence et al., 2008; Malaizé et al., 2011; Das et al., 2013), stalagmites (Frappier et al., 2007b), corals (Kilbourne et al., 2011), rock samples (Kolodny et al., 2009), organic material extracted from sediment cores (Lambert et al., 2008), and tree ring cellulose (Li et al., 2011). Here we focus on their use in i) tree rings; ii) speleothems; and iii) coastal sediments, as we believe these represent potentially important new areas of research that should be the focus of additional work by the paleotempestological community.

2.5.2.1 Tree rings

Time series of oxygen isotopes have shown decadal to multi-decadal variations in TC activity (Lawrence and Gedzelman, 1996; Miller et al., 2006). Since oxygen isotope values in tree ring cellulose mainly reflect the source water used by the tree, TC water depleted in $\delta^{18}O$ should be discernable in the stable isotopic signature of tree rings (Miller et al., 2006). As precipitation from a TC infiltrates the soil it will be assimilated by the tree, leaving its isotopic signature within the cellulose that fed off that specific event. However, depending on local edaphic and geomorphic conditions, this TC water may only be captured in the cellulose up to a few weeks after an event (Miller et al., 2006). Tree species with shallow root systems, such as most *Pinus* (pine) species, will be more affected by soil water, making them particularly sensitive species for detecting TC activity (Anderson et al., 2002). Many factors can affect the amount of TC-derived water which will be incorporated into tree ring cellulose, such as the amount of precipitation available in the immediate vicinity of the tree and the infiltration and drainage capacity of the soil (Miller et al., 2006). Because of these factors, the isotope values can be a reliable proxy of TC past frequency, but not of intensity (Miller et al., 2006). In addition, certain physiological effects can affect the isotope values, such as carbonyl and water interactions that happen during biosynthesis, water-sucrose exchanges through the xylem, and oxygen fractionation due to leaf transpiration (Anderson et al., 2002). Luckily, these physiological effects are typically consistent within the same species, meaning that they can be largely controlled for by undertaking a species-specific tree-ring analysis (Anderson et al., 2002, Miller et al., 2006). Moreover, tree ring isotopic records are sensitive to dating uncertainties due to false and missing rings, but these problems can be mitigated for by developing a large dataset (often 50-100 trees) and cross-dating to develop a master chronology (Speer, 2010) to help select the most reliable samples for isotopic analysis.

2.5.2.2 Speleothems

Like tree-rings, speleothems also represent a promising, albeit little-used, source of stable isotopic data of past TC strikes that is of high temporal resolution (Frappier et al., 2007b; Malmquist, 1997). Speleothems are accretions formed by the dissolution of limestone or dolomite in karstic subterraneous caverns, passages and water basins which are formed by soil water percolating and infiltrating underground (Ford and Williams 2007). The limestone drip solution solidifies in layers, which in regions with well-defined seasonal precipitation can produce annual-scale features. In the case of TCs, the $\delta^{18}O$ depleted precipitation will leave its isotopic signature in the speleothems (McDermott, 2004). For example, Frappier et al. (2007b) reconstructed a 23 year record of TC activity using a rapidly forming calcite stalagmite in Belize. The $\delta^{18}O$ and $\delta^{13}C$ data generated from this stalagmite covered the period AD 1977 to 2000 at weekly to monthly resolution. The study showed that excursions in $\delta^{18}O$ and $\delta^{13}C$ were highly correlated with known TC strikes, indicating that the method likely has utility in longer (pre-instrumental) speleothem records (Frappier et al., 2007b).

The use of speleothems for paleotempestology has many advantages, not the least of which is the high temporal resolution possible. In addition, karstic environments can be completely sheltered from exterior meteorological factors such as temperature and humidity, meaning that changes in stable isotopic ratios are more likely to be associated with TCs (McDermott, 2004). Moreover, caves are generally humid, limiting the evaporation of the precipitated water, thus limiting kinetic fractionation (McDermott, 2004). Despite this, not all caves and speleothems are appropriate for sampling. Frappier (2008) defined a screening process to help identify the most sensitive speleothems for paleotempestological research, which consisted of the following criteria: 1) sampling fast-growing speleothems to ensure short-lived hurricane events are recorded; 2) sampling in caves surrounded by thin soils to enhance the infiltration of TC rainwater; and 3), analyzing speleothems that have had minimal re-crystallization or disturbance.

2.5.2.3 Organic Chemical Proxies

The use of organic geochemical proxies (OGP) in paleotempestology is an understudied area but it may bring important new insight where established proxies cannot (Das et al., 2013; Lambert et al., 2008). OGPs can be used to identify the source of the organic matter in sediment cores, such as whether it is terrestrial, lacustrine or marine, and in doing so identify changes in the state of a wetland that might be related to TC activity (Das et al., 2013). Specifically, an isolated coastal freshwater lake will have organic matter with relatively lower $\delta^{13}C$ and $\delta^{15}N$ values than organic matter from a state in which it is flooded or inundated after a storm surge (Das et al., 2013). Nutrient supplies from marine water intrusion and enhanced light penetration will stimulate algal growth (i.e., eutrophication; Lambert et al., 2008), and the marine organic matter entering the basin will have higher $\delta^{13}C$, $\delta^{15}N$, and C/N values compared to lacustrine organic matter (Das et al., 2013; Lambert et al., 2008). These proxies were investigated at Lake Shelby, Alabama, and excursions in those isotopic ratios correlated closely with hurricane-generated sand layers at this site (Lambert et al. 2008). Indeed the results of this study showed that 11 catastrophic hurricanes hit the Lake Shelby coast over the last 682 years and that the ability to detect severe hurricanes using this isotopic method was significantly increased over the established proxies (Das et al., 2013).

2.6 General Limitations

In addition to proxy limitations, paleotempestological reconstructions can also be hampered by the characteristics of the study site, sea level change, and other processes (Wallace et al., 2014). At the site level, long-term changes in barrier height and width can affect the ability of overwash to enter a lagoon, with increases in these dimensions (due to geomorphic processes such as enhanced sedimentation) reducing the sensitivity of a site to overwash and hence appearing as though fewer hurricane strikes occurred (Otvos, 2011). In addition, other processes that result in the deposition of coarse grained material, such as floods due to (non-hurricane) high energy precipitation events, aeolian processes, high tides, and sediment winnowing, might help concentrate coarser particles and yield a “false positive” (i.e., a sand layer not deposited by a hurricane)(Otvos, 2009; Otvos, 2011). Relative sea level rise is also a potentially complicating factor, as lower past sea level positions would decrease the sensitivity of a lagoon or a coastal lake to overwash as the shoreline would have been located in a more seaward position in the past (Liu and Fearn, 2000). It is therefore helpful to understand local relative sea level history at a given site when interpreting long paleotempestological records to assess whether an apparent decrease in coarse layers with time is due to a real decrease in hurricane activity or a different past shoreline position. In addition, the question of tsunamis is frequently raised in the literature (e.g. Toomey et al., 2013), and there are no clear methods for differentiating between tsunami- and hurricane-generated deposits (McCloskey and Keller, 2009). Despite this, the occurrence of tsunamis is much less frequent than that of hurricanes, at least in the western North Atlantic basin (McCloskey and Keller, 2009), and tsunamis are unlikely to be significant contributors to coastal sedimentary deposits. Finally, anthropogenic factors can disrupt sedimentation in coastal environments (Lane et al., 2011; McCloskey and Liu, 2012b) making the detection of recent hurricanes in the sedimentological record difficult.

2.7 Future directions

Based on the work in this paper, we suggest three areas where we believe the paleotempestological community could focus its research efforts:

2.7.1 The development of an online paleotempestological database

We argue that the building of a searchable, publically and freely available, online database archiving the raw data from these studies would greatly enhance research efforts in this field. The database need not be restricted to the western North Atlantic region but could be global and would include information on the proxy data (e.g., grain size measurements, isotopic values), chronologies and age-depth models, details about the sampling site (e.g., physiographic information about lagoon barrier height and width, vegetation, etc.), and the technology used to collect the sample (e.g., coring equipment). The methodologies used, even though often available in publications, would allow researchers to better understand the potentials and limitations of the data from each site. The availability of this information would also facilitate the comparison of records within and between sites, providing more information on spatial and temporal variability in paleotempestological records. Some online resources do already exist; for example, the National Climatic Data Center (NCDC) of the National Oceanic and Atmospheric

Administration (NOAA) has a “Paleotempestology Resource Center” page (http://www.ncdc.noaa.gov/paleo/hurricane/links.html), although it was last updated in February 2012 and contains few datasets. It should also be noted that some paleotempestological records are also available through the Paleoclimatology Data Search engine of the NCDC website (and researchers who have contributed data should be thanked), but a single database devoted to paleotempestology would be effective for researchers in this field. One possibility would be to model such a database after the Neotoma Paleoecology Database, which in addition to searchable data also includes information on news highlights, events, and public outreach activities in the area of paleoecology (http://www.neotomadb.org/about/category/about).

2.7.2 Regional-scale syntheses of paleotempestological data

Given the recent proliferation of paleotempestological records from individual sites (Table 2.1) and the increasing spatial density of coverage in the western North Atlantic region (Figure 2.1), we argue that it is time to go beyond just the generation of individual paleotempestological records and their comparison to other datasets in papers (e.g., Peros et al., 2015) to begin to more systematically analyze temporal and spatial differences in paleotempestolgical records. How consistent are the presence of “active” hurricane periods identified at some sites (e.g., Donnelly and Woodruff, 2007) across space? If these periods occur elsewhere, is their occurrence synchronous or do they occur in a time-transgressive manner? A time-transgressive model of enhanced hurricane activity has been proposed that involves a latitudinal migration of the Intertropical Convergence Zone (ITCZ) as a driving mechanism during the middle to late Holocene (McCloskey et al., 2012; van Hengstum et al., 2016). Testing of hypotheses related to identifying the main drivers of centennial- to millennial-scale hurricane patterns would be enhanced by generating a time-series of region-wide maps highlighting active versus inactive period variability. Such maps would be analogous to fossil pollen-based reconstructions of North American temperature anomalies (Viau et al., 2006) and would more easily permit potential driving factors (e.g., sea surface temperatures, ITCZ position) to be compared to the paleotempestological data in order to better understand the causes of long-term hurricane variability.

2.7.3 The generation of new paleotempestological records from areas on the margins of hurricane tracks

The space in which North Atlantic hurricanes occupy today is shown in Figure 2.3. The southern boundary of this zone is approximately parallel to the north coast of South America whereas the northern boundary is more diffuse and extends north of the Canadian Atlantic Provinces. Most paleotempestological reconstructions have been undertaken at sites near the center of this zone, such as the northern Gulf of Mexico coast (e.g., Liu and Fearn, 2000), Belize (e.g., McCloskey and Keller, 2009), and the Bahamas (e.g., van Hengstum et al. 2016). We propose that it would be beneficial to the understanding of long-term processes controlling hurricane frequencies and patterns to also examine sites at the margins of this zone, as different atmospheric and oceanic circulation patterns in the past (i.e., warmer sea surface temperatures) may have increased the space over which this zone occurs, particularly at its northern limit. For this reason, we suggest that an investigation of sites in the Canadian Atlantic Provinces and the southern Caribbean would be advantageous. A cursory analysis of potential coring locations, based on some of the criteria outlined by Wallace et al. (2014), indicates the presence of a few potential sites on the islands of Bonaire and Grenada (Figure 2.3). Likewise, there are many coastal lakes and ponds located on the Atlantic coast of Nova Scotia that could be examined. One potential difficulty that may be encountered at high latitude sites could be differentiating tropical cyclones from mid-latitude winter storms (i.e., "nor'easters") in the paleotempestological record but this can be accomplished by selected coring locations that are oriented such that winter storms have minimal impact (Boldt et al., 2010). Indeed, the idea of examining hurricane track boundaries is analogous to the concept of studying major ecological boundaries (i.e., "ecotones") in paleoecology and palynology as it is in these locations that change is expected to be most prominent and detectable in the fossil record (McAndrews, 1966; Williams et al. 2009).

2.8 Conclusion

When Hippensteel (2010) writes about the pursuit of the perfect proxy for paleotempestology reconstructions, he focuses on sedimentary- and ecological-based indicators. Sedimentary research related to the identification of coarse sand layers, ecological work identifying offshore foraminifera, and the use of other proxies such as loss-on-ignition, are still indispensable and robust methods for paleotempestological research and have helped advanced the field considerably. However, new technologies (e.g., XRF core scanning) and non-established paleoenvironmental archives (at least as applied to paleotempestology, such as tree rings) provide an opportunity to expand the scope of paleotempestological research to new sites and to generate records at considerably higher temporal resolution, sometimes at the annual or even seasonal scale.

For example, researchers have begun to use stable isotope geochemistry (Das et al., 2013; Frappier et al., 2007b; Kilbourne et al., 2011; Lawrence et al., 2008; Li et al., 2011), XRF core scanning (McCloskey and Liu, 2012a; Naquin et al., 2014), and X-radiography (Boldt et al., 2010; Hawkes and Horton, 2012; Lane et al., 2009) to study past TC variability. Stable isotopes from tree rings have the potential for increasing both the spatial and temporal (i.e., seasonal) resolution of paleotempestological studies, although they have not yet been widely applied, and it is unclear if long (e.g. 1000 year) timescales can be generated with them. Analyzing the geochemical properties of speleothems is also a very promising method for studying paleotempestology but it is an area of research that remains in its infancy. However, the sampling protocol for speleothems described by Frappier (2008) opens the door to potentially seasonal-scale resolution at much longer (>10 000 years) timescales than many other existing methods allow.

In this paper we also reviewed the spatial distribution of paleotempestological studies in the Atlantic Basin and showed that many gaps exist along the coast of eastern North America, in the Gulf of Mexico, and in the Caribbean. There are a number of reasons for this, but the use of a wider range of proxy indicators by the paleotempestological community will help fill these gaps by increasing the number of potential sites from which data can be generated. Such efforts will help to develop a more comprehensive and spatially homogenous coverage of paleotempestological records to be able to better test hypotheses concerning the factors that drive TC frequency changes in the Atlantic Basin (e.g., ITCZ Hypothesis, McCloskey et al., 2012; van Hengstum et al., 2016). In addition, synoptic-scale analyses of TC variability will also be assisted with the building of publically-available online databases where paleotempestological records can be housed, accessed, and analyzed, with the view to producing regional-scale syntheses.

Table 2.1 List of original peer-reviewed publications on Paleotempestology in the western North Atlantic basin.

			Proxy							Chronology		
	Author	Year	Grain-size	LOI	Geochemistry	XRF	X-Ray	Micropaleontology	Model	^{14}C	^{137}Cs	^{210}Pb
1	Adomat and Gischler	2016	x					x		x		
2	Aharon and Lambert	2009								x		
3	Bertran et al.	2004	x							x		
4	Boldt et al.	2010	x			x	x			x	x	
5	Brandon et al.	2013	x			x	x			x	x	x
6	Brandon et al.	2014	x			x	x			x	x	
7	Brown et al.	2014	x	x						x	x	
8	Burn and Palmer	2015				x				x		
9	Buynevich and Donnelly	2006	x							x		
10	Buynevich et al.	2007								x		
11	Cheung et al.	2007							x			
12	Cochran et al.	2009	x	x						x		
13	Collins et al.	1999		x			x	x				x
14	Das et al.	2013			x					x		
15	Denommee et al.	2014	x							x		x
16	Donnelly	2005	x							x		
17	Donnelly and Woodruff	2007	x			x				x	x	
18	Donnelly et al.	2001a	x							x	x	
19	Donnelly et al.	2001b	x							x	x	
20	Donnelly et al.	2004	x	x						x	x	
21	Donnelly et al.	2015	x	x		x				x	x	
22	Ercolani et al.	2015	x	x				x		x		x
23	Frappier et al.	2007b			x						x	
24	Gischler et al.	2008	x							x		
25	Hawkes and Horton	2012	x	x			x	x				
26	Hippensteel	2008						x				
27	Hippensteel and Garcia	2014	x					x		x		
28	Hippensteel and Martin	1999	x					x		x		
29	Hippensteel et al.	2013	x					x		x		
30	Horton et al.	2009	x	x				x				
31	Kiage et al.	2011	x	x						x		
32	Kilbourne et al.	2011			x							

33	Lambert et al.	2008			x					x		
34	Lane et al.	2011	x	x			x	x		x	x	x
35	Lawrence et al.	2008			x							
36	Li et al.	2011			x							
37	Liu and Fearn	2000	x	x						x		
38	Liu and Fearn	1993	x							x	x	
39	Liu et al.	2008	x	x								
40	Liu et al.	2011	x	x								
41	Malaizé et al.	2011	x	x	x		x			x		
42	Mattheus and Fowler	2015	x							x		
43	McCloskey and Keller	2009	x	x						x		
44	McCloskey and Liu	2012a	x	x		x				x		
45	McCloskey and Liu	2012b	x	x						x		
46	Naquin et al.	2014	x	x		x				x		
47	Nikitina et al.	2014	x	x						x	x	
48	Peros et al.	2015	x	x				x		x	x	
49	Reese et al.	2008	x	x								
50	Scileppi and Donnelly	2007	x	x		x				x		
51	Scott et al.	2003	x	x			x	x		x		
52	Toomey et al.	2013	x			x	x			x		x
53	van Hengstum et al.	2014	x	x						x	x	x
54	van Hengstum et al.	2016	x	x			x			x		
55	Wallace and Anderson	2010	x							x		
56	Williams	2013	x	x				x		x	x	
57	Williams	2010	x	x				x				
58	Williams	2009	x					x				
59	Woodruff et al.	2008	x						x	x	x	

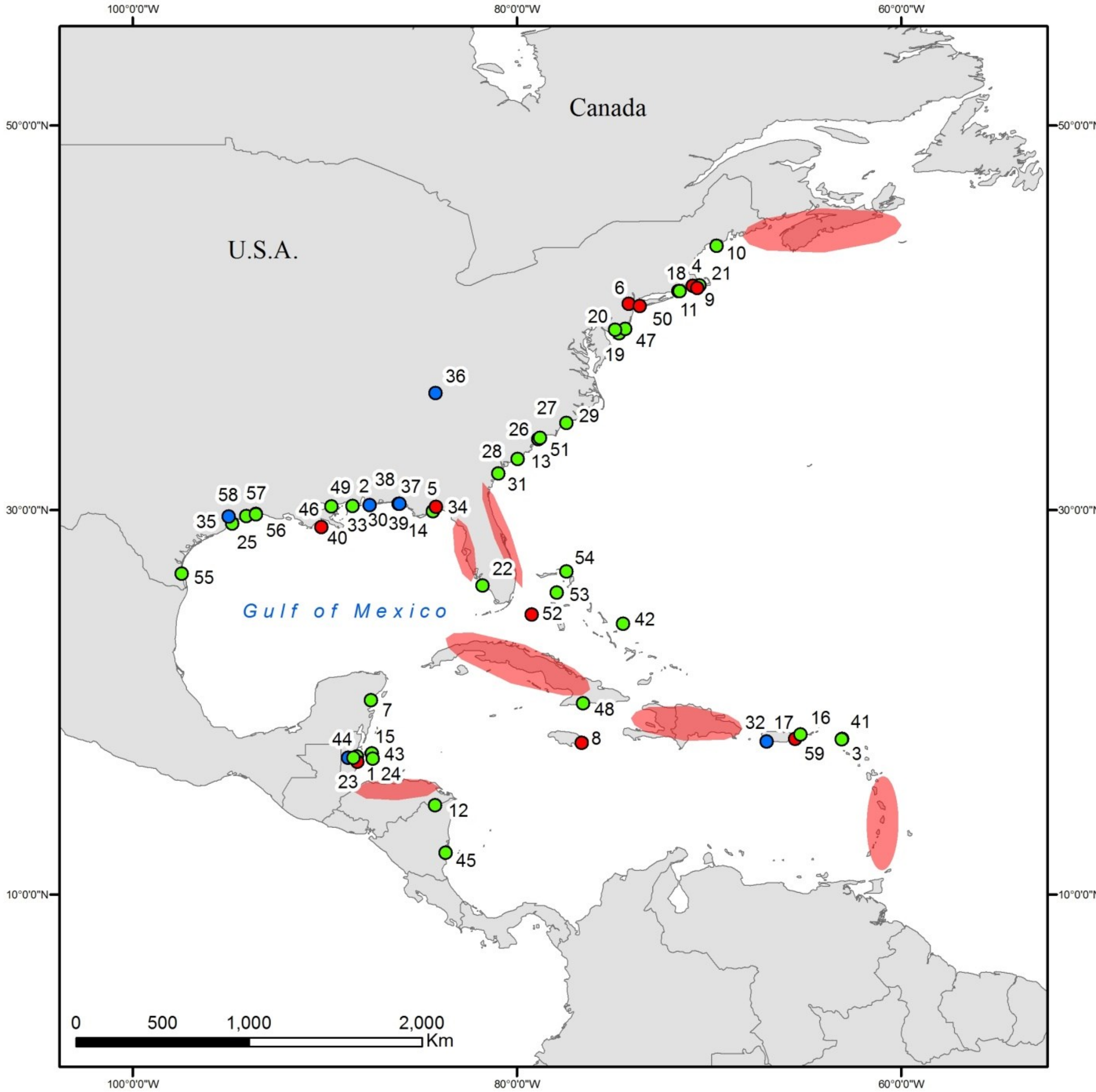

Figure 2.1 Map of peer-reviewed study sites from Atlantic tropical cyclone. Red points represent studies that used XRF, blue points are studies that used geochemistry, and the green points represent studies that primarily used more established methods. Number corresponds to Study ID (Table 2.1). Red areas are identified spatial gaps.

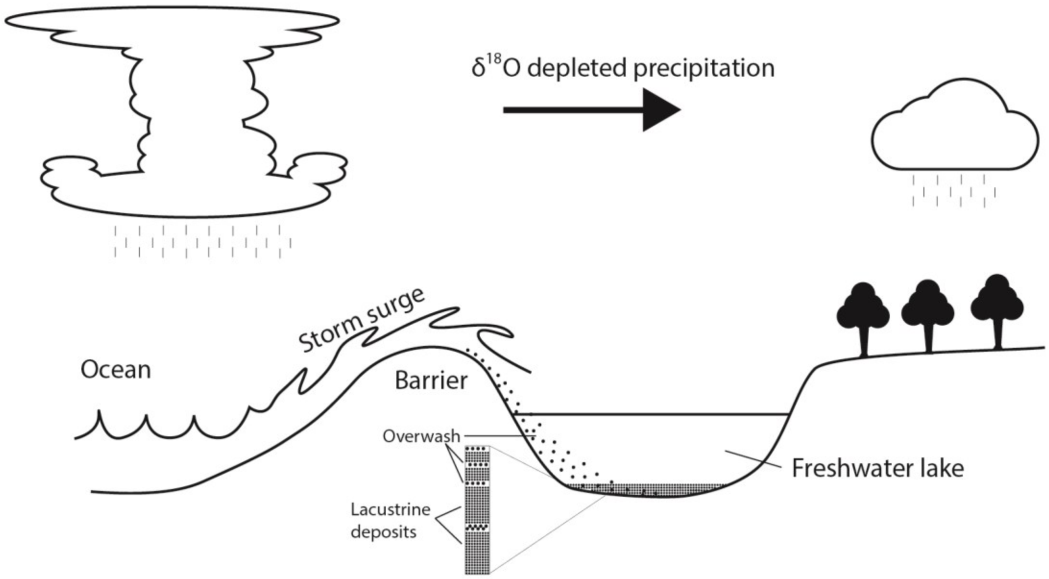

Figure 2.2 Effects of an advancing TC: storm surge breaching a barrier and bringing overwash into a freshwater coastal setting. Clouds carrying ^{18}O depleted precipitation moving inland from the storm.

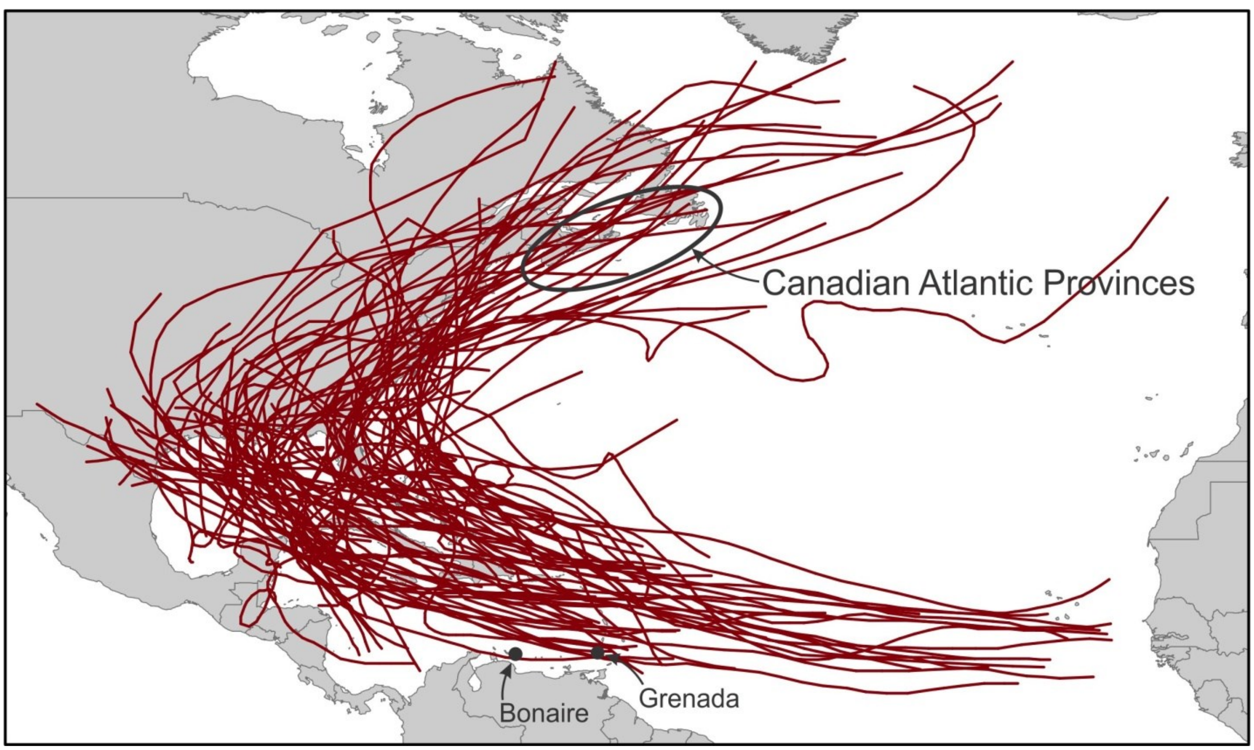

Figure 2.3 Paths of all tropical cyclones and major hurricanes from 1851 to 2004 that crossed the United States (National Oceanic and Atmospheric Administration, Tropical Prediction Center/National Hurricane Center).

Chapter 3 – Development of a Paleotempestological Database and its Potential Application in Testing Hypotheses for Variations in Tropical Cyclone Activity in the Western North Atlantic Basin

3.1 Abstract

Paleotempestology, the study of past tropical cyclone (TC) activity using geological proxy techniques, utilizes data from a broad range of sources. This paper presents a database that includes data from 59 paleotempestological studies. This database, housed at the National Oceanographic and Atmospheric Association (NOAA), contains the most up-to-date paleotempestological proxy data available for TC reconstructions for the western North Atlantic basin during the past 8,000 years. From this database a robust subset of four studies was chosen using stringent criteria and was compared to a less stringently chosen subset of 37 studies to reconstruct TC variability in the western North Atlantic basin to investigate the Bermuda High Hypothesis. We provide evidence based on two different approaches that shifts in the Bermuda High do impact the movement of TC tracks. TCs followed the western edge of the high pressure system while it was in a southwest position from < 3000 cal yr BP to ~1000 cal yr BP and then the pressure system went through a millennial scale shift to a northeastern position at ~1000 cal yr BP when TCs curled up the North American Coast.

This chapter has been submitted for publication as: *Oliva F., Peros M., Viau A., Bouchard M. (2017) Testing the Bermuda High Hypothesis through Tropical Cyclone Activity in the Western North Atlantic Basin.* The Holocene.

3.2 Introduction

Paleotempestology, the study of past tropical cyclones (TCs) using different geological methods (Liu, 2004), is a now an established field with at least 59 published peer reviewed articles (Table 2.1) dedicated to the reconstruction of past TC activity along the Atlantic Coast of North America, Central America, and the insular Caribbean (Oliva et al., 2017).

Short instrumental records are often not long enough to properly model future TCs including their path, intensity and frequency. Geological proxy data allows the instrumental record to be extended over longer timescales in order to improve predictability (Henderson et al., 2009). In the case of TCs, reliable instrumental data only began to be collected in the mid to late 1940s, making the identification of trends and patterns and their attribution particularly difficult (Bradley, 2000; Knutson et al., 2010).

Oliva et al. (2017) suggested that a publicly available online database of reconstructed TC strikes, along with raw proxy data, sampling site details, and the methods of data collection and generation would greatly contribute to efforts to understand TC variability in the western North Atlantic basin during the Holocene. We expect that future analyses using this database, rather than just an examination of individually selected sites, will lead to a better understanding of the long-term climate forcing(s) that influence hurricane tracks, intensity, and frequency along the North Atlantic eastern seaboard, and help in the generation of new hypotheses on TC variability for this region.

In this paper, we present a new database that includes the TC reconstructions from 59 peer-reviewed studies. Secondly, we compare an analysis of a 37 study subset selected using one single criterion (henceforth referred to as "full subset") against an analysis of four studies chosen with more stringent inclusion criteria (henceforth referred to as "restricted subset"). Based on these analyses we then present a robust reconstruction of TC strikes in the western North Atlantic in order to test the Bermuda High Hypothesis.

Although major climate forcings (e.g. North Atlantic Oscillation (NAO)) (Knowles & Leitner, 2007; Liu, 2004) and the latitudinal position of the Intertropical Convergence Zone (ITCZ) (van Hengstum et al., 2016) may have an impact on the frequency of TCs, we only explore the impact of the position of the Bermuda High pressure system in relation to TC activity in the western North Atlantic basin (Knowles & Leitner, 2007; Liu and Fearn, 2000; Liu, 2004) as an example of the use of our new database.

The Bermuda High Hypothesis argues that a northeast to southwest seesaw shift of this high pressure system has an impact on tropical cyclone tracks in the western North Atlantic basin. When the Bermuda High is in the northeast position, TCs will follow the western edge of the high pressure system and curl up the northern North American coast. Conversely, when it is in its southwestern position, TCs will again tend to follow the western outer edge of the high pressure system and get pushed into the Gulf of Mexico. We test this hypothesis by studying the oscillation in the distribution of TCs strikes between the northern North American Coast and the Gulf of Mexico.

The Bermuda High Hypothesis has often been cited in the literature as a potential driver of millennial-scale shifts in TC tracks (Liu & Fearn, 2000; Liu, 2004) and it has only been tested using various visualization techniques (Knowles & Leitner, 2007), but not quantitatively. This Bermuda High Hypothesis is closely linked with the North Atlantic Oscillation (NAO), an oscillation in the pressure gradient between the Icelandic low and the Bermuda (Azores) high pressure systems. The movement of the Bermuda High towards the southwest reduces the pressure gradient in the Atlantic shifting the NAO into a negative phase and vice-versa (Hurrell et al., 2003).

3.3 Methods

3.3.1 Data Manipulation – Database Development

A review of all peer-reviewed journal articles on the paleotempestology of the western North Atlantic was done and showed that at least 59 studies have been published for this region (Oliva et al., 2007). The paleotempestological reconstructions in these studies are from sedimentary archives in coastal areas (e.g., coastal fresh water lake, lagoon) along the eastern North American seaboard, Gulf of Mexico, and the Caribbean. A number of proxy indicators were used to infer past TC strikes, with sediment grain size analysis being the most common technique (e.g. Liu & Fearn, 1993), although benthic foraminifera and stable isotopes have also been used (e.g. Peros et al., 2015, Miller et al., 2006). In some studies, individual TC events are identified, usually on the basis of single event beds present in a sediment core (e.g. Liu et al., 2008). Other studies, where sediment rates have been relatively slow, the authors identify intervals of more or less active hurricane activity based on grain size changes that last decades to hundreds of years (e.g. Donnelly & Woodruff, 2007). Intervals are recorded as calendar dates (year BP, BC, AD or CE, calibrated in most cases from radiocarbon years BP to calendar ages before present: 1950), along with event frequency or return period (e.g. 1 in 100 years).

Events and intervals were recorded using only the authors' interpretations of event dates, associated errors, and event return periods, based on their interpretation of the dating model and associated isotopic chemistry, lithology, grain size distribution, palynological and/or micropaleontological evidence of past TC events. These were recorded in the database: 1) directly from the body of the text; 2) from summary tables provided by the authors; and/or 3) digitized from scaled graphics presented as figures in the paper. The latter method of data acquisition from graphical interpretations of the data carry on average an inherent error on the order of +/- 50 years associated with digitizing low resolution rasters embedded in the PDF format of the articles. Further event and interval metadata are described in the supporting information (Appendix 1).

3.3.2 Full subset analysis

From the 59 studies in our database, we selected 37 for an exploratory spatial data analysis (ESDA) of the data. The 37 studies were chosen based on one single criterion: the study must contain quantitatively dated intervals or events and not simply periods of heightened or lessened activity. The two types of data, intervals and events, were formatted to a uniform data type and collated into a single table (Table 3.1). With ~8000 years of data, the bin size was determined by using the Square-root choice, a common method which involves rounding up the square root of 8000 years (89.44 years) to 100 years. For single event entries with error bars greater than 100 years, the event frequency was calculated as 100 [yrs] / range [yrs]. For single event entries with error bars less than or equal to 100 years, the 100-year event frequency was assumed to be 1. Event frequencies were then assigned to each 100-year bin, whereby if either tail of the error bar interval falls within a given 100-year interval, the 100-year event frequency is assigned to that 100-year interval bin and to every bin within that interval range. For study locations with overlapping intervals or single event error bars, the mean event frequency is calculated for each 100-year bin at each study location. The overall range of data for each study location is from present (1950) to the oldest assessed event age. Within these overall ranges, 100-year periods with no recorded events are assumed to have an event frequency of zero or no TC events.

3.3.3 Bermuda High Hypothesis Analysis

We subdivided both the full and the restricted subsets into two groups based on geographic location: the western Atlantic Coast with latitude greater than 31.5°N: the North Coast, and to the south of 31.5°N including Florida, the Gulf of Mexico and the Caribbean: the South Coast. This was done in order to identify the location of TC strikes in the optic of testing the Bermuda High Hypothesis. This approach allows us to distinguish between the paths of TCs that made landfall north up the eastern North American Coast, and the paths of TCs being pushed south into the Gulf of Mexico under the influence of the Bermuda High pressure system.

Then in order to test the Bermuda High Hypothesis in a more robust way, we used much more stringent selection criteria to select four sedimentological studies based on literature (e.g. Mann et al., 2009) homogeneity and proxies (Figure 3.1; Table 3.2) to perform a comparison analysis from which to draw our conclusions.

The stringent selection criteria for our restricted subset included:

a) The study must have a complete record covering the desired period (2000 BP to present). In order to certify a robust analysis, it is important that all the of the records span the same timeline, to not have any discontinuities or false return intervals (Mann et al, 2009).

b) The age model needs to have a sufficiently robust dating method to have a confidence level in the reconstructions.

c) The results must contain quantitatively dated intervals or events and not simply periods of heightened or lessened activity.

d) The study must have a minimum sensitivity or threshold of category 2 hurricanes. As with Mann et al. (2009), the chosen sites may slightly vary in their sensitivity of threshold category they can record. The importance is that sites register TCs of similar intensities and not to compare high intensity hurricanes to extra-tropical storms.

e) Sites with any ambiguity in their path, such as Cuba, were omitted to avoid false positives (i.e. record a strike on the South Coast but curl northward before entering the Gulf).

f) The study must be situated in the Gulf of Mexico or along the eastern seaboard Coast of North America.

3.4 Results

3.4.1 Database development

The database consists of a total of 152 single TC events and 83 intervals of relatively active TC periods from ~8000 cal yr BP to the present in 59 studies. A map of the spatial distribution of paleotempestological records (Figure 3.2) in the database illustrates the spatial coverage of sites and the total number of detected TC strikes (Figure 3.2a) at those locations and the duration of those records (Figure 3.2b). The overall distribution of records shows good coverage for the northeastern United States, the northern Gulf of Mexico, but relatively sparse coverage for Cuba, Hispaniola, and the Lesser Antilles (Oliva et al., 2017).

3.4.2 Full Subset Analysis

Combined event frequencies per 100 years and the number of active sites for the North and Southe Coasts are plotted in Figure 3.4a and 3.4b, respectively. "Active sites" refers to the number of paleotempestological records for that time interval whether TC strikes was recorded or not. The frequency results show a generally inverse relationship between northern (red) and southern (black) sites for the present to ~3400 cal yr BP, although both regions show low TC activity from ~2200 to 1900 cal yr BP. Tropical cyclone activity is generally high at the southern sites from ~5400 to 2200 cal yr BP, with the exception being the periods from 3300 to 2800 cal yr BP and 4700 to 4000 cal yr BP. There are too few northern sites that date to this interval to be reliable, although the period from 3300 to 2900 cal yr BP does appear to have been active in the north.

Given the decrease in the number of sites that have records older than a few millennia, we focus the total events portion of the analysis on the last 2000 years. Figure 3.5 shows each reconstructed strike from the present to 2000 cal yr BP. The size of the green points shows the number of strikes for each site in 100 year intervals, and the integer value in each frame denotes the total number of TC strikes recorded at all sites during that time (the black points indicate no strikes are recorded). In general, the results show that TC frequency was higher over the last few centuries (from 600-501 cal yr BP, or approximately AD 1500, to the present), compared to the period from 2000 to 600 cal yr BP. An exception is 1000-901 cal yr BP, which records a higher number of total TC strikes, particularly in the northern Gulf of Mexico. The period from 2000 to 1500 cal yr BP is especially quiet.

3.4.3 Restricted Subset Analysis

The two sites from the North Coast (Donnelly et al., 2015; Scott et al., 2003; Figure 3.3) show heightened activity from the present to ~1800 cal yr BP. Donnelly et al.'s (2015) results confirm heightened activity in New England form 550 to 275 cal yr BP and from 1800 to 800 cal yr BP.

Scott et al.'s (2003) study concludes strikes along the North Coast in -39, -4, 520, 667, 738, 927, 1298, 1727 and 2972 cal yr BP. The two sites from the South Coast show (McCloskey and Liu, 2012; Liu and Fearn, 2000; Figure 3.3) heightened activity from present to 1000 cal yr BP (McCloskey and Liu, 2012) and from 1000 cal yr BP to beyond 3000 cal yr BP (Liu and Fearn, 2000).

3.5 Discussion – Testing the Bermuda High Hypothesis

3.5.1 Full Subset Analysis

The inclusion of 37 studies based on one general criterion, to include only studies that contain quantitatively dated intervals or events and not simply periods of heightened or lessened activity, has advantages and disadvantages. Although this type of analysis suffers from many statistical and analytical shortcomings due to the use of multiple proxies, different dating standards, unknown site sensitivity, non-continuous records and the possibility of false positives due to site location, it serves as an example of the potential use of our new database for important analyses that can help future research and hypothesis testing.

The frequency of TCs is high for both the North and South Coasts from the present to 100 cal yr BP, indicating that the Bermuda High pressure system may be in a slightly neutral position or in the midst of shifting from one position to the next (Figure 3.4). From a climate period standpoint, there is an increase to 14 events in the 901-1000 cal yr BP period in both regions (Figure 3.5). This coincides with warming temperatures and the onset of the Medieval Climate Anomaly (MCA) and also matches a previously detected period of higher activity based on sedimentary evidence and a statistical model (Mann et al., 2009). The MCA was characterized by having a strong positive NAO during its entire duration (Trouet et al., 2009) which matches with many of the strikes occurring on the North Coast (Figure 3.5). The same happens with a peak of 21 events in both regions from 401-500 cal yr BP (Figure 3.5), during a slightly warmer period of the LIA. Our findings support the claim that a shift of the Bermuda High occurred ~6800 cal yr BP as the overall frequency of tropical cyclone strikes along the South coast diminished (Figure 3.4). The shift at 3200 cal yr BP, on the other hand, would not have been caused by a millennial-scale shift to the southwest but moreso by a decadal-scale shift to the northeast (Figure 3.4). The hyperactive period that Liu and Fearn (2000) identified as having occurred from 900 to 3600 ^{14}C yr BP (843±47 to 3906±10 cal yr BP), indicates that the Bermuda High underwent a slow shift toward the northeast for a period of ~700 years followed by a clearly active period along the south coast from 2000 to 3000 cal yr BP (Figure 3.4).

3.5.2 Restricted Subset Analysis

Here, we applied very stringent criteria to filter out studies to include only 4 of 59 studies available in our new database. This more conservative approach has been suggested to yield better results with much higher confidence than as compared to the more liberal approach we presented above (Mann et al., 2009).

McCloskey and Liu (2012) acknowledge that their activity pattern does not correspond with the majority of the reconstructions in the Gulf of Mexico and USA coast. Taking this into consideration, the results from Liu and Fearn (2000), Donnelly et al. (2015) and Scott et al. (2003) support a period of heightened activity on the North coast from the present until ~1800 cal yr BP and from 1000 cal yr BP to earlier than 3000 cal yr BP. This supports Liu and Fearn's (2000) conclusion that there was a northeastern shift in the position of the Bermuda High at ~1000 cal yr BP.

Over the last 3000 years, results from the full and restricted subset analyses both show an increased activity along the South coast after ~2100 cal yr BP with a sharp decline in activity along the North coast at ~1800 cal yr BP. With the inclusion of the McCloskey and Liu (2012) study, the results also coincide from present to 1000 cal yr BP, when there was activity in both regions (Figure 3.7).

A number of forcing mechanisms have been proposed to explain millennial-scale TC variability in the North Atlantic region. One such potential forcing, referred to as the Bermuda High Hypothesis, represents a shift in the Bermuda High pressure system which creates a corridor for TCs to migrate northwards before hitting the east coast of North America when the system is in its northeastern position (Figure 3.6a) (Liu and Fearn, 2000; Liu, 2004). Conversely, TCs are generally steered towards the Gulf of Mexico when it is in its southwestern position (Figure 3.6b) (Liu and Fearn, 2000; Liu, 2004).

Although it is well known that there is multi-decadal variability in instrumentally observed tropical cyclones, the discovery of overlapping millennial-scale variability can explain the effect of greater climate forcings on tropical cyclones in the western North Atlantic basin (Liu, 2004).

Liu and Fearn (2000) originally suggested a shift in the Bermuda High to the southwest at 3200 cal yr BP and a shift northeast in 6800 cal yr BP. Other shifts in the position of the Bermuda High pressure system may also exist on interannual and interdecadal timescales (Liu, 2004). For example, Knowles & Leitner (2007) tested this hypothesis with modern data using various visualization techniques in Geographic Information Systems (GIS). They concluded that there was potential for interannual and interdecadal shifts in the Bermuda High position which affected the movement of tropical cyclones (Knowles & Leitner, 2007).

3.5.3 Limitations

There are several limitations to testing the Bermuda High Hypothesis. The first, main limitation is the multitude of factors that can have an impact on TC paths, such as the NAO, sea-surface temperatures, other high and low pressure systems as well as other major teleconnections such as El Niño–Southern Oscillation (ENSO). Another limitation is the bias to reconstructions along the South Coast which could falsify results along with the arbitrary decision to cut off the coasts at 31.5°N could pose other issues.

3.6 Conclusion

The available data provides evidence for changes in TC activity over the last 8000 years. However, because older records are less well represented, along with other shortcomings of using a database with diversity in research methods and robustness, we cannot have the same confidence in large-scale reconstructions from all time periods (full subset analysis) as using stringent inclusion criteria (restricted subset analysis). Conclusions from this study are:

a) The development of this paleotempestology database was necessary and represents an essential tool for the advancement of the field. Although this database remains in its infancy and may suffer from spatial and temporal gaps (Oliva et al., 2017), this study shows emerging trends both in time and space spanning the past 8,000 years. The new paleotempestology database is housed in the National Oceanographic and Atmospheric Association's (NOAA) Paleoclimatology World Data Center (WDC) archives and is readily available for researchers for free download (https://www.ncdc.noaa.gov/paleo/study/21391).

b) Our results provide evidence for shifts in the Bermuda High pressure system as having had an impact on TC tracks, by guiding TCs into the Gulf of Mexico when the Bermuda High pressure system is in its southwestern position and allowing TCs to more easily move northwards when the high pressure system is in its northeastern position, at least on millennial to centennial timescales. Our results also support the conclusion of Liu and Fearn (2000) that a shift northeast occurred, or at least started at ~1000 cal yr BP using two different approaches.

c) Our findings show an active period starting at ~900 cal yr BP (Liu, 2004), at the onset of the MCA (Mann et al., 2009), leading us to believe that variations in total TC strikes can be due to multi-centennial climate variability (e.g. LIA, MCA).

d) Transition periods between the SW/NE positions of the Bermuda High are represented by similar numbers of TC strikes along both coasts (e.g. ~1000 to ~1800 cal yr BP). This leads to the interpretation that transitional periods or a more central position of the Bermuda High leads to non-preferential distribution of tropical cyclones along the western North Atlantic coasts

Table 3.1 Table of 37 studies used for full subset analysis, including location and date range of archive (0 cal yr BP ≥ 1950).

Author	Publication year	Latitude	Longitude	cal yr BP min	cal yr BP max
Adomat and Gischler	2016	16.99	-88.28	840	7825
Aharon and Lambert	2009	30.26	-87.66	295	795
Boldt et al.	2010	41.65	-70.79	191	1865
Brandon et al.	2013	30.10	-84.34	1	2012
Brandon et al.	2014	40.52	-74.19	60	175
Brown et al.	2014	20.10	-87.57	0	7000
Buynevich and Donnelly	2006	41.57	-70.64	12	945
Buynevich et al.	2007	43.74	-69.79	136	1375
Cochran et al.	2009	14.65	-84.24	170	660
Das et al.	2013	30.32	-86.12	0	1000
Denommee et al.	2014	17.25	-87.57	0	1150
Donnelly and Woodruff	2007	18.09	-65.52	0	5054
Donnelly et al.	2001	39.19	-74.66	129	512
Donnelly et al.	2001	41.38	-71.52	135	543
Donnelly et al.	2004	39.41	-74.36	550	1250
Donnelly et al.	2015	41.54	-70.63	275	800
Ercolani et al.	2015	26.07	-81.79	500	500
Gischler et al.	2008	17.25	-87.57	165	1305
Hippensteel and Garcia	2014	34.52	-77.41	450	800
Kiage et al.	2011	31.89	-80.97	0	1100
Lambert et al.	2008	30.26	-87.66	0	490
Lane et al.	2011	29.93	-84.34	627	3755
Liu and Fearn	2000	30.32	-86.15	0	3200
Liu et al.	2008	30.26	-87.66	166	1060
Malaizé et al.	2011	18.13	-63.05	250	2680
McCloskey and Keller	2009	17.14	-88.30	2500	4500
McCloskey and Liu	2012	16.90	-88.29	200	6700
Nikitina et al.	2014	39.37	-74.89	25	1569
Peros et al.	2015	19.95	-76.54	250	1800
Scileppi and Donnelly	2007	40.60	-73.63	900	2800
Scott et al.	2003	33.76	-78.79	0	5667
Toomey et al.	2013	24.71	-79.24	0	3800
van Hengstum et al.	2014	25.70	-77.91	300	800
van Hengstum et al.	2016	26.79	-77.42	100	1000
Wallace and Anderson	2010	26.25	-97.20	940	2072
Williams	2013	29.79	-93.57	99	312
Woodruff et al.	2008	18.09	-65.52	0	2500

Table 3.2 Table of four studies used in restricted subset analysis, including location and date range of archive (0 cal yr BP ≥ 1950).

Author	Publication year	Latitude	Longitude	Location	cal yr BP min	cal yr BP max	Site sensitivity (category)
Donnelly et al.	2015	41.54	-70.63	Massachusetts, USA	0	2000	2
Liu and Fearn	2000	30.32	-86.15	Louisiana, USA	0	3200	4
McCloskey and Liu	2012	16.90	-88.29	Belize	0	6700	3
Scott et al.	2003	33.76	-78.79	South Carolina, USA	0	5667	3

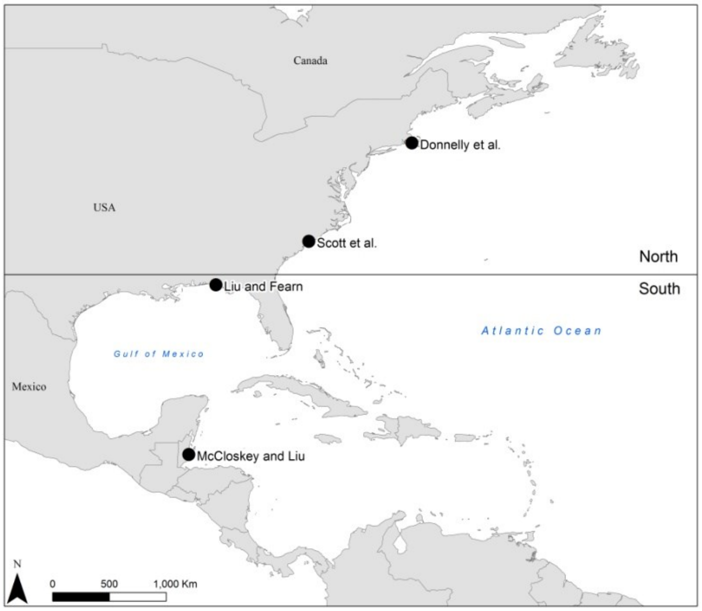

Figure 3.1 Location of four studies (restricted subset) used to test the Bermuda High Hypothesis.

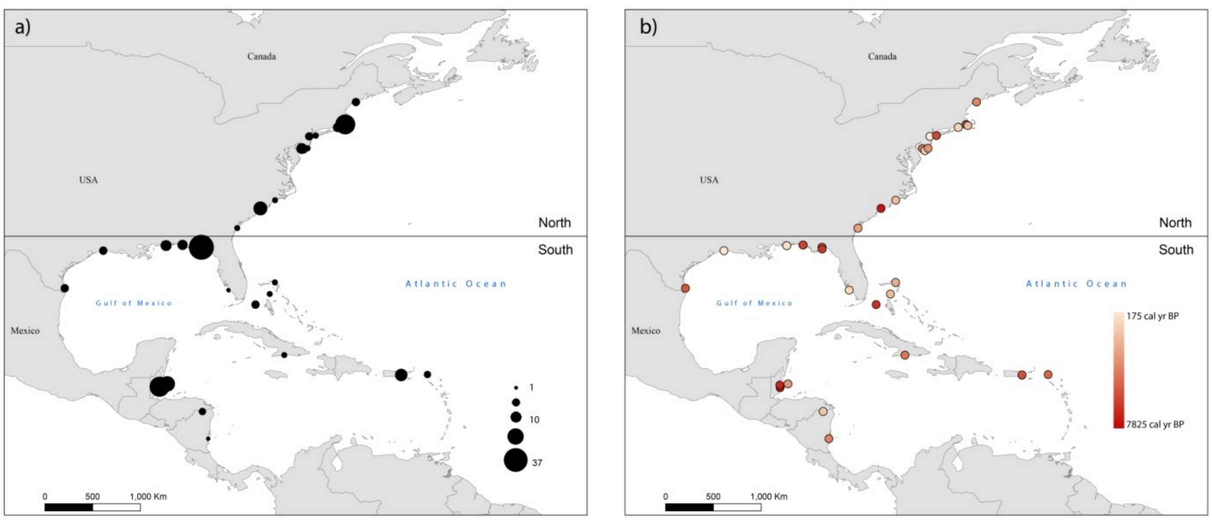

Figure 3.2 Map of hurricane strikes over the last ~8000 years with the North/South line used to separate the sites. a) Size of points corresponds to the relative number of detected strikes for that location, and b) The age of the archive where the darker the color, the older the record.

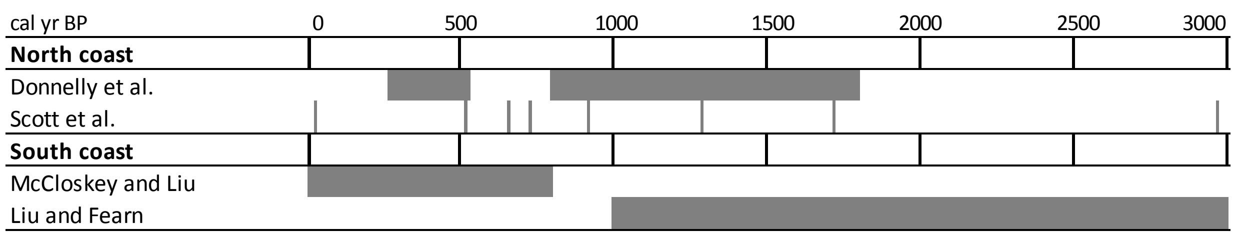

Figure 3.3 Reconstruction of periods of heightened TC activity from 0 to 3000 cal yr BP from subset of four studies. The grey bars indicate periods of heightened TC activity.

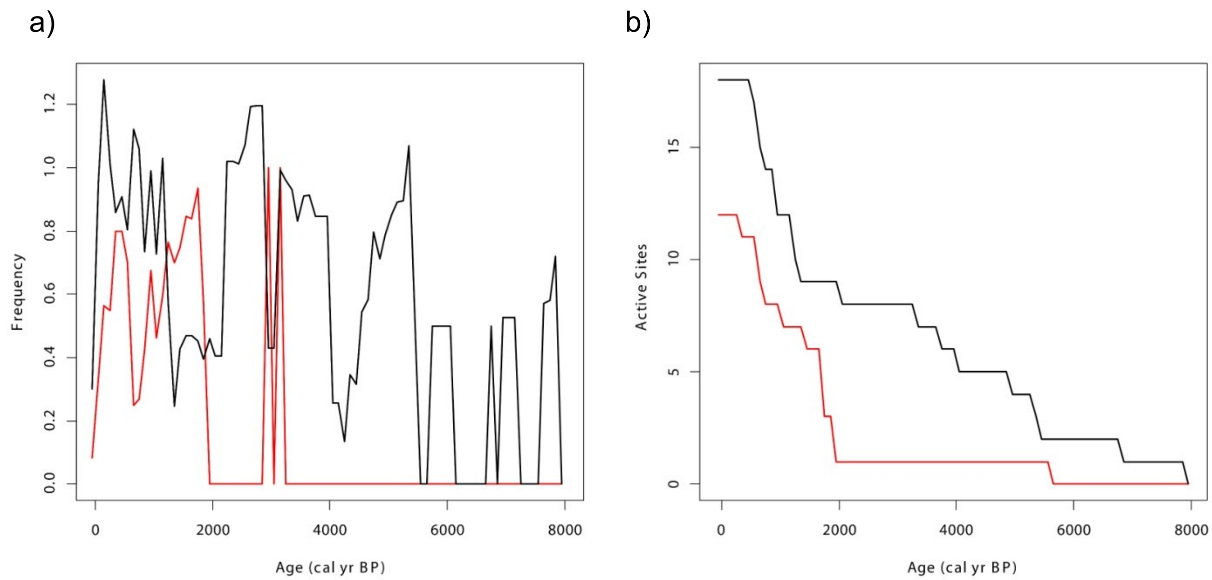

Figure 3.4 a) Frequency of hurricane strikes per 100 years, and b) total number of studies used for that bin per region over the last 8000 years. The red line represents the North coast (> 31.5°N) and black line the South coast (< 31.5°N).

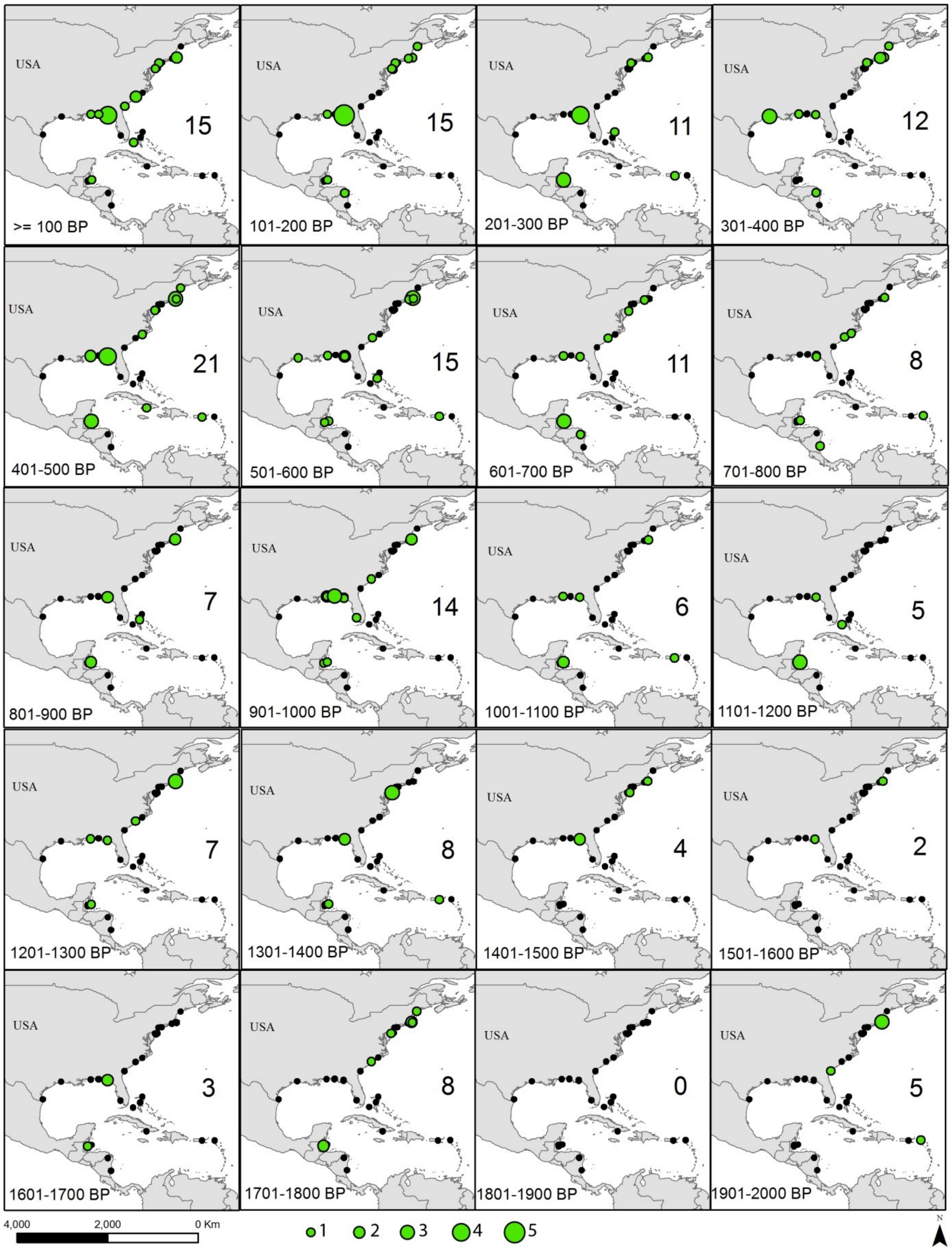

Figure 3.5 Number of TC strikes in the full subset analysis per study per 100 year intervals from the present to 2000 cal yr BP. The size of the green points indicates the number of strikes for that time interval as identified in the legend. The integer value in each frame represents the total number of TC strikes in that time interval for all sites. The black points represent sites with no reconstructed strikes.

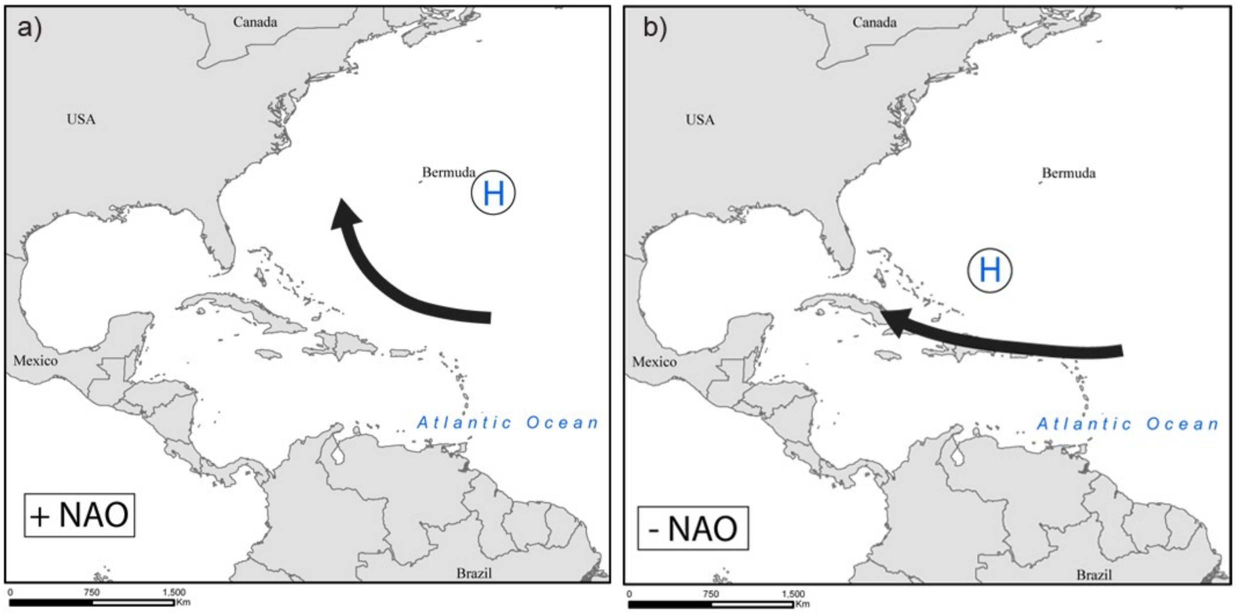

Figure 3.6 Movement of tropical cyclones around the oscillating mid-Atlantic Bermuda High pressure system: a) the Bermuda High pressure system in its most north-easterly position when it is associated with a positive NAO and b), in its most south-westerly position when it is associated with a weak or negative NAO (Liu, 2004).

Figure 3.7 TC activity along the North (> 31.5°N; Blue) and South (< 31.5°; Red) coasts over the last 3000 years. Lines are frequency from full subset analysis (37 studies). Shaded areas represent heightened TC activity from restricted subset analysis for both regions, North (> 31.5°N; Blue) and South (< 31.5°; Red).

Chapter 4 – X-Ray Fluorescence for Inference of Tropical Cyclone Activity in the Western North Atlantic Basin

4.1 Abstract

This study presents a multi-proxy reconstruction of tropical cyclone (TC) activity for the past 800 years from Nova Scotia, Canada. Two sediment cores were extracted from a small lake on the Atlantic coast of the province and were dated by ^{210}Pb and ^{14}C, and analyzed for organic matter content, benthic foraminifera and thecamoebians, sediment grain size, and a range of elements and elemental ratios determined by XRF core scanning. Our results show that peaks in grain size, which we interpret to represent overwash by TC wave activity and storm surges, are generally correlated with abrupt increases in Br, Br/Cl, and Br/Ti. XRF-derived Br measurements on sediment cores are an indicator of marine organic carbon (MOC), and the increases in Br (and its associated ratios) likely reflect incursions of marine water and nutrients into the pond due to TC storm surges. Based on the results, we identify two periods of low TC activity: one from ~1150 to 1475 and the other from 1670 to the present, with the intervening period from ~1475 to 1670 CE, a time of more frequent and possibly higher magnitude TC activity. Our findings are consistent with similar recent research from Salt Pond, Massachusetts, which shows a similar pattern of TC activity. Our work also extends the paleotempestological record in the North Atlantic to higher latitudes, permitting hypotheses concerning variability in TC activity to be more accurately tested, and it provides data that may help inform us about how TC activity in Atlantic Canada will change.

This chapter has been submitted for publication as: *Oliva F., Viau A., Peros M., Reinhardt EG., Nixon CF., Morin A. (submitted) A high-resolution multi-proxy reconstruction of tropical cyclone variability during the past 800 years from Nova Scotia, Canada.* Marine Geology.

4.2 Introduction

North Atlantic tropical cyclones (TCs), also known as hurricanes, and their associated winds and storm surges, have resulted in major impacts on coastal ecosystems and human infrastructure (Emanuel, 2003). Continuous and reliable instrumental data, which extends back at most ~70 years, and historical data, which can go back hundreds of years but is often incomplete (Liu 2013), do not provide the long-term perspective necessary for reconstructing past and modelling future trends in TC activity (Toomey et al., 2013). For example, Mann et al. (2009) suggested that there may have been enhanced TC activity during the Medieval Climate Anomaly (MCA, 900-1200 CE) in the North Atlantic, which could be an analogue for future warming expected for this region (Rhein et al., 2013), but long-term paleotempestological reconstructions to test this idea are rare.

A range of physical environments have been used to reconstruct past TC activity. These environments, which must preserve sediments and generally be positioned facing the ocean, include lagoons (e.g. Peros et al., 2015) and coastal fresh-water lakes (e.g. Liu and Fearn, 1993). In this study, we present an 800-year, high-resolution record of TC activity from a lagoon on the Atlantic coast of central Nova Scotia, Canada. The Canadian Maritimes have been the focus of limited paleotempestological research (e.g. Scott and Medioli, 1980), despite there being regularly affected by TC activity (Hurricane Juan, for example, was responsible for billions of dollars of damage when it struck the coast of Nova Scotia in September 2003)(McTaggart-Cowan et al. 2006). Our work therefore adds important new data to a region close to the north-western limit of North Atlantic TCs. Indeed, by increasing the spatial coverage of paleotempestological studies to understudied regions (Oliva et al., 2017), we may be able to better examine how large-scale climatic events, such as the West African Monsoon, the El Niño–Southern Oscillation (ENSO), and the position of the Bermuda High, influence TC activity over multiple timescales (Toomey et al., 2013; Liu and Fearn, 2000).

Various field techniques and laboratory analyses have been used in paleotempestological research (Oliva et al., 2017). The most widely used approach includes established laboratory analyses such as sediment grain-size and organic matter content, and analyses of micropaleontological indicators sampled from sediment cores extracted from coastal settings (e.g. Liu and Fearn, 1993, 2000; Donnelly et al., 2001a, 2001b, 2004; Scott et al., 2003; Buynevich and Donnelly, 2006; Hippensteel, 2008; Liu et al., 2008, 2011; Williams, 2009, 2010, 2013; Kiage et al., 2011; Lane et al., 2011; McCloskey and Liu, 2012; Hippensteel et al., 2013; van Hengstum et al., 2014; Peros et al., 2015). Other more recent approaches include: 1) multi-proxy analyses of deep-sea cores (Toomey et al., 2013); 2) X-ray fluorescence (XRF) and geochemical analyses of sediments (Woodruff et al., 2008, Brandon et al., 2014); and 3), tree cellulose and speleothem isotopic analyses (Miller et al., 2006; Frappier et al., 2007). Over the last two decades, X-ray fluorescence (XRF) core scanners have become increasingly utilized in paleoenvironmental research. Originally used to identify the elemental composition of marine cores, XRF core scanning is increasingly used on lake and terrestrial sediments (Rothwell and Croudace 2015). The latest XRF core scanners, such as the Cox Analytical Systems ITRAX, are capable of sub-mm resolution (µ-XRF) (Oliva et al., 2017; Rothwell and Croudace, 2015). Elemental proxy data can provide high-resolution time series useful for the study of variations in chemistry, mineralogy, and biological primary productivity, which may ultimately be linked to climatic and environmental change (Croudace et al., 2006). The most commonly used elements used in paleoenvironmental reconstructions include bromine (Br), calcium (Ca), iron (Fe), strontium (Sr), potassium (K) and titanium (Ti), as well as ratios calculated from these elements (Rothwell and Croudace, 2015).

A relatively large body of paleotempestological research has now been conducted along the north shore of the Gulf of Mexico and the eastern seaboard of the United States (Oliva et al., 2017), but little is known about past TC activity north of New England. In this study we use a multiproxy approach (XRF core scanning, grain-size, loss on ignition, and micropaleontological data) to study a small oligohaline lake (Robinson Lake) on the western seaward edge of Chezzetcook Inlet for the purpose of reconstructing past TC activity for this region. Robinson Lake was chosen due to its proximity to the ocean and because of the presence of a stable barrier, which is important to ensure marine incursions are rare. Conducting research in Nova Scotia contributes to filling important geographical data gaps in the coverage of paleotempestological data and helps us understand past TC dynamics at the northern margin of the Atlantic hurricane zone (Oliva et al., 2017).

4.3 Study Site

In selecting our field site, it was of primary importance to locate a coastal lake known to be affected by TCs. Robinson Lake was hit directly by Hurricane Juan on September 29th, 2003 (NOAA, 2017) and local residents confirmed that the barrier had been breached during that event (personal communication, John Donahue, 2014). The second criterion was that, under normal and average conditions, the lake water is fresh or low-salinity (as opposed to marine). Robinson Lake was tested in several locations and found to have an average salinity of < 5‰, classifying it as oligohaline. Next, the study site needed to be non-tidal, confirming its separation from the marine system. Finally, a stable barrier, elevated high enough above mean sea level, was required to ensure that the lake was not getting regularly breached during normal high tides or storms.

Located at the northern edge of modern tropical cyclone paths, Robinson Lake is located at sea-level at 44°39.114’N 63°16.631’W, on the western margin of the mouth of Chezzetcook Inlet (Figure 4.1). Chezzetcook Inlet has been previously studied by groups led by Dr. David Scott and the late Dr. Franco Medioli at Dalhousie University, for micropaleontology (e.g. Scott and Medioli, 1980), sea-level change (e.g. Gehrels et al., 2005), as well as salt marsh evolution (Chague-Goff et al., 2001). Chezzetcook Inlet is a shallow estuarine environment with extensive networks of intertidal mudflats and salt marshes (Scott, 1977). The inlet formed ~4000 yr BP as a result of relative sea-level rise due mainly to the ongoing glacioisostatic adjustment of Nova Scotia (i.e., crustal subsidence; Scott et al., 1995) along with a forebulge going through the area ~1700 yr BP (Laidler & Scott, 1996). European settlement began around 200 years ago in this area; that, and modern infrastructure development in the recent past, has contributed to changes in sedimentation rates at the head of the inlet (Scott, 1980). Relative sea level was ~1 m lower 1000 years ago in Chezzetcook Inlet (Gehrels et al., 2005; Scott et al., 1995), but we do not believe this would have been sufficient to affect our results as storm surges accompanying TCs would still have impacted Robinson Lake in the early part of our record.

Robinson Lake (Figure 4.1) is separated from the Atlantic Ocean at the southern edge by a natural barrier that was reinforced by a causeway after Hurricane Juan in 2003 (Figure 4.1b), and at the northern end by a salt marsh leading into Three Fathom Harbour (Figure 4.1c). At the northern end, the salt marsh is presently ~1 m above sea-level and eye-witness accounts (personal communication, John Donahue, 2014) suggest it has been inundated during past major events (e.g., Hurricane Juan in 2003). This indicates that the entry of marine water and sediment into Robinson Lake can potentially occur overtop the southern barrier, and also via the salt marsh to the north. Robinson Lake is shallow (~2m), with a thick layer of submerged aquatic grasses. The vegetation surrounding Robinson Lake consists of dense stands of black spruce (*Picea mariana*). Many of the trees in these stands are dead, apparently due to the effects (e.g., wind-throw, soil salinization) of Hurricane Juan. Geologically, Robinson Lake is underlain by slate, greywacke and quartzite bedrock (McBride, 1978), but many of the surface features were formed during the most recent glacial period, and include drumlins, moraines, and other glacial depositional landforms (Scott, 1977).

4.4 Methods

4.4.1 Field work

The field work, which was undertaken in fall 2014, consisted of coring Robinson Lake using a Livingstone piston corer and a hollow tube fitted with a piston. Two cores were extracted: RL01, near the causeway in the center of the lake; and RL02, ~40m further inland (Figure 4.1a). Cores were taken at both locations to refusal from a customized platform. The hollow tube and piston were used to collect the water-sediment interface intact while each subsequent drive with the Livingstone piston corer was done approximately 1 m from each other with approximately 30 cm of overlap to ensure continuity. The water-sediment interface cores were extruded vertically near the field site directly into labeled bags at continuous 1 cm intervals. All cores and sediment samples were wrapped in plastic and aluminum foil and placed in split ABS tubes for transportation and then refrigerated at 4°C for preservation. Water chemistry, which included salinity, pH, dissolved oxygen, conductivity, total dissolved solids, and temperature, was recorded using a YSI Multiparameter meter at 3 different locations and at different depths to ensure that water chemistry was characterized throughout Robinson Lake.

4.4.2 Laboratory analyses

The sediment cores were subsampled at continuous 1 cm intervals for grain-size analysis using a Microtrac S3500 laser particle size analyzer (lpsa). Pre-treatment of the samples included using 30 % hydrogen peroxide (H_2O_2) to eliminate organic matter and also sodium hexametaphosphate $(NaPO_3)_6$ to disperse the sediment. Organic matter and non-organic carbonate values were established using LOI (Heiri et al., 2001), by burning the dried samples at 550°C and 950°C respectively and calculating the difference in mass. Core drives from site RL01 (1000 µm intervals) and RL02 (400 µm intervals) were scanned for elemental composition by XRF using an ITRAX Cox Core scanner at McMaster University's core laboratory. All drives were also scanned at 400µm intervals for density by x-radiography. The unconsolidated materials comprising the top 5 cm of core RL01 and the top 15 cm of core RL02 were used for establishing a chronology by lead-210 dating, and were not scanned by XRF due to their heterogeneous textures and water content. The lake's foraminiferal assemblages and thecamoebians were identified and summed at every 5cm from core RL02.

4.4.3 Chronology

The chronology was established using lead-210 (^{210}Pb) and radiocarbon (^{14}C) dating. Lead-210 was used for high-resolution dating of the upper portion of the cores and to establish a modern sedimentation rate, while radiocarbon dating was used to establish the older chronological sequence. The lead-210 analyses were performed at the Geotop laboratory in Montréal, Canada. The lead-210 chronology was built using the constant rate supply (CRS) method, which assumes a varying accumulation rate which is what would be expected at a site with slow lacustrine sedimentation interrupted by episodes of rapid accumulation due to marine intrusions following a TC or major storm (Ghaleb, 2009). Radiocarbon dating was performed at the University of Ottawa's André Lalonde AMS (accelerator mass spectrometry) Laboratory. Autochthonous organic detritus and freshwater shells were used to date the cores and the results were calibrated using the IntCal13 dataset (Reimer et al., 2013). Age-depth models were generated using a Bayesian model in BACON (Blaauw and Christen, 2011).

4.5 Results

4.5.1 Core lithology and micropaleontology

Core RL01 is 112 cm in length and consists almost entirely of fine-grained mud, with an average grain-size ranging between 12 to 48 µm, and one peak of very-fine sand at ~70 cm depth (110 µm; Figure 4.2a). Organic matter content is less than 25% throughout (Figure 2a; LOI550). Core RL02 is 101 cm long and is silt-rich with an average grain size ranging from 12 to 48 µm (Figure 4.2b; GS). The organic matter content in RL02 ranges from ~2 to 44% (Figure 2b; LOI550) and varies along the core. Optical images from both cores (Figure 4.2) are similar, with darker material and a more pronouced stratigraphy near the top of the cores and lighter, more compact sediment, near the center. Visual inspection of the high-resolution optical imaging and x-radiography reveals sedimentary structures in both cores. Both cores have darker, finer sediment at the top and base, with a clear transition to greyish, coarser sediments starting at ~35 cm depth at RL01 and ~37 cm depth at RL02, and continuing to deeper levels (Figure 4.2). The entire lengths of both cores have fine, well-defined laminations, which is a strong indication that there is little to no vertical mixing. There is no evidence for a depositional hiatus in either core.

The micropaleontological results (not plotted) for core RL02 show that it is dominated by benthic foraminifera such as *Trochammina* spp., a typical high-marsh environment foraminifer which occurs throughout the entirety of the core, along with the thecamoebians *Centropyxis aculeata* and *Centropyxis constricta*. More marine species of thecamoebians were also found throughout the core, and are known to dominate coastal lakes because of their tolerance for salt spray and are often present in lakes that have transitioned from marine to freshwater conditions (Scott et al., 2001). The very deepest part of the core contains a higher (> 6/cc) abundance of foraminifera and a variety of species (*Trochammina* spp., *Miliammina* spp. and *Quinqueloculina*) and is devoid of thecamoebians, indicating a potential marker for the first full separation of Robinson Lake from the Atlantic.

4.5.2 Chronology

The recent chronology of both cores varies past ~5 cm of depth according to the lead-210 dating results (Table 4.1; raw counts: Appendix 2). The average modern accumulation rate of RL01 is 0.09 cm/year, while the average modern accumulation rate of RL02 is 0.13 cm/year.

Radiocarbon dating on cores RL01 and RL02 shows an average accumulation rate of 0.13 cm/year and 0.10 cm/year, respectively. Age-depth models developed with the radiocarbon dates and lead-210 results are shown in Figure 4.4. One date from core RL02 (Table 4.2; UOC-2053) was left out of the age-depth model due to probable contamination error. The accumulation rates vary between the cores, with core RL01 showing an inflexion at 25-35 cm depth, and core RL02 showing a more linear trend (Figure 4.3). In both cases, the age-depth models indicate that sedimentation began at or just after 800 cal yr BP (~1150 CE).

4.5.3 XRF elemental composition

The XRF results produced information on over 50 elements but here we plot: a) some of the most abundant elements; and b) those elements that may be important for TC detection. A complete plot of all XRF data can be found in Supplementary Information.

In core RL01 (Figure 4.2a), there is high activity in Ti, Sr, Fe, and Cl in the top 25 cm. Peaks and dips in Si, Ti, Fe, and Sr all correlate while variations in Cl are inversely related to these elements. Bromine (Br) does not appear to fluctuate until 32 cm depth. There is a relatively large peak in Si and Ti that correlates at 54.7 cm depth, and also coincides with a decrease in Br and

Cl. Another peak in Si is present at 101.5 cm depth, which matches an increase in Ti and an overall decrease in Br. Iron (Fe) also fluctuates but appears to follow a similar pattern to that of Ti and Si. Overall, Br and Cl show different patterns compared to Si, Ti, Fe, Ca, and Sr; Br exhibits very low and stable values from 70 to 110 cm and from 5 to 32 cm, and higher background levels and numerous peaks between 32 and 70 cm. Chlorine generally mirrors the organic matter content (as measured by loss on ignition), and gradually increases toward the top. The peaks in mean grain size are not closely reflected in any of the elements but generally coincide with the high Br values in the central portion of the core.

In core RL02 (Figure 4.2b), the XRF results are similar, and show values that generally correlate between Si, Ti, and Fe (with higher values in these elements apparent between 38 and 72 cm). Calcium (Ca) and Sr correlate as well, and show generally decreasing values upcore. Bromine (Br) and Cl show patterns that are broadly similar to that of core RL01, with high values of Br between 44 and 66 cm and increasing values of Cl towards the surface. At a more detailed level, there is one Si peak and one Ti peak that occurs 66.2 cm depth, which also coincides with a dip in Br. Another peak in Si is present at 98.3 cm depth, coincident with an increase in Ti and Sr and an overall decrease in Br. As in core RL01, Br generally mirrors the mean grain-size results, with higher values in this element between 40 and 67 cm depth. However, Si and Ti also parallel the grain size results in core RL02, with higher values in the central portion of the core.

A Principal Components Analysis (PCA) was undertaken to further analyze relationships between the elemental XRF data and other variables (e.g., mean grain size and LOI) (Figure 4.4) (Rothwell and Croudace, 2015). Biplots of PCA scores for both cores show strong positive correlations between Si and Ti, and a strong negative correlation with organic matter content (LOI550), consistent with the visual inspection of these data (Figure 4.2). For core RL01, grain size (GS) shows a low correlation with Si, Ti, and organic matter, whereas there is a weak positive relationship between Si, Ti and grain size in RL02. In core RL01, Br is negatively correlated with grain size and somewhat positively correlated with it in RL02. In RL01, Br is not correlated with Si, Ti, or Sr, but varies positively with these elements in RL02. In both cores, Cl shows a positive relationship with organic matter and an inverse relationship with grain-size, possibly due to the fact that Cl, as a strong oxidizing agent, has an ability to bind with organic matter (Greenwood and Earnshaw, 1997). For the most part, the PCA results are similar between cores, although the relationships that Br has with various elements (e.g., Si, Ti, Sr) and grain size differs between cores RL01 and RL02.

4.5.4 XRF ratios

A number of elemental ratios were also calculated to better understand the environmental history of Robinson Lake and reconstruct TC activity in the region. Because of the high variability in Br and the similarities in it between cores (Figure 4.2), we calculated ratios involving Br, specifically Br/Cl and Br/Ti (Figure 4.5). XRF-measured sedimentary Br and Br/Cl values have been interpreted to be a reliable indicator of marine organic carbon (MOC)(Ziegler et al. 2008; Cartapanis et al., 2014). We also calculated Br/Ti to estimate the relative contribution of marine versus terrigenous input into Robinson Lake (Ziegler et al., 2008; Haug et al., 2001; Gregory et al., 2015). In both cases (Br/Cl and Br/Ti), we assumed that the presence of high values of Br represent marine incursions caused by TC storm surges and wave activity. In addition to ratios of Br, we also calculated more established elemental ratios, such as Ti/Ca and Fe/Ca, which are often used in marginal-marine and marine environments as an indicator of terrestrial input (i.e., precipitation induced runoff)(Gregory et al., 2015). The premise behind the use of these indicators in our study is that they could represent TC-driven precipitation events or variations due to long-term climate change.

Elemental ratios are plotted alongside mean grain size in Figure 4.5. The results show similarities between both cores: Ti/Ca and Fe/Ca are both highly correlated within cores RL01 and RL02, and show gradually increasing values towards the present in both cores, possibly indicative of enhanced runoff in the area over the last 800 years. No peaks in sediment grain size appear to correlate with changes in Ti/Ca or Fe/Ca in either core (with the exception of one peak in grain size at ~52 cm in core RL01 that is concurrent with a drop in Ti/Ca and Fe/Ca), indicating that sedimentation due to TC-induced precipitation was limited. The results for Br/Cl and Br/Ti are considerably different, however, with activity in these ratios common between 35 and 72 cm, where large increases in grain size are also common in both cores (see grey bar, Figure 4.5). Very little activity in recorded in Br/Cl or Br/Ti below this zone; above this zone, only Br/Ti shows any variation, mostly in core RL01. The concurrence of relatively coarse-grained sediments, in conjunction with elevated Br levels, likely represents a period of frequent marine incursion into Robinson Lake.

4.5.5 Tropical cyclone detection and attribution

The grain-size variation in both cores is likely an indicator of fine, “background” sediment being overlain by coarser material, likely deposited during episodes of rapid sediment transfer (Toomey et al., 2013). To attribute environmental proxy changes to TC activity, we matched peaks in mean grain size, Br, and Br/Ti from core RL01 to known historical TCs for the last 150 years (Figure 4.6a). Several peaks in these proxies correlate with historically recorded TCs (Table 4.3) that made landfall within 50 km of the study site (Figure 4.6b). Specifically, the Br/Ti record shows a large peak around 1991 which may be attributable to the “Perfect Storm” of 1991, a mid-latitude storm which absorbed Hurricane Grace and then struck the coast of Nova Scotia as a Tropical Storm in early November of that year. In addition, peaks in Br and Br/Ti date to around 1933, when the Outer Banks Hurricane struck the coast of Nova Scotia as an extratropical cyclone. Finally, a peak in mean grain size dates to 1857 (with a 2-sigma age range of 1841 to 1870 CE), and may be associated with an unnamed tropical cyclone that came within the vicinity of the coast in 1863. A number of other lower magnitude extra-tropical cyclones have struck the coast over the last 150 years (Table 4.3), but none seem to be registered in any of our proxy data, indicating that the site and our proxies are sensitive to only high-magnitude events with sufficient wave energy and storm surge to transport sediment and MOC into Robinson Lake.

The differences between grain size and Br and Br/Ti may relate to the specific characteristics of each TC event, as they pertain to storm surge height, wave activity, and flooding. For example, in the case of the 1933 Outer Banks Hurricane, the fact that this is recorded in the Br record suggests that its main impact at Robinson Pond was flooding (possibly across the salt marsh to the north), which delivered MOC into the pond, but that wave activity offshore was not sufficiently strong to deliver coarse-grained sediment into the basin at the location of core RL01. Likewise, the 1863 TC resulted in the transport of coarse-grained sediment into Robinson Lake, but the input of MOC was relatively limited, indicating that large-scale flooding did not accompany this event. Moreover, changes in pore-water density and organic matter content at the top of core RL01 may also account for some of the variability in Br and Ti concentrations, as XRF-derived elemental data can be sensitive to these and other factors (Rothwell and Croudace, 2015). Additional work will be necessary to better understand the sensitivities of these proxies to TC activity and why certain storm events are recorded in the sedimentary record while other are not. Nevertheless, our results indicate that grain size, and elemental Br and ratios based on it, do record high magnitude TC events at this site, and that our 800-year sedimentary record likely contains a fairly complete record of high magnitude TC activity, with low magnitude events being under-represented or missing.

4.6 Discussion

4.6.1 High resolution TC reconstruction

Inferring marine intrusions and overwash resulting from TC activity using high-resolution (e.g. sub-millimetre scale) analyses such as XRF core scanning may help better identify individual TC events, especially at sites with low sedimentation rates. This provides a potential advantage over other lower resolution (e.g. centimetre scale) reconstructions which yield multi-year or even decadal-scale data (Oliva et al., 2017) based solely on grain-size or organic matter (i.e., loss-on-ignition) analysis.

The grain size and Br results are plotted in Figure 4.7 as a function of age and show a number of events that represent past TC strikes. In both cores, the peaks in grain size are usually associated with peaks in Br, Br/Cl, and Br/Ti, indicating the overwash of marine sediment and input of marine organic carbon (MOC) into Robinson Lake. A closer inspection of the data shows an offset in the timing of these events between cores RL01 and RL02, with the RL01 data appearing older. The most likely explanation for this discrepancy is the age-depth model for core RL01 (Figure 4.3), which shows two dates (UOC-2047, 570 +/- 19 ^{14}C yr BP and UOC-1065, 343 +/- 52 ^{14}C yr BP) that, if removed, would generate a near-linear age-depth relationship, similar to that of RL02. Given that these dates were made on bulk organic detritus, the likelihood of a hard-water error that would produce an erroneously old age is high. Thus, we argue that core RL02 has the more reliable age-depth model, and use it as the basis for our overall chronology.

Both cores show evidence of TC strikes at approximately 1475 CE, 1530 CE, 1575 CE, with events also likely at 1240 CE and 1670 CE (in addition to the 1863, 1933, and 1991 CE events, as discussed above). This cluster of strikes (from approximately 1475 to 1670 CE) corresponds to a period of heightened TC activity inferred from grain size data from Salt Pond, Massachusetts (Donnelly et al., 2015), which occurs from ~1400 to 1675 CE. With both sites recoding similar patterns, we infer that the Canadian Maritime provinces and New England states, in the last 800 years, experienced a period of low TC frequency from ~1150 to 1400 CE, a period of high frequency from ~1400 to 1675 CE, and a period of low frequency from 1675 to the present. Indeed, the period from ~1475 to 1670 in the Chezzetcook area saw considerably more frequent TC activity than it does today.

The question of TC magnitude is difficult to resolve from sedimentary data, due to the fact that a "small" peak in grain size may represent a TC strike farther away, or with lower wind speed and wave action, than a lower magnitude event closer to the coring site (Brandon et al., 2014; Woodruff et al., 2008). The magnitude of the peaks in grain size and Br during the prehistoric period at Robinson Lake suggests that not only were TCs more frequent, but that they either were of higher magnitude, struck closer to the coast, or had particularly high storm surges and wave energies, compared to any event recorded in the last 150 years, with the possible exception of Hurricane Juan in 2003 (which our sedimentary record does not cover). Indeed, the pattern of higher magnitude peaks in this period is also seen at Salt Pond (Figure 4.7), where Donnelly et al. (2015) indicated that coarse-grained event beds dating from 1300 to 1700 CE point to TCs with intensities greater than any that occurred during historic times. Thus the data from Robinson Lake also points to not only higher-frequency, but also higher magnitude events between ~1475 to 1670 CE. One important difference between Salt Pond and Robinson Lake is the presence of the salt marsh behind the latter location; in the past a lower elevation of the marsh surface might have meant that marine incursion via the north was easier, which could account for higher peaks in indicators such as Br. However, the fact that sediment grain size is also high during the period from ~1475 to 1670 CE, and that coarse sediment is unlikely to be transported hundreds of meters across the salt marsh surface, indicates that the most likely explanation for these peaks is high magnitude TC activity.

4.6.2 Tropical cyclones and climate

The lack of evidence for TC activity from ~1150 to 1400 CE in Nova Scotia and Massachusetts suggests that climate conditions were unsuitable for the formation of high magnitude TCs, that they did not reach more northern latitudes, or that TC tracks at this time were such that they did not make landfall in this region. Warm sea-surface temperatures (SSTs) are one of the driving factors behind TC formation and trajectory (Tory & Frank, 2010). Relatively cool sea surface temperatures have been noted at this time for this region (Cronin et al., 2010; Keigwin, 1996;

Wanamaker et al., 2008; Donnelly et al., 2015), and these may have reduced TC intensity so that few to no events are recorded at these sites. The active period, from ~1400 to 1675 CE, is generally correlated with warmer SSTs (Cronin et al., 2010; Keigwin, 1996; Wanamaker et al., 2008), which consequently may have led to more intense TCs which were capable of transporting sediment and MOC into Robinson Lake. Finally, the decrease in TC activity from ~1675 to at least the middle of the 19th century may be indicative of the coldest period of the Little Ice Age, which would have brought cooler SSTs to the North Atlantic, again decreasing TC intensity at the northern limit of TC tracks. Despite this, it is important to note that TC activity is controlled by more than just SSTs, with vertical wind shear and other processes being important for their formation, duration, and direction, and future work should consider a greater range of climatological forcings to explain the data at Robinson Lake.

4.6.3 The use of XRF core scanning as a TC indicator

Finally, our work highlights the potential of XRF core scanning as a potential tool for paleotempestological research. Obvious advantages of XRF core scanning include the speed at which data can be generated and the temporal resolution that is possible, especially at sites of low sedimentation rate (Oliva et al., 2017). However, our main finding involves the use of Br (and ratios based on it) as an indicator of TC-transported MOC. In this regard, our work complements previous research by Das et al. (2013) who used organic geochemical proxies such as $\delta^{13}C$, $\delta^{15}N$, C%, N%, and C/N measured on sediment organic matter to infer shifts to marine-like conditions in coastal lakes based on input of marine water and nutrients. Further work should focus on better understanding how these geochemical proxies both complement, and provide different information than, established indictors such as grain size analysis (Oliva et al. 2017). In addition, the element zinc (Zn) has an inverse relationship to grain-size in cores RL01 and RL02 (Figure 4.8), consistent with the conclusion of Brandon et al. (2014), who showed that that Zn and other industry-derived heavy metals have particularly low concentrations during TC events, indicating that this is another potential indicator of TC activity. Finally, our results do not show a strong relationship between detrital elements, such as Ti, Si, and Fe, and TCs (Naquin et al., 2014), but at other sites increases in these elements may reflect sedimentation due to overland run-off, particularly during TCs with high rainfall or at sites with steep-sided basins.

4.6.4 Limitations

Limitations exist in critically assessing the downcore validation without matching results to well-known events (i.e. Hurricane Juan in 2003). Different sampling protocols will need to be tested and established, perhaps such as freeze cores, to allow for sub-sampling at the same resolution (i.e. sub-mm) of the unconsolidated material at the top of the core as the that of the XRF core scanning.

4.7 Conclusion

In this paper, we show that XRF core scanning is a powerful tool to complement traditional sedimentary analyses of TCs activity from a particular site. Our study presents such an analysis for the first time from the Maritime Provinces of Canada. Oliva et al. (2017) demonstrated the need for reconstructions from this region to reach further north on the eastern North American seaboard in order to provide data on the "northern margin" of the northern Atlantic TC zone. Our main findings are that:

a) TC activity was low between ~1150 to 1475 CE and 1670 to the present, and that the coast experienced more frequent and probably higher magnitude TC strikes between ~1475 and 1670 CE than it currently does, possibly as a result of higher sea surface temperatures during this interval;

b) These results are consistent with data from Salt Pond, Massachusetts, which shows a similar pattern of TC activity for the last 800 years;

c) XRF-derived Br values (and ratios of Br, such as Br/Cl and Br/Ti), may be useful indicators of TC activity;

d) XRF core scanning is a potentially powerful tool to complement other more established indicators, such as sediment grain size analysis, in paleotempestological research.

e) Future work should focus on better understanding the full potential and limitations of geochemical indicators of TC activity and also identifying other sites in the Canadian Maritimes that can provide better dated, longer, and higher-resolution records of past TC strikes. Such information is critical for helping us better understand how TC activity in the coming decades will affect eastern Canada.

Table 4.1 Modern ^{210}Pb chronology of cores RL01 and RL02 built with the CRS method.

	Year,CE)	
Depth,cm)	RL01	RL02
0.5	2012	2009
1.5	2009	2007
2.5	2006	2005
3.5	2000	2001
4.5	1993	1996
5.5	1986	1991
6.5	1980	1988
7.5	1969	1982
8.5	1951	1978
9.5	1931	1971
10.5	1902	1964
11.5	1891	1953
12.5	1866	1937
13.5		1913

Table 4.2 Radiocarbon dates for cores RL01 and RL02. *was not used in age modelling.

Core	Sample Id	Total depth,cm)	^{14}C yr BP	Material	Age,2σ calibrated calendar year A.D.) (IntCal13)
RL01	UOC-1065	32	343 - 52	Organic detritus	500-305
RL01	UOC-2049	38	570 - 19	Organic detritus	636-594(56%): 563-535 (39%)
RL01	UOC-1066	61	576 - 38	Organic detritus	652-527
RL01	UOC-2050	71	560 - 23	Shell	na
RL01	UOC-1067	84	734 - 45	Organic detritus	740-563
RL01	UOC-1064	106	820 - 62	Shell	901-563
RL02*	UOC-2053	42	525 - 20	Organic detritus	621-611 (4%): 554-513 (92%)
RL02	UOC-2052	57	273 - 22	Organic detritus	430-358 (50%): 330-287 (45%)
RL02	UOC-1736	73	577 - 62	Shell	na
RL02	UOC-1735	79	573 - 65	Organic detritus	661-513
RL02	UOC-2051	85	605 - 30	Organic detritus	654-544
RL02	UOC-1734	100	823 - 60	Organic detritus	907-847 (12%): 832-668 (83%)

Table 4.3 Instrument recorded tropical cyclones to make landfall within 50 km of study sites (*NOAA*, 2017).

Year	Strength at landfall	Month and day of landfall
1991	Tropical Storm	Nov-02
1943	Extra-Tropical Cyclone	Sep-15
1937	Extra-Tropical Cyclone	Sep-26
1933	Tropical Cyclone	Sep-18
1918	Extra-Tropical Cyclone	Sep-06
1900	Extra-Tropical Cyclone	Oct-29
1899	Extra-Tropical Cyclone	Oct-06
1896	Extra-Tropical Cyclone	Oct-14
1887	Extra-Tropical Cyclone	May-19
1879	Extra-Tropical Cyclone	Nov-20
1877	Extra-Tropical Cyclone	Nov-29
1871	Tropical Cyclone	Oct-12
1863	Tropical Cyclone	Aug-22

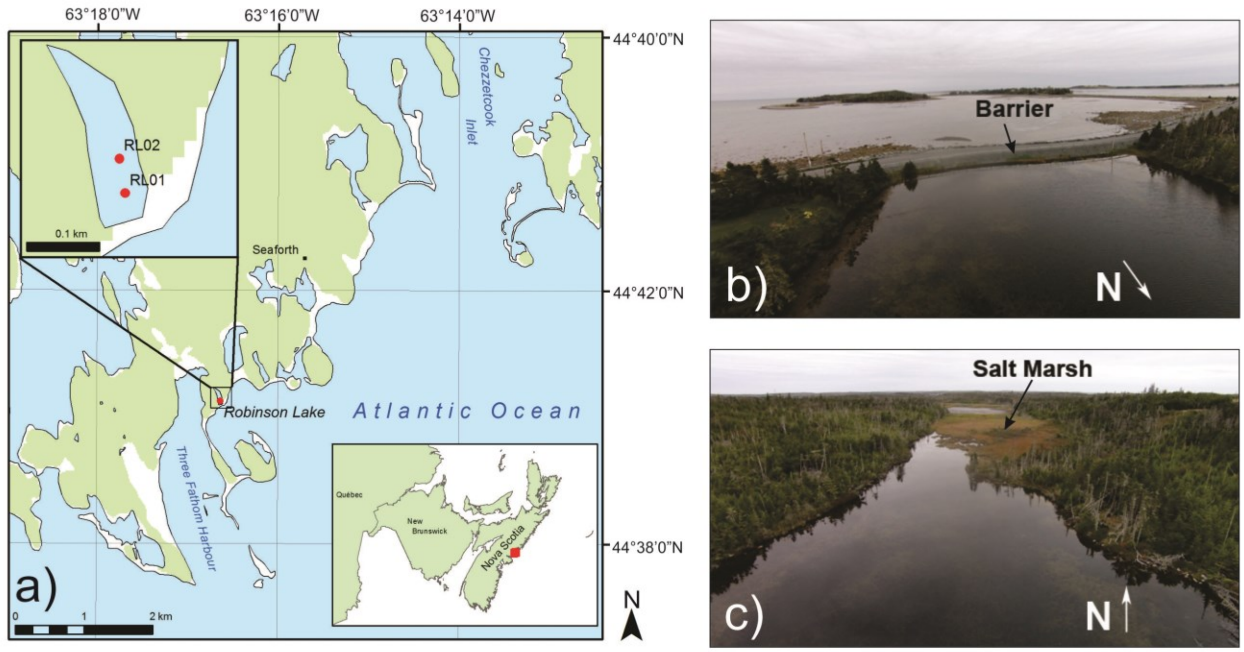

Figure 4.1 a) Location map of Robinson Lake in the Chezzetcook Inlet, Nova Scotia, Canada. Inset: Location of coring sites RL01 and RL02 in Robinson Lake. b) Photograph of the Robinson Lake barrier looking south towards the Atlantic Ocean; and c), Photograph looking north toward the salt marsh with the northern tip of Three Fathom Harbour at the very back of the image.

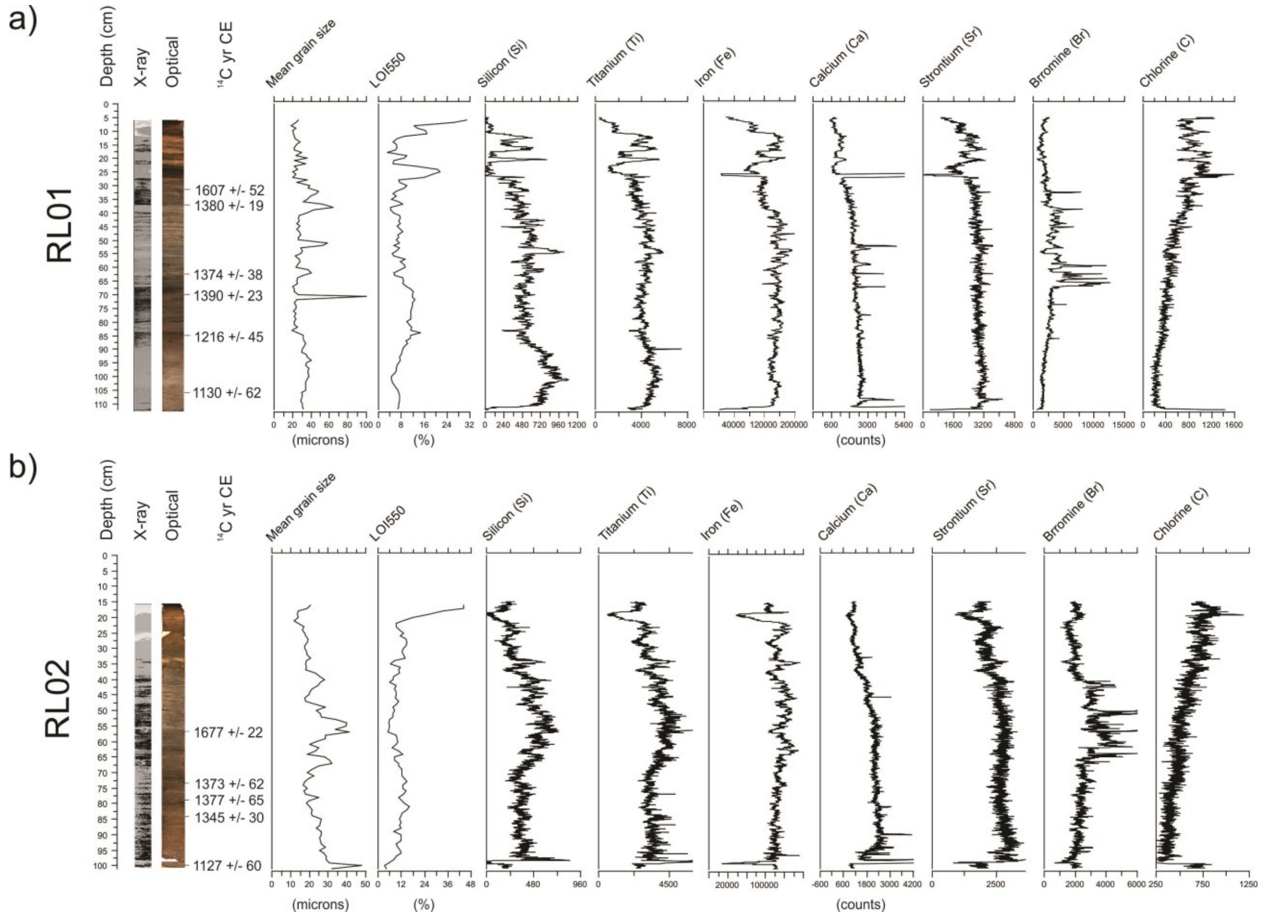

Figure 4.2 Plots of X-ray, optical imaging, uncalibrated 14C dates, and select proxy data from cores RL01 (a) and RL02 (b) by depth (cm). The proxy data for both cores includes mean grain-size (µm), organic matter content (%); LOI550, silicon (Si), titanium (Ti), iron (Fe), calcium (Ca), strontium (Sr), bromine (Br) and chlorine (Cl) based on the XRF core scanning in counts/s.

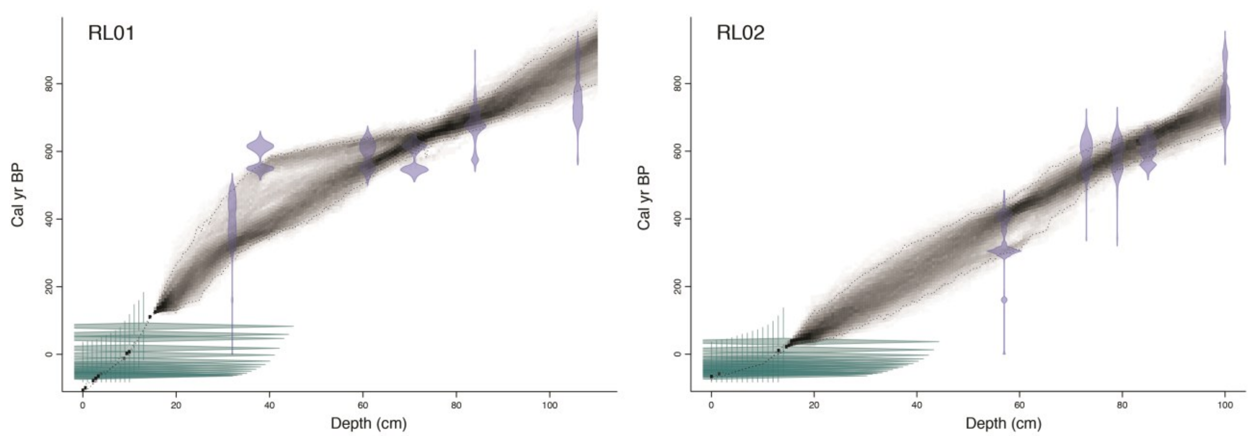

Figure 4.3 BACON age model in years (CE) using lead-210 (green) and calibrated radiocarbon dates (blue) for cores RL01 and RL02.

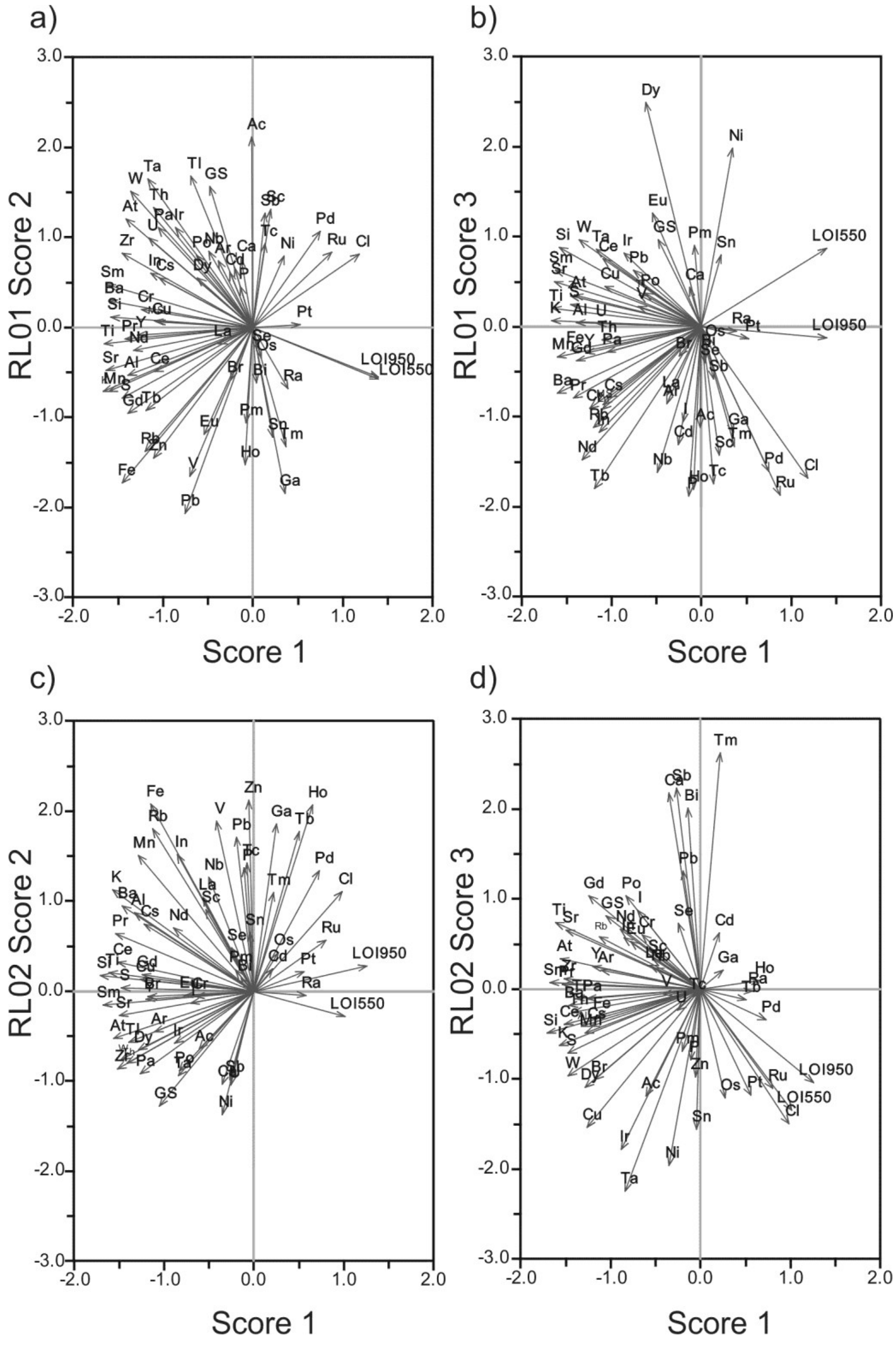

Figure 4.4 Principal component analysis (PCA) of all elements and mean grains size (GS) and loss on ignition data; a) Score 1 vs. 2 of RL01; b) Score 1 vs. 3 of RL01; c) Score 1 vs. 2 of RL02; d) Score 1 vs. 3 of RL02

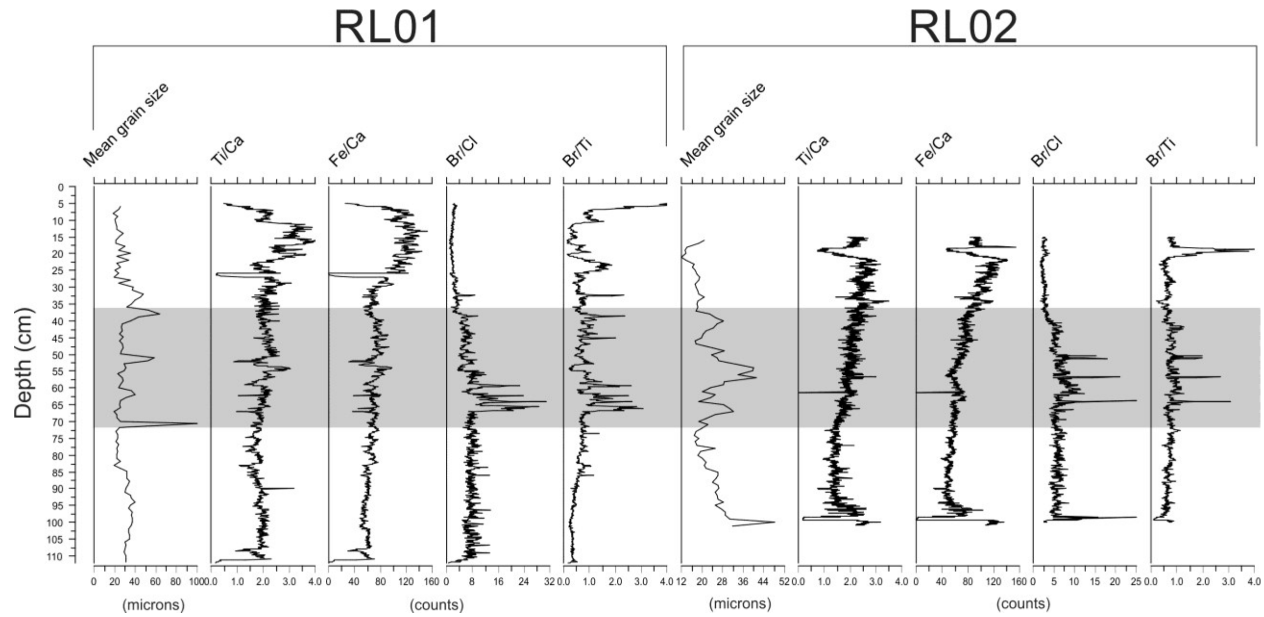

Figure 4.5 Mean grain-size (μm), Ti/Ca, Fe/Ca, Br/Cl and Br/Ti for cores RL01 (1000 μm resolution) and RL02 (400 μm resolution) plotted by depth. The grey bar represents a zone of heightened TC activity based on peaks in grain size, Br, Br/Cl, and Br/Ti.

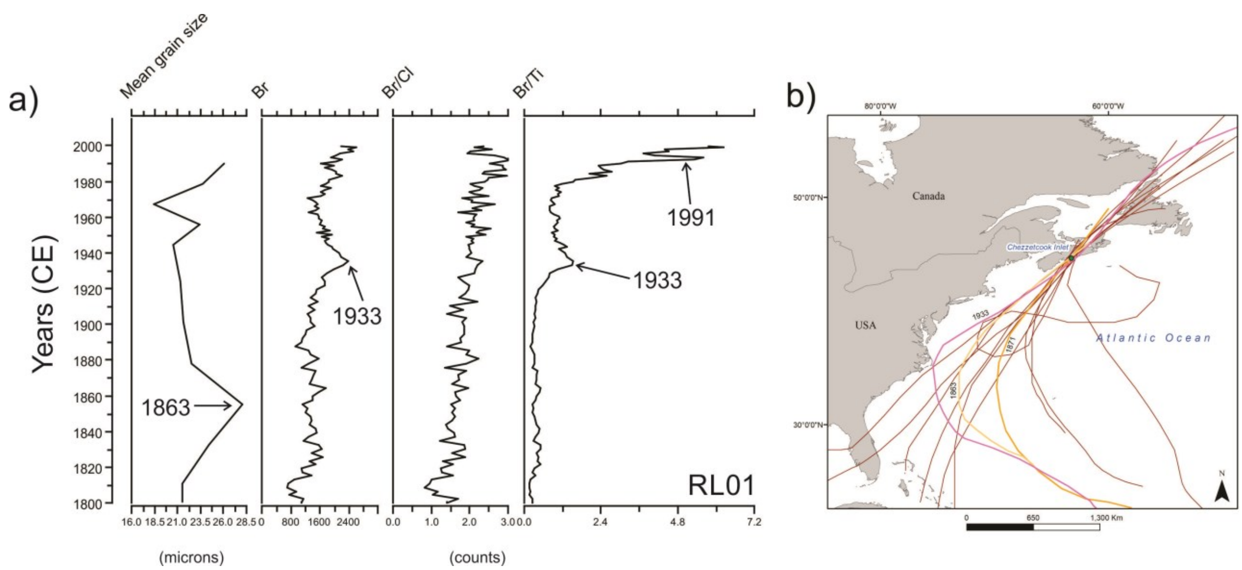

Figure 4.6 a) Mean grain size (μm), Br, and Br/Ti plotted by year CE peaks identified representing likely TC strikes in 1863, 1933, and 1991; b) map of TCs that made landfall within 50 km of Chezzetcook Inlet since 1863.,Track data: (NOAA, 2017).

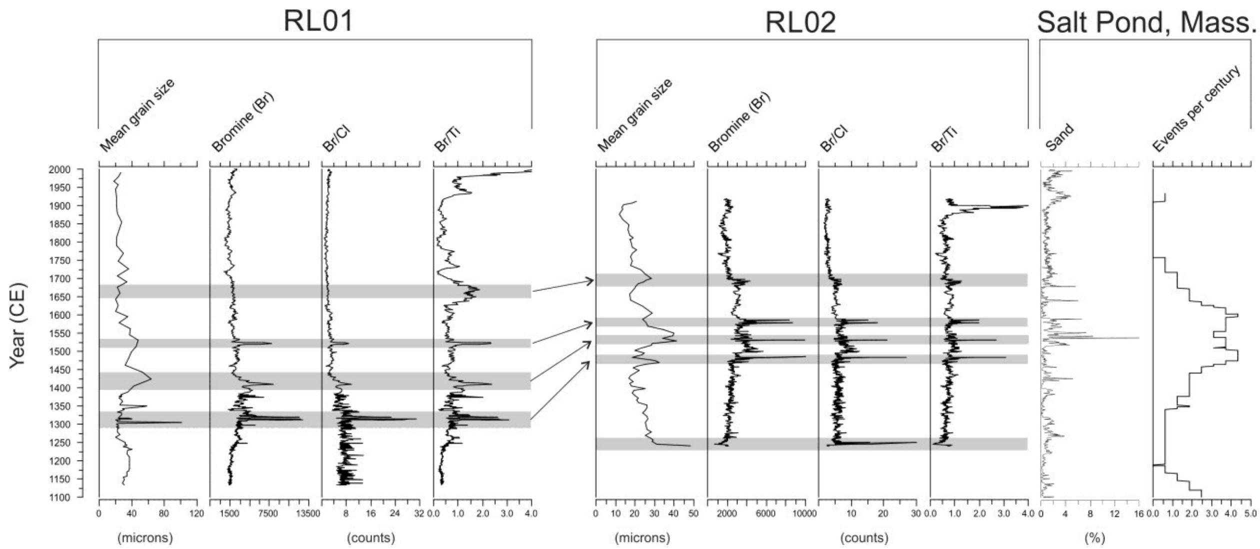

Figure 4.7 Grain-size (µm), Br, Br/Cl and Br/Ti for cores RL01 (1000 µm resolution) and RL02 (400 µm resolution). Percent sand and reconstructed TC events per century from Salt Pond, Massachusetts (Donnelly et al. 2015), plotted on the right. The grey bars represent TC events in the prehistoric portion of the Robinson Lake record, and the arrows represent likely correlations between cores RL01 and RL02.

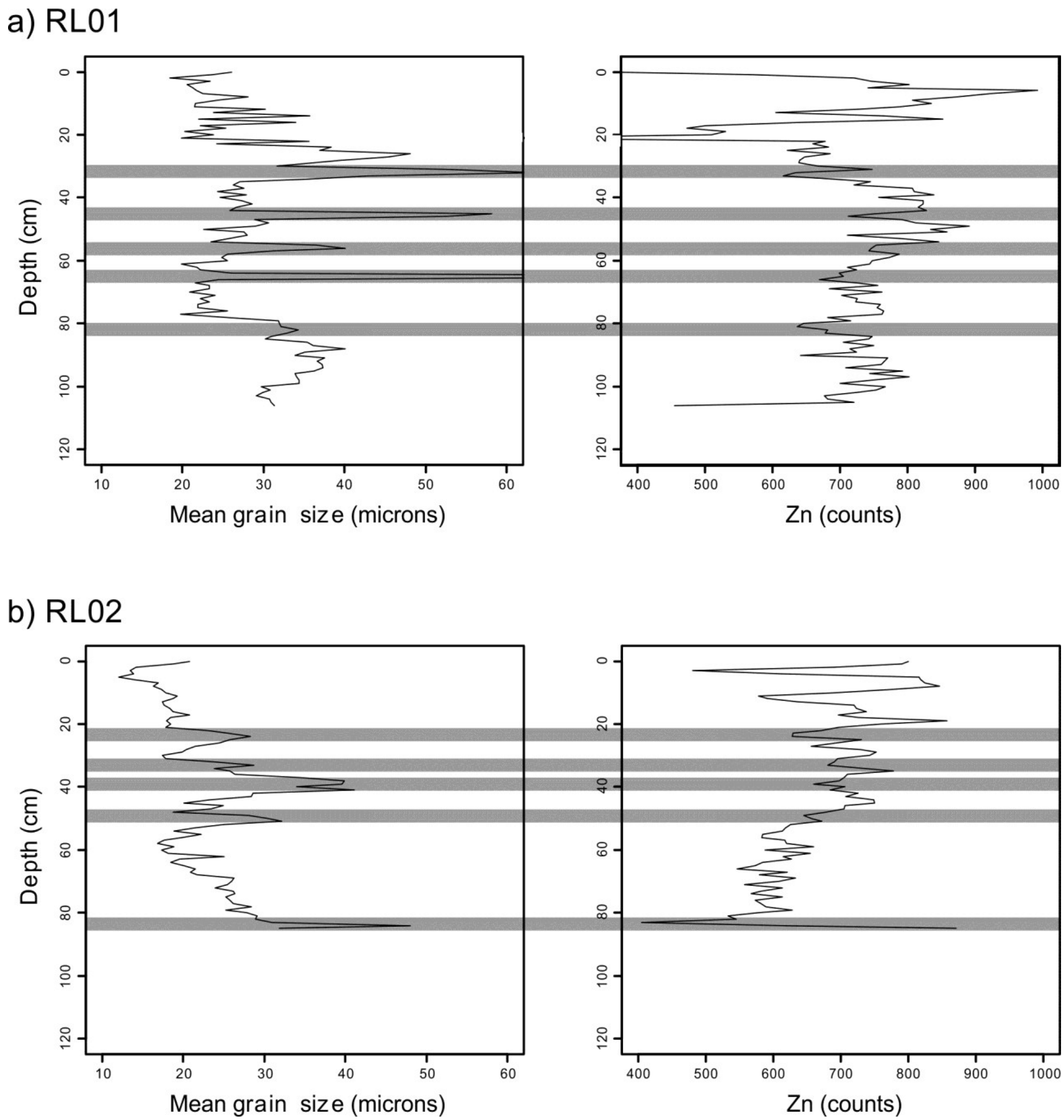

Figure 4.8 Grain-size (µm) and Zn,counts/s; averaged by cm) in cores a) RL01 and b) RL02. Grey bars show the inverse relationship between these proxies.

Chapter 5 – On the use of oxygen isotopes from tree ring α-cellulose to reconstruct past tropical cyclones in the Canadian Maritime region

5.1 Abstract

In this study, we explore the potential use of stable oxygen isotopes in tree ring α-cellulose to reconstruct past local tropical cyclone (TC) activity surrounding areas of known TC strikes in Nova Scotia, Canada. Cores of *Picea mariana* trees were extracted adjacent to Robinson Lake, Chezzetcook Inlet, Nova Scotia in order to test more contemporary and historically documented records of TC activity in this region. TCs precipitate ^{18}O-depleted rain, leaving a unique signature in the source water trees use to form the cellulose. Using an ARIMA AR-1 model to detrend the data, local and regional TCs were reconstructed and compared. Local reconstructions led to most (> 95%) hurricanes and all major hurricane (± 1 year) being recorded in the oxygen isotope record, whereas the regional reconstruction shows no major hurricane, only a few hurricanes (< 40%) and one TC event having a higher uncertainty (> 1 year).

This chapter is in preparation to be submitted for publication as: *Oliva F., Peros M., Viau A., Porter T., Faucher B. (in prep) On the use of oxygen isotopes from tree ring α-cellulose to reconstruct past tropical cyclones in the Canadian Maritime region.* Canadian Journal of Earth Sciences.

5.2 Introduction

Although tropical cyclones (TCs) are a well-studied phenomenon, little is known about long-term trends and variability. Paleotempestology is a discipline which uses proxy records to reconstruct TC activity over long periods of time in order to uncover longer-term patterns in TC behavior, which may assist in our predicting how TCs will change under a warming climate (Oliva et al., 2017). Traditionally, geological proxies such as grain-size analysis has been used in paleotempestology (e.g. Donnelly and Woodruff, 2007; Liu, 2013). Newer geochemical techniques and proxies have now emerged such as X-ray fluorescence (e.g. Brandon et al., 2013) and stable isotope geochemistry (e.g. Frappier et al., 2007). Collectively, these methods permit researchers to reconstruct TC paths and frequencies, but the inference of intensities or magnitudes is still difficult to produce (Oliva et al., 2017; Miller et al., 2006).

Tropical cyclones have unique isotopic signatures with their precipitation being depleted by up to 10‰ in the heavy stable isotope of oxygen (^{18}O) compared to locally produced rainwater (Lawrence and Gedzelman, 1996). The depleted $\delta^{18}O$ value of TC precipitation is due to fractionation which leads to the preferential incorporation of ^{18}O in the condensate during cloud formation (Grissino-Mayer et al., 2010). Although the water in the eye of the TC has a lower $\delta^{18}O$ composition than that at the periphery of the storm, Lawrence and Gedzelman (1996) show that the depletion can still be recorded up to several hundred kilometers away, ensuring that stable isotopes of oxygen (O) can be used as geochemical indicators of TC activity.

In terms of its use in tree rings, Miller et al. (2006) generated a time series of O isotopes in tree ring α-cellulose, which is pure cellulose free of monosaccharide, lignin and other plant secondary chemicals (Gaudinski et al., 2005) to show decadal to multi-decadal variations in TC activity at a site in the state of Georgia in the USA. The oxygen isotopic composition of the α-cellulose in the tree rings was thought to reflect the isotopic composition of the source water, which was incorporated into the longleaf pine (*Pinus palustris*) trees through their shallow root systems (Anderson et al., 2002; Miller et al., 2006). For this study, a conifer species was chosen instead of a deciduous tree where the isotopic composition of tree ring α-cellulose will reflect less the isotopic composition of the source water as more fractionation occurs in the leaf, altering the signature after O exchange in the xylem (McCarroll and Loader, 2004).

The objective of this study is to assess the viability of using stable oxygen isotopes from α-cellulose in *Picea mariana* (black spruce) to reconstruct past TCs in the region. We do this through the collection of samples of *P. mariana* from two tree stands in the Chezzetcook Inlet area of Nova Scotia. *Picea mariana* is a common component of the boreal forest north to the Arctic tree line and can be found in temperate wet areas such as littorals and bogssuch as the moist areas in the vicinity of Chezzetcook Inlet. The root system of *P. mariana* is generally shallow, normally occurring within the upper 20 cm of the organic horizon in the soil (Klinka, 2000). This results in near-surface groundwater being an important contributor to the tree's water budget, making *P. mariana* a good candidate to record TC events (Anderson et al., 2002; Miller et al., 2006).

5.3 Study Sites

Two field sites were selected based on their being affected by historic TCs. The first site is located adjacent to Robinson Lake (Figure 5.1), on the western margin of Chezzetcook Inlet (Figure 5.1), and experienced considerable flooding and standing water from Hurricane Juan in 2003 (NOAA, 2016) (personal communication from John Donahue, 2014). Two trees (RLT2 and RLT8) trees were chosen for analysis from the *P. mariana* forest which we sampled (located at 44°39'10"N 63°16'45"W, at ~5 m AMSL). The land is flat and separates Robinson Lake from Robinson Marsh and Three Fathom Harbor. The forest is dense, with a high volume of snags and fallen trees, many of which died during Hurricane Juan in August 2003 (personal communication from John Donahue, 2014). The position of the individual trees varies as RLT2 is ~140 m from the shoreline and ~5 m from the edge of Robinson Marsh whereas RLT8 is ~40 m away from the shoreline and ~20 m from Robinson Marsh.

The second site is located near the community of East Petpeswick, at 44°40'51"N 63°09'32"W (~5 m AMSL), 10 km east of Robinson Lake. Like the forest at Robinson Lake, the peninsula of East Petpeswick consists of a flat monospecific stand of *P. mariana*. Two cores from one tree (EPT1A and EPT1B) were chosen for analysis from this site. The difference that sets it apart from Robinson Lake is that it is a much healthier tree stand, with generally larger individuals, and fewer snags and fallen trees. It is also less densely populated than the Robinson Lake stand. This indicates that the impacts of Hurricane Juan (and perhaps other TCs) were less severe at this site, providing a control site against which to compare the data from nearby Robinson Lake. The analyzed tree, EPT1 is ~60 m from the shoreline and less than 10 m from the nearby, unnamed pond.

5.4 Methods

5.4.1 Field

Trees were cored using a standard increment borer at breast height in the fall of 2014. Only healthy, adult individuals were cored. To ensure as complete a record as possible and two radii, trees were cored from bark-to-bark through the pith (Porter et al., 2013) and twice from opposing sides of the tree when the diameter of the tree was greater than the length of the instrument. A total of eight cores were taken at Robinson Lake and nine at East Petpeswick, which were stored in large straws and labelled by location. The tree-ring series used for isotope analysis were dated by ring-counting, and ring-width measurements were cross-dated using the COFECHA software (Holmes, 1983).

5.4.2 Stable Isotopes

5.4.2.1 Lab

In the laboratory all cores were air dried, glued on wooden mounts and sanded using a belt sander with grits ranging from 80 to 600. Sub-samples of cores from three trees (four cores) were chosen for stable isotope analysis. For the chronology, the rings of each sample was counting from the outer bark towards the pith. The isotope analysis was not done on the entire cores. Series were chosen to 1) capture a variation of years, 2) have continuous series with adequate rings for sub-sampling and 3) to stay within budgetary constraints. The sub-samples, separated using medical scalpels (McCaroll and Loader, 2004) were divided by early- (EW) and latewood (LW) and placed in 50 ml centrifuge tubes. The α-cellulose was extracted from the tree rings using the Brendel method but modified to include extra steps of rinsing and alkaline hydrolysis (Gaudinski et al., 2005). The analysis was conducted at the G.G. Hatch Isotope Laboratory at the University of Ottawa, Canada. The weighed samples were placed in the Temperature Conversion Elemental Analyzer (TC/EA) for pyrolysis at 1450°C. The resulting gases were introduced into the Delta plus XP Isotope Ratio Mass Spectrometer via Conflo IV interface for analysis. Duplicates were ran every 10 samples. The 1σ analytical precision for oxygen isotopes is ± 0.4‰.

5.4.2.2 Data

The raw data was normalized to VSMOW using at least two standards (Porter and Middlestead, 2012). A 1-year autoregressive (AR-1) Box-Jenkins model was used on the data to remove potential effects of auto-correlation due to trends in seasonality (Miller et al., 2006). An autoregressive integrated moving average (ARIMA) model was used in the R program to produce modeled data. The model predicted values were subtracted from the observed to produce residual values (Miller et al., 2006). The residuals were then evaluated to identify instances of anomalously low $\delta^{18}O$ from the EW and LW (Miller et al., 2006). We chose -1 in the residuals as the critical value for distinguishing tree rings with TC signatures (Miller et al., 2006) from other possible major. The data from every tree is presented as the local time-series data, and a median of the local data was then used to create a regional time-series data.

5.5 Results

5.5.1 Local Time-Series Data

The results of the $\delta^{18}O$ in the tree ring α-cellulose varies from 19‰ to 29‰ in the EW and 17‰ to 28‰ in the LW (Figure 5.2). The most variable is RLT2 with a range of 10 ‰ over the 18 year record. The next most variable is EPT1A, with a variance of 6 ‰ in its 17 year record, RLT8 has a 5 ‰ variance and EPT1A has a variance of 4 ‰. All sites average in the 24-26 ‰ range at the exception of a few outliers. The two cores from the same tree (EPT1) show very similar values with slight differences.

The residuals from the ARIMA model are presented in Figure 5.3. As with the $\delta^{18}O$ values (Figure 5.2), EPT1A, EPT1B and RLT8 show less variation than RLT2. The first three cores hover around 0 oscillating between 5 and -5, indicating that the modeled data and the observed data are similar. RLT2 shows much more variation, not going lower than -5 but reaches highs of 15. The residuals from the cores in tree EPT1 show similar trends but are more variable than the $\delta^{18}O$ values.

5.5.2 Regional Time-Series Data

The data from all sites was combined by using the median to make a regional time series from 1987 to 2010 CE to cover years with at least 2 data points. The combined $\delta^{18}O$ record shows high variability between 1988 and 1993, followed by relatively stable but upward trending values from 1993 to 1995, followed by some variability in the LW between 2005 and 2009. In general, the EW is isotopically lighter than the LW and shows much more stability, with the exception of the measurement in 1989 (Figure 5.4).

In the combined EW chart (Figure 5.5) four anomalies were found, dating to 1987, 1989, 1990 and 1993. In the LW chart (Figure 5.5), four anomalies were also detected, in 1989, 1992, 2005, and 2008.

5.6 Discussion

There are two main situations that can impact the accuracy of the reported TCs through tree ring stable oxygen isotopes. First, some tree rings lack a clear boundary between the EW and LW (Figure 5.6), leading to a subjective separation/sampling during laboratory work. This can potentially lead to TCs appearing in the wrong sub-sample. Next, TCs precipitating anomalously low $\delta^{18}O$ late in the season when the tree is no longer producing cellulose, and is therefore in dormancy. This can lead to the low $\delta^{18}O$ signal being diluted through winter precipitation or stored in photosynthates and then used as source water for the tree in the following year's EW (McCarroll and Loader, 2004).

5.6.1 Local TC Reconstruction

The two years with the most anomalous values are 1998 and 2010 (Table 5.1). These years saw major hurricanes hit Nova Scotia in mid to late August (Table 5.2; Figure 5.7). The next lowest residual values are 1996, 2007 and 2008 where a major hurricane hit the coast in September 1996, another hit in early November 2007 and two hurricanes hit in September 2008.

Years with anomalously low $\delta^{18}O$ which are separated into three categories:

1) EW results that match with documented storms: Tropical Storm Ana (1985) and Hurricane Allison (1995);

2) LW results that correspond with documented storms: Hurricane Dean (1989) and Hurricane Gustav (2002), and;

3) EW results synchronous with late storms from the previous year: Hurricanes Bertha and Lili (1990) in 1991, Unnamed Hurricane (1991) in 1992, Major Hurricane Bonnie (1998) in 1999, Major Hurricane Floyd (1999) in 2000, Hurricane Gordon (2000) in 2001 and Hurricane Karen (2001) in 2002.

These results indicate that late-season TCs are more likely going to be recorded in the following year's EW at this latitude due to trees being dormant earlier than lower latitudes (Miller et al., 2006). A possible explanation for this is that trees can still be producing photosynthates while dormant which lead to the carbohydrates (sugars) being stored in the rhizosphere, the soil surrounding the roots, to supplement growth the following season. The demand from trees for these stored carbohydrates increases with dormancy length, and therefore latitude (Hopkins et al., 2013).

On September 29th 2003, Hurricane Juan hit the coast of Nova Scotia with the eye travelling within a few kilometers of the study sites (Figure 5.8). No signal was found in 2003, however EPT1A does have an anomalously low $\delta^{18}O$ for late 2004, a year in which *no* TC came within 250 km of the coast of Nova Scotia (Table 5.2). Although we would suspect this TC to be to in the LW of 2003 or EW of 2004, the limitations of the subjective separation of EW and LW per annual tree ring mentioned above could explain this discrepancy. This same argument can be used to explain the anomalously low $\delta^{18}O$ in the 2011 LW, after a major hurricane hit the coast in September 2010 and none in 2011.

5.6.2 Regional TC Reconstruction

Although individual *P. mariana* appear to better record TCs than others, a regional mean of the data gives a more conservative look. The anomalies in our regional reconstruction (Figure 5.5) show no major hurricanes and < 40% of documented hurricane strikes within ~250 km (Table 5.2). Moreover the 1993 values in the EW show no TC within 2 years, thus increasing the error associated with the regional record. This result suggests that pooled samples or regional medians or means may not be effective for reconstructing TCs from tree rings as is the case in more southern regions (McCarroll and Loader, 2004).

5.6.3 Limitations

As previously discussed, some limitations in using trees at these latitudes for reconstructing TCs can lay within the earlier drop in temperature in the fall than further south, limiting the TC season where trees are not in dormancy.

The lack of defined boundaries between rings sometime lead to a subjective separation of the EW and LW, which can lead to diluting, and effectively changing the isotopic value in the subsequent growing season.

Although unlikely because *P. mariana* cross-dates well regionally (Grissino-Mayer, 1993), another limitation is missing or false rings, skewing the chronology down core (e.g. Caldwell et al., 2006).

5.7 Conclusion

The potential widespread use of $\delta^{18}O$ in tree ring α-cellulose in paleotempestology is very promising. Whenever this proxy technique is used, modern data is needed to understand the dynamics of that region and the species being used. This proxy is also useful for modern reconstructions in aiding with methods that normally lack these time periods, such as X-ray fluorescence. The main conclusions drawn from this research are:

1) This region is very promising for reconstructing TCs through stable O isotopes, but much greater sampling depth over a wider region to include more of the swath covered by Hurricane Juan is needed to create a more robust regional record.

2) Although the confidence of using a regional record is intuitively higher than using individual trees, our results suggest that computing a regional record may smooth through real local records (Local > 95% of hurricanes as compared to regional < 40% of hurricanes) in this region.

3) Due to the early dormancy of *P. mariana* at these latitudes, many late season TCs only show up in the EW of the following year.

4) We suggest that $\delta^{18}O$ in tree ring α-cellulose for this latitude might give more insight by not separating EW and LW but completing the analysis on the entire ring. This needs further testing and comparison with the separation of the rings as the oxygen isotope measurements from the LW could get diluted within the EW from a difference in cellulose quantity.

Table 5.1 Years with low $\delta^{18}O$ anomalies in residuals from ARIMA (AR-1) per tree. Grayed area length of record for each tree.

EW	EPT1A								1999	
	EPT1B									
	RLT2			1991		1995		1998		
	RLT8	1985			1992			1998		2000
LW	EPT1A									
	EPT1B							1998		
	RLT2		1989				1996	1998		
	RLT8						1996			
EW	EPT1A		2002							
	EPT1B						2008	2010		
	RLT2	2001			2005					
	RLT8									
LW	EPT1A		2002	2004			2008	2010		
	EPT1B					2007		2010	2011	2013
	RLT2									
	RLT8		2002			2007		2010		

Table 5.2 List of TCs that came within 250 km of central Nova Scotia (NOAA Hurricane Center, 2017).

	Maximum strength	Strength at site	Name	Date
1983				
1984	MH	TS	DIANA	SEP 8-16
1985	TS	ET	ANA	JUL 15-19
1986				
1987				
1988	TS	TS	ALBERTO	AUG 5-8
	TS	TD	CHRIS	AUG 21-30
1989	H	H	DEAN	JUL 31 - AUG 9
1990	H	H	BERTHA	JUL 24 - AUG 9
	H	ET	LILI	OCT 6 - 14
1991	H	TS	----	OCT 31 - NOV 6
1992				
1993				
1994				
1995	H	ET	ALLISON	JUN 3-6
	TS	TS	BARRY	JUL 5-10
1996	MH	H	HORTENSE	SEP 3-15
1997				
1998	MH	TS	BONNIE	AUG 19-30
1999	MH	ET	FLOYD	SEP 7-17
2000	H	ET	GORDON	SEP 14-18
	ST	ET	----	OCT 25-29
2001	H	TS	KAREN	OCT 11-15
2002	H	H	GUSTAV	SEP 8-12
2003	H	H	JUAN	SEP 24-29
2004				
2005	H	ET	OPHELIA	SEP 6-17
2006	TS	ET	BERYL	JUL 18-21
2007	H	ET	NOEL	OCT 28 - NOV 2
2008	H	H	KYLE	SEP 25-29
	H	ET	HANNA	AUG 28 - SEP 7
2009	MH	H	BILL	AUG 15-24
2010	MH	H	EARL	AUG 25 - SEP 4
2011				
2012				
2013	TS	ET	ANDREA	JUN 5-7

Figure 5.1 Tree core locations in central Nova Scotia, Canada.

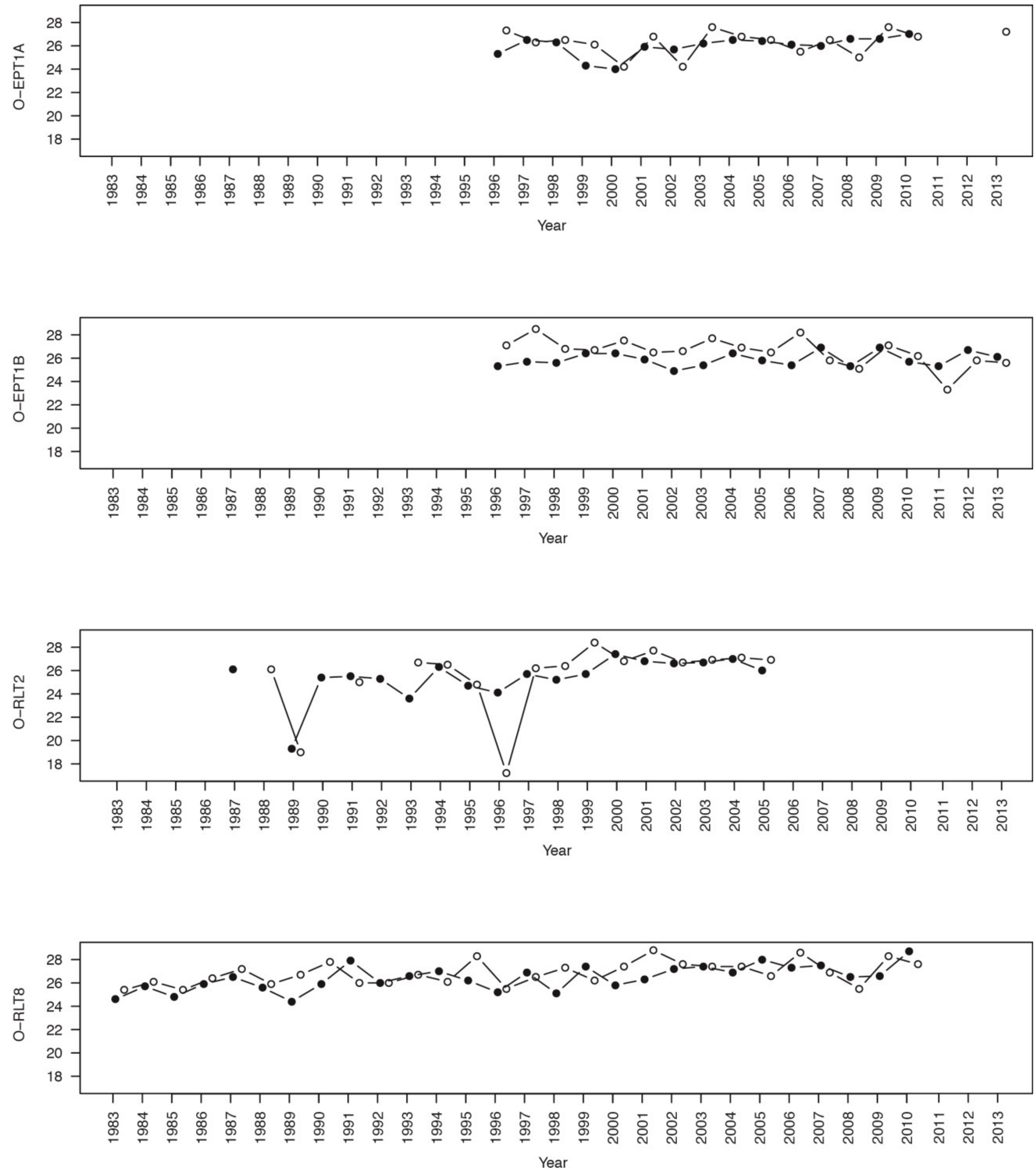

Figure 5.2 δ^{18}O values in per mil (‰) for EW (black circles) and LW (hollow circles) for the four individual trees. Values are plotted as the EW on the tickmark of the year and LW shortly thereafter. Connecting lines in graph absent between non-consecutive points (i.e. missing data).

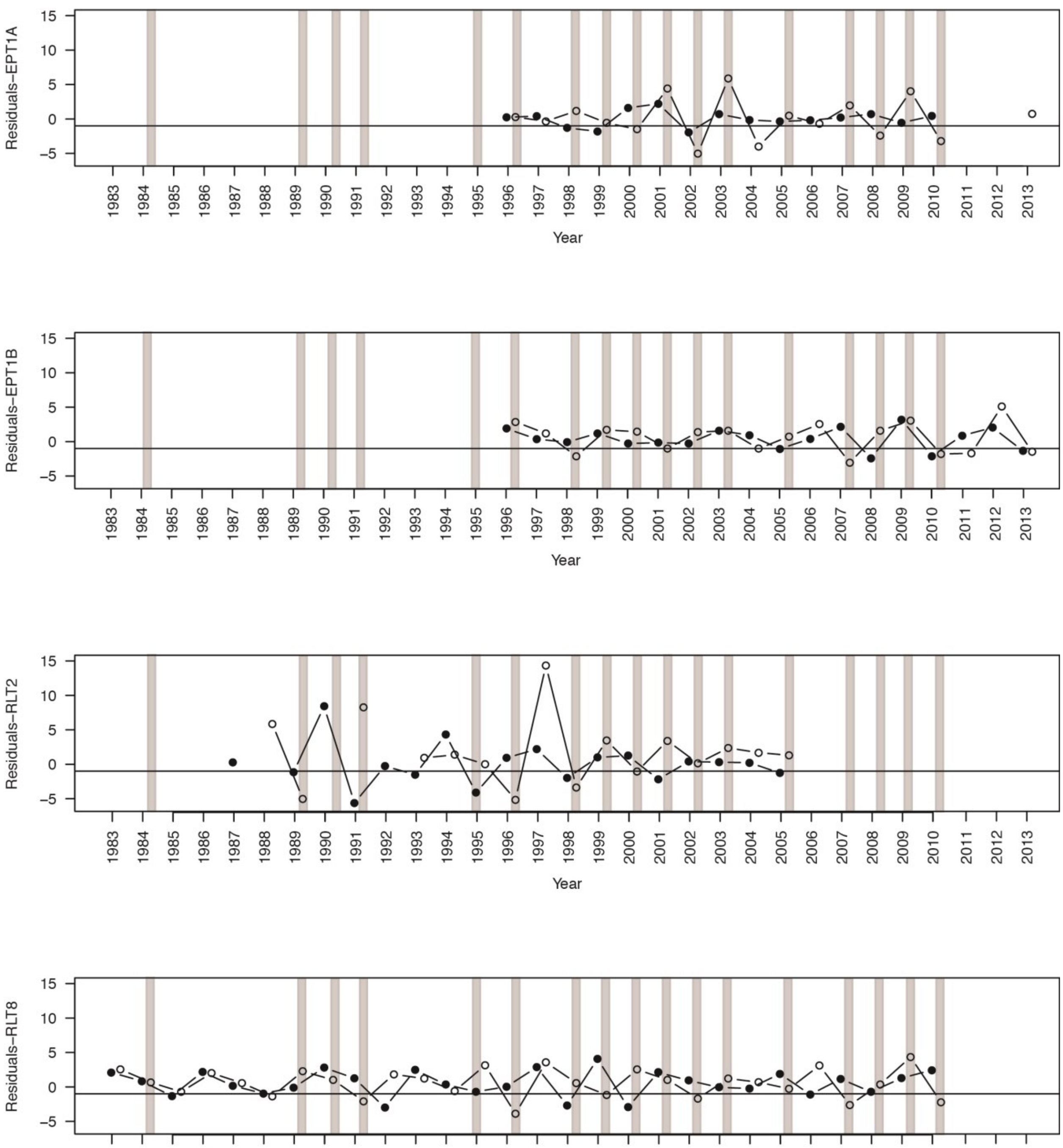

Figure 5.3 Residuals plotted against time for EW (black circles) and LW (hollow circles) for the four individual trees. Values are plotted as the EW on the tickmark of the year and LW shortly thereafter. Connecting lines in graph absent between non-consecutive points (i.e. missing data). Threshold (-1) indicated by line (Miller et al., 2006). Grey bars represent every hurricane and major hurricane (Table 5.2).

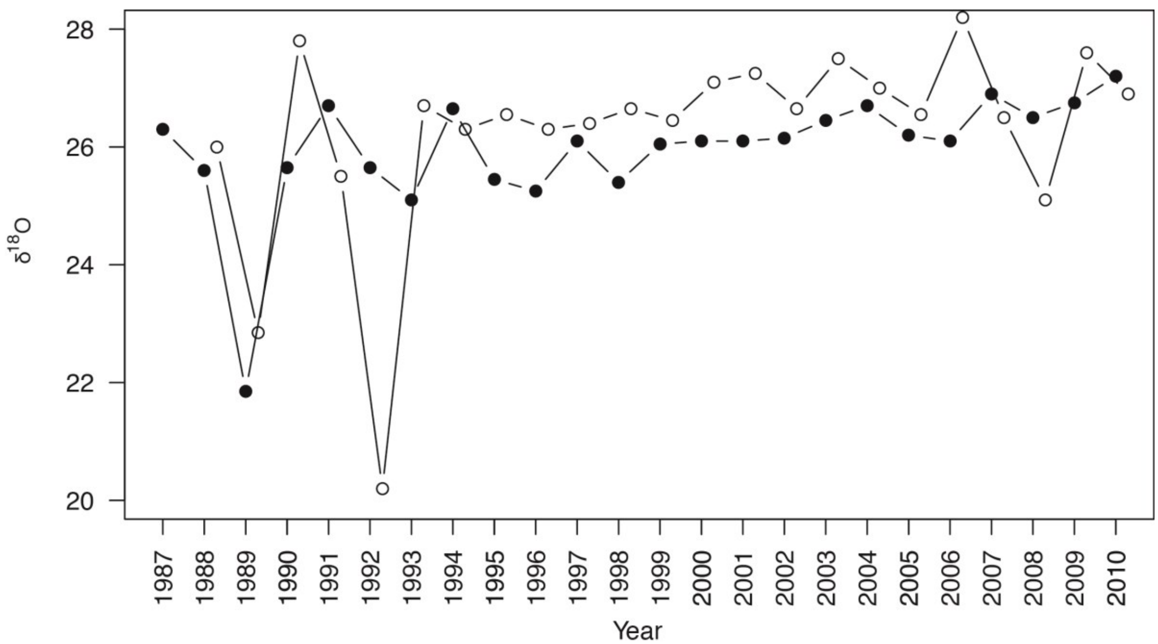

Figure 5.4 $\delta^{18}O$ values in per mil (‰) for EW (black circles) and LW (hollow circles) in a regional setting. Values are plotted as the EW on the tickmark of the year and LW shortly thereafter.

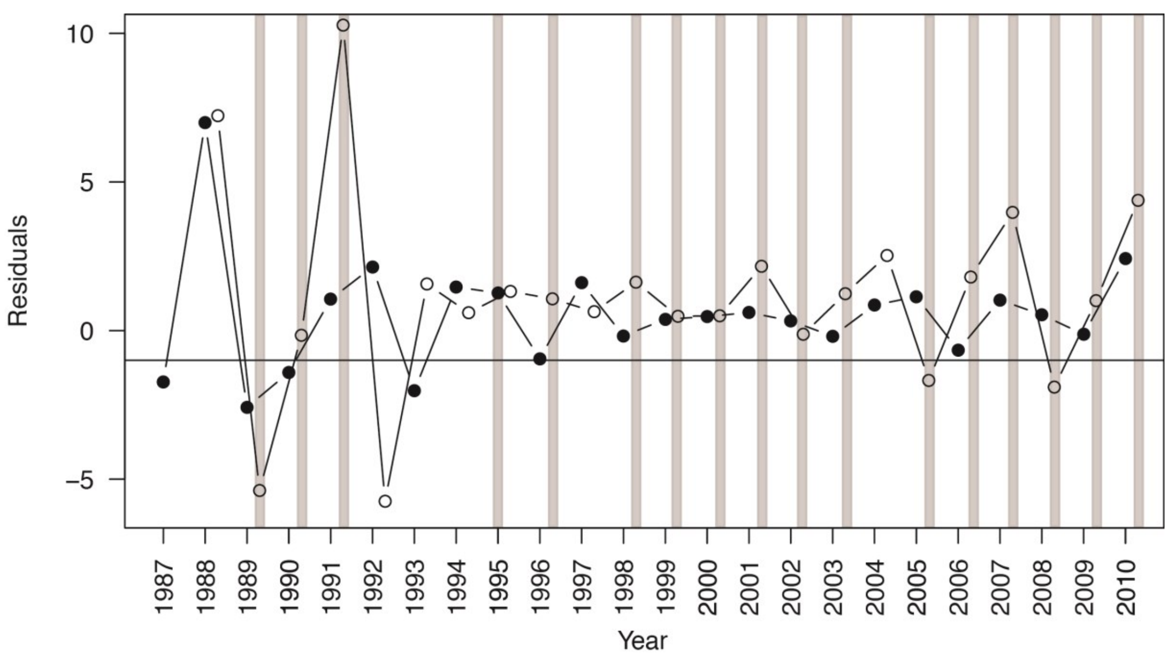

Figure 5.5 Residuals plotted against time for EW (black circles) and LW (hollow circles) in a regional setting. Values are plotted as the EW on the tickmark of the year and LW shortly thereafter. Threshold (-1) indicated by line (Miller et al., 2006). Grey bars represent every hurricane and major hurricane (Table 5.2).

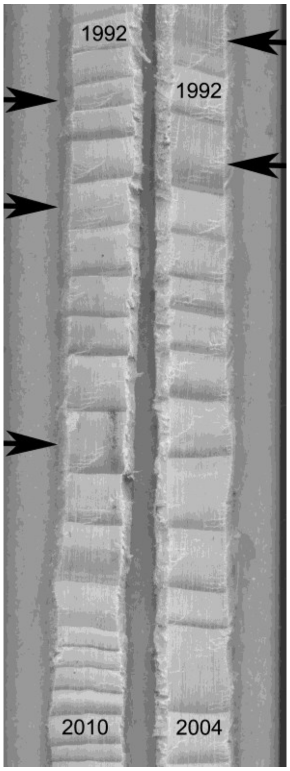

Figure 5.6 Scan section of core RLT8. Black arrows showing blurred boundaries between EW and LW.

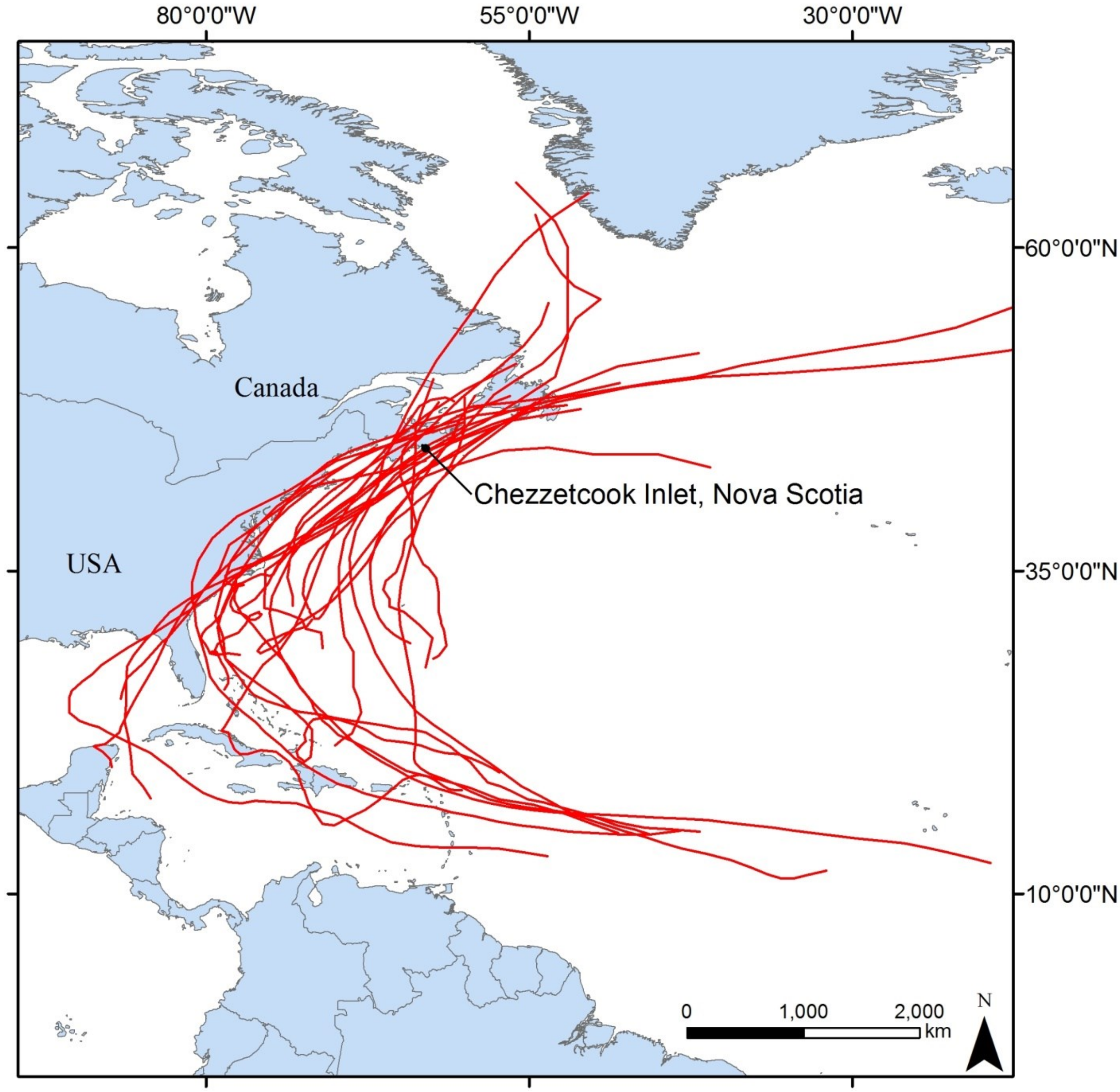

Figure 5.7 Map of TCs that came within 250 km of central Nova Scotia (NOAA Hurricane Center, 2017).

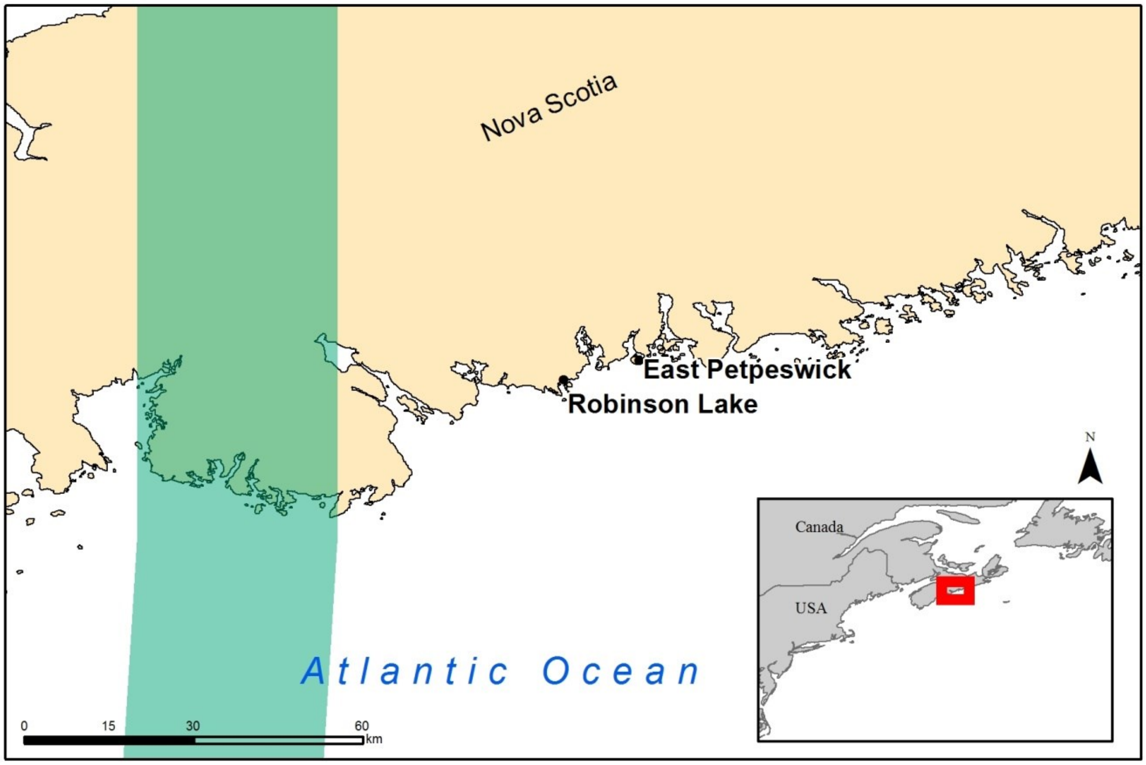

Figure 5.8 Map showing track of Hurricane Juan. Size of line shows approximate diameter of eye of hurricane at landfall (35 km)(Bowyer, 2003).

Chapter 6 – Conclusion

6.1 Summary and Conclusions

6.1.1 Objective 1

The first objective of the thesis is to *"*compile, synthesize and analyze of the available information in paleotempestology and create tools for researchers in the discipline to use*"* was achieved by writing the most comprehensive to date review of paleotempestological research in the western North Atlantic basin (Chapter 2). While studying the 59 peer-reviewed papers that were published at the time of writing the manuscript, I found that although newer technologies such as XRF can add to the breadth of research possible in paleotempestology, traditional sedimentary research remains invaluable. These traditional analyses, such as paleoecological work with foraminifera, grain-size analyses and loss on ignition are tested and robust methods that provide indispensable data. These analyses used in conjunction with high-resolution analyses provide high-quality reliable quantitative data. Geographical gaps in the data were also observed by reviewing the spatial distribution of the 59 studies. These gaps notably exist in the northern section of the eastern North American coast, the southern section of the Gulf of Mexico and in the Caribbean.

Following the work in Chapter 2, Chapter 3 was written to meet the first objective of the thesis. This chapter explores the available paleotempestological data in much detail and tests it against various hypotheses, such as the Bermuda High Hypothesis (Liu, 2004). The resulting database from the work in these two chapters has been housed at the National Oceanographic and Atmospheric Association's (NOAA) World Data Center for Paleoclimatology and NOAA National Centers for Environmental Information. In this study, I take a broad, careful look at the temporal and spatial trends in TC activity over the last 8000 years and a closer look at four studies based on stringent criteria, to test the Bermuda High Hypothesis over the last 3000 years. Evidence was also provided that a centennial to millennial seesaw shifts in the Bermuda High pressure system from a northeasterly position to a southwesterly position affects TC tracks. Results also show that variations in total TC strikes can be due to multi-centennial variations in climate forcings such as during the LIA and MCA.

6.1.2 Objective 2

The second objective was to "contribute data by pushing known geochemical limits of proxy analysis*"; this* was achieved by using X-ray fluorescence to analyze sediment cores at sub-millimetre scales for dozens of elements (Chapter 4). From the results at this site, we uncover two quiescent periods between ~1150 to 1475 CE and 1670 to the present and a higher magnitude of activity from ~1475 to 1670 CE. These results are consistent with results from New England (Salt Pond, Massachusetts; Donnelly et al., 2015). Results also show that Bromine (Br) and its associated ratios are useful indicators of TC activity.

In order to meet the second objective, Chapter 5 explores the method of using $\delta^{18}O$ isotopes in tree ring α-cellulose for reconstructing past TC and the limitations to this method at Nova Scotia's latitude in a more modern timeframe. This chapter permitted us to conclude that reconstructing TCs in this region using stable oxygen isotopes is very promising. We also uncovered that the data from single trees contrarily to regional records uncovers more TCs, but possibly with greater error. The $\delta^{18}O$ in tree ring α-cellulose at this latitude may give more insight if the tree rings are not separated by early- and latewood. Finally, since these trees fall into dormancy in the early fall; they fail to record passing TCs in mid and late fall in the proper ring, and often record them in the spring earlywood.

6.2 Key Contributions

This thesis presents several key contributions to advance knowledge in the discipline of paleotempestology.

A much needed comprehensive review of the present state of paleotempestology by reporting on current and evolving trends. All of the emerging methods are presented and explained, including known limitations of their use.

Work was also done to present a new, comprehensive and robust database housed at NOAA for future researchers. This database, suggested as future work in Chapter 2 was welcomed by reviewers for Chapter 3. This database is a repository that researchers can use can also continue to contribute data. The analyses conducted on this data are very promising and helped cement Liu and Fearn's (2000) hypothesis of a millennial-scale shift in the Bermuda High pressure system

This thesis also provides not only the first, but also very high-resolution TC reconstruction north of Massachusetts. This was a first step in filling geographical gaps highlighted in Chapter 2. This study did not only present a history of TCs, but also contributed to the science behind using XRF and breaking down the use and limitations of individual elements for TC reconstructions in the Canadian maritime region.

Miller et al. (2006) along with few others (e.g. Grissino-Mayer et al., 2010) have used stable oxygen isotopes in tree ring α-cellulose in the southern USA (e.g. Georgia). In chapter 5, we contribute the first analysis of these isotopes for coniferous trees at higher latitudes (Nova Scotia) and worked at uncovering the limitations and uses of stable oxygen isotopes for this region.

6.3 Future Research Directions

6.3.1 Regional-Scale Syntheses and Filling Spatial Gaps

As highlighted in the *Future Directions* section of Chapter 2, there is little that has be accomplished in regional-scale syntheses of paleotempestological data. Although we touch on this in Chapter 3, much more work needs to be done, especially as new high-quality studies are being published. This goes hand-in-hand with another deficiency in the field which is the big spatial gaps that exist north of New England, on either side of the Florida panhandle and in the Caribbean. As studies emerge from these fringe locations, and higher-resolution data get published from already studied areas, full Atlantic basin syntheses could bring forth some important information about trends and cycles that we may be unaware of. The consistency of the presence of “active” hurricane periods identified at some sites (e.g., Donnelly and Woodruff, 2007) and in this thesis across space needs to be further looked at and tested.

6.3.2 Major Climate Forcings

I suggest more work be done in correlating TC records, and possibly the aforementioned regional syntheses, to major climate forcings and potential driving factors. Important climate forcings which could have an impact on TCs are the North Atlantic Oscillation (NAO) (Knowles & Leitner, 2007; Liu, 2004), the north-south position of the Intertropical Convergence Zone (ITCZ) (van Hengstum et al., 2016), El Niño / southern oscillation (ENSO) and further testing of the Bermuda High Hypothesis would be necessary (Liu and Fearn, 2000).

6.3.3 Geochemical Proxies

There are still many remaining questions in the use of geochemical proxies, such as stable oxygen isotopes and XRF to reconstruct TCs. With stable oxygen isotopes, further statistical testing needs to be done and much greater sampling depth. This method has only been used in a handful of studies in tree rings (Miller et al., 2006) and in speleothems (Frappier et al., 2007). A greater sampling depth could potentially yield good regional data with a low signal to noise ratio. As we understand more and more the different elements and ratios in different regions, the use of XRF has immense potential for being a very powerful analytical tool. Droves of data can be stored in repositories and potentially used in a myriad of disciplines, opening the door to very interesting future collaborations.

6.4 Thesis Limitations

With paleotempestology being a fairly novel discipline, many questions remain surrounding the theses, methods and tests presented in the dissertation.

In Chapter 2, limitations were found to exist in the literature. These include geographical gaps where little or no studies have been conducted, such as north of New England (Oliva et al., 2017). In Chapter 3, one of the very inherent limitations is the error associated with records digitized from graphs. An average of ± 50 years was deemed suitable as an error associated with these records, but they were left out of the Bermuda High Hypothesis test, as much uncertainty remains. Limitations also exist in the paleo-reconstructions (Chapter 4), with issues arising with downcore validation as the upper most parts of sediment cores were not analyzed at the same resolution as the consolidated material downcore. To complete Chapter 5, future work will also have to be conducted on more trees to obtain a more robust regional result of depleted ^{18}O isotope signal in tree ring α-cellulose. As well as deciphering the isotopic composition of locally produced precipitation to better depict anomalies.

References

Adomat, F., and E. Gischler (2017), Assessing the suitability of Holocene environments along the central Belize coast, Central America, for the reconstruction of hurricane records, *International Journal of Earth Sciences*, *106*(1), 283–309, doi:10.1007/s00531-016-1319-y.

Aharon, P., and W. J. Lambert (2009), Radiocarbon deficiencies of US Gulf Coast lakes compromise paleo-hurricane records, *Quaternary Research*, *71*(3), 266–270, doi:10.1016/j.yqres.2009.01.004.

Anderson, W. T., S. M. Bernasconi, J. A. McKenzie, M. Saurer, and F. Schweingruber (2002), Model evaluation for reconstructing the oxygen isotopic composition in precipitation from tree ring cellulose over the last century, *Chemical Geology*, *182*(2), 121–137.

Ascough, P., G. Cook, and A. Dugmore (2005), Methodological approaches to determining the marine radiocarbon reservoir effect, *Progress in Physical Geography*, *29*(4), 532–547, doi:10.1191/0309133305pp461ra.

Ball, D. F. (1964), Loss-on-ignition as an estimate of organic matter and organic carbon in non-calcareous soils, *Journal of Soil Science*, *15*(1), 84–92.

Bertran, P., D. Bonnissent, D. Imbert, et al. (2004), Paléoclimat des Petites Antilles depuis 4000 ans BP : l'enregistrement de la lagune de Grand-Case à Saint-Martin. *C.R. Geoscience,* 336, 1501-1510.

Blaauw, M., and J. A. Christen (2011), Flexible Paleoclimate Age-Depth Models Using an Autoregressive Gamma Process, *Bayesian Analysis*, *6*, 457–474, doi:10.1214/11-BA618.

Boldt, K. V., P. Lane, J. D. Woodruff, and J. P. Donnelly (2010), Calibrating a sedimentary record of overwash from Southeastern New England using modeled historic hurricane surges, *Marine Geology*, *275*(1–4), 127–139, doi:10.1016/j.margeo.2010.05.002.

Bradley, R. S. (2000), Past global changes and their significance for the future, *Quaternary Science Reviews*, *19*(1–5), 391–402, doi:10.1016/S0277-3791(99)00071-2.

Brandon, C. M., J. D. Woodruff, D. P. Lane, and J. P. Donnelly (2013), Tropical cyclone wind speed constraints from resultant storm surge deposition: A 2500 year reconstruction of hurricane activity from St. Marks, FL: PALEO-HURRICANE ACTIVITY IN ST. MARKS, FL, *Geochemistry, Geophysics, Geosystems*, *14*(8), 2993–3008, doi:10.1002/ggge.20217.

Brandon, C. M., J. D. Woodruff, J. P. Donnelly, and R. M. Sullivan (2014), How Unique was Hurricane Sandy? Sedimentary Reconstructions of Extreme Flooding from New York Harbor, *Scientific Reports*, *4*, 7366, doi:10.1038/srep07366.

Brown, A. L., E. G. Reinhardt, P. J. van Hengstum, and J. E. Pilarczyk (2014), A Coastal Yucatan Sinkhole Records Intense Hurricane Events, *Journal of Coastal Research*, *294*, 418–428, doi:10.2112/JCOASTRES-D-13-00069.1.

Brown, M. E. (2006), Hurricanes and Typhoons: Past, Present, and Future (review), *Southeastern Geographer*, *46*(2), 323–324, doi:10.1353/sgo.2006.0017.

Burn, M.J., S.E. Palmer (2015), Atlantic hurricane activity during the last millennium, *Scientific Reports,* 5, 12838

Burton, M.L., Hicks, M.J. (2005), Hurricane Katrina: preliminary estimates of commercial and public sector damages, *Marshall University: Center for Business and Economic Research*.

Buynevich, I. V., and J. P. Donnelly (2006), Geological Signatures of Barrier Breaching and Overwash, southern Massachusetts, USA, pp. 112–116, Journal of Coastal Research, Brazil.

Buynevich, I. V., D. M. FitzGerald, and R. J. Goble (2007), A 1500 yr record of North Atlantic storm activity based on optically dated relict beach scarps, *Geology*, *35*(6), 543–546.

Caldwell, M. M., G. Heldmaier, R. B. Jackson, O. L. Lange, and H. A. Mooney (2006), *Growth Dynamics of Conifer Tree Rings: Images of Past and Future Environments.*, Springer, Dordrecht.

Canadian Disaster Database (CDD) (2015) Public Safety Canada. Government of Canada. http://cdd.publicsafety.gc.ca/. Visited March 27th 2015.

Cartapanis, O., K. Tachikawa, O. E. Romero, and E. Bard (2014), Persistent millennial-scale link between Greenland climate and northern Pacific Oxygen Minimum Zone under interglacial conditions, *Climate of the Past*, *10*(1), 405–418, doi:10.5194/cp-10-405-2014.

Chague-Goff, C., T. S. Hamilton, and D. B. Scott (2001), Geochemical evidence for the recent changes in a salt marsh, Chezzetcook Inlet, Nova Scotia, Canada,

Chenoweth, M. (2006), A Reassessment of Historical Atlantic Basin Tropical Cyclone Activity, 1700–1855, *Climatic Change*, *76*(1–2), 169–240, doi:10.1007/s10584-005-9005-2.

Cheung, K. F., L. Tang, J. P. Donnelly, E. M. Scileppi, K.-B. Liu, X.-Z. Mao, S. H. Houston, and R. J. Murnane (2007), Numerical modeling and field evidence of coastal overwash in southern New England from Hurricane Bob and implications for paleotempestology, *Journal of Geophysical Research*, *112*(F3), doi:10.1029/2006JF000612.

Cochran, D. M., C. A. Reese, and K. Liu (2009), Tropical Storm Gamma and the Mosquitia of eastern Honduras: a little-known story from the 2005 hurricane season, *Area*, *41*(4), 425–434, doi:10.1111/j.1475-4762.2009.00886.x.

Collins, E. S., D. B. Scott, and P. T. Gayes (1999), Hurricane records on the South Carolina coast: can they be detected in the sediment record?, *Quaternary International*, *56*(1), 15–26.

Cronin, T. M., K. Hayo, R. C. Thunell, G. S. Dwyer, C. Saenger, and D. A. Willard (2010), The Medieval Climate Anomaly and Little Ice Age in Chesapeake Bay and the North Atlantic Ocean, *Palaeogeography, Palaeoclimatology, Palaeoecology*, *297*(2), 299–310, doi:10.1016/j.palaeo.2010.08.009.

Croudace, I. W., A. Rindby, and R. G. Rothwell (2006), ITRAX: description and evaluation of a new multi-function X-ray core scanner, *Geological Society, London, Special Publications*, *267*(1), 51–63.

Cuven, S., P. Francus, and S. F. Lamoureux (2010), Estimation of grain size variability with micro X-ray fluorescence in laminated lacustrine sediments, Cape Bounty, Canadian High Arctic, *Journal of Paleolimnology*, *44*(3), 803–817, doi:10.1007/s10933-010-9453-1.

Das, O., Y. Wang, J. Donoghue, X. Xu, J. Coor, J. Elsner, and Y. Xu (2013), Reconstruction of paleostorms and paleoenvironment using geochemical proxies archived in the sediments of two coastal lakes in northwest Florida, *Quaternary Science Reviews*, *68*, 142–153, doi:10.1016/j.quascirev.2013.02.014.

Dean, W.E. Jr. (1974), Determination of Carbonate and Organic Matter in Calcareous Sediments and Sedimentary Rocks by Loss on Ignition: Comparison with Other Methods, *Journal of Sedimentary Petrology,* 44, 242-248

Denommee, K. C., S. J. Bentley, and A. W. Droxler (2014), Climatic controls on hurricane patterns: a 1200-y near-annual record from Lighthouse Reef, Belize, *Scientific Reports*, *4*, doi:10.1038/srep03876.

Donnelly, J. P., and J. D. Woodruff (2007), Intense hurricane activity over the past 5,000 years controlled by El Niño and the West African monsoon, *Nature*, *447*(7143), 465–468, doi:10.1038/nature05834.

Donnelly, J. P. et al. (2001a), 700 yr sedimentary record of intense hurricane landfalls in southern New England, *Geological Society of America Bulletin*, *113*(6), 714–727.

Donnelly, J. P., S. Roll, M. Wengren, J. Butler, R. Lederer, and T. Webb (2001b), Sedimentary evidence of intense hurricane strikes from New Jersey, *Geology*, *29*(7), 615–618.

Donnelly, J. P., J. Butler, S. Roll, M. Wengren, and T. Webb (2004), A backbarrier overwash record of intense storms from Brigantine, New Jersey, *Marine Geology*, *210*(1–4), 107–121, doi:10.1016/j.margeo.2004.05.005.

Donnelly, J. P., A. D. Hawkes, P. Lane, D. MacDonald, B. N. Shuman, M. R. Toomey, P. J. van Hengstum, and J. D. Woodruff (2015), Climate forcing of unprecedented intense-hurricane activity in the last 2000 years: DONNELLY ET AL., *Earth's Future*, *3*(2), 49–65, doi:10.1002/2014EF000274.

Elsner, J. B., J. P. Kossin, and T. H. Jagger (2008), The increasing intensity of the strongest tropical cyclones, *Nature*, *455*(7209), 92–95, doi:10.1038/nature07234.

Emanuel, K. (2003), T ROPICAL C YCLONES, *Annual Review of Earth and Planetary Sciences*, *31*(1), 75–104, doi:10.1146/annurev.earth.31.100901.141259.

Ercolani, C., J. Muller, J. Collins, M. Savarese, and L. Squiccimara (2015), Intense Southwest Florida hurricane landfalls over the past 1000 years, *Quaternary Science Reviews*, *126*, 17–25, doi:10.1016/j.quascirev.2015.08.008.

Ford, D., and P. Williams (2007), Karst Hydrogeology and Geomorphology. John Wiley and Sons, Ltd. Chichester. 562 pp.

Frappier, A., T. Knutson, K.-B. Liu, and K. Emanuel (2007a), Perspective: coordinating paleoclimate research on tropical cyclones with hurricane-climate theory and modelling, *Tellus A*, *59*(4), 529–537, doi:10.1111/j.1600-0870.2007.00250.x.

Frappier, A. B. (2008), A stepwise screening system to select storm-sensitive stalagmites: Taking a targeted approach to speleothem sampling methodology, *Quaternary International*, *187*(1), 25–39, doi:10.1016/j.quaint.2007.09.042.

Frappier, A. B., D. Sahagian, S. J. Carpenter, L. A. González, and B. R. Frappier (2007b), Stalagmite stable isotope record of recent tropical cyclone events, *Geology*, *35*(2), 111–114.

Gaudinski, J. B., T. E. Dawson, S. Quideau, E. A. G. Schuur, J. S. Roden, S. E. Trumbore, D. R. Sandquist, S.-W. Oh, and R. E. Wasylishen (2005), Comparative Analysis of Cellulose Preparation Techniques for Use with ^{13}C, ^{14}C, and ^{18}O Isotopic Measurements, *Analytical Chemistry*, *77*(22), 7212–7224, doi:10.1021/ac050548u.

Gehrels, W. R., J. R. Kirby, A. Prokoph, R. M. Newnham, E. P. Achterberg, H. Evans, S. Black, and D. B. Scott (2005), Onset of recent rapid sea-level rise in the western Atlantic Ocean, *Quaternary Science Reviews*, *24*(18–19), 2083–2100, doi:10.1016/j.quascirev.2004.11.016.

Ghaleb, B. (2009), Overview of the methods for the measurement and interpretation of short-lived radioisotopes and their limits, *IOP Conference Series: Earth and Environmental Science*, *5*, 012007, doi:10.1088/1755-1307/5/1/012007.

Gischler, E., E.A. Shinn, W. Oschmann, et al. (2008), A 1500-Year Holocene Caribbean Climate Archive from the Blue Hole, Lighthouse Reef, Belize. *Journal of Coastal Research* 24(6): 1495-1505.

Greenwood, N. N., and A. Earnshaw (1997), *Chemistry of the elements*, 2nd ed., Butterworth-Heinemann, Oxford ; Boston.

Gregory, B. R. B., M. Peros, E. G. Reinhardt, and J. P. Donnelly (2015), Middle–late Holocene Caribbean aridity inferred from foraminifera and elemental data in sediment cores from two Cuban lagoons, *Palaeogeography, Palaeoclimatology, Palaeoecology*, *426*, 229–241, doi:10.1016/j.palaeo.2015.02.029.

Grissino-Mayer, H. D. (1993), An updated list of species used in tree-ring research, *Tree-Ring Bulletin*, *53*, 17–43.

Grissino-Mayer, H. D., D. L. Miller, and C. I. Mora (2010), Dendrotempestology and the Isotopic Record of Tropical Cyclones in Tree Rings of the Southeastern United States, in *Tree Rings and Natural Hazards*, vol. 41, edited by M. Stoffel, M. Bollschweiler, D. R. Butler, and B. H. Luckman, pp. 291–303, Springer Netherlands, Dordrecht.

Gupta, B. (1999), *Modern Foraminifera*, Kluwer Academic Publishers, Dordrecht.

Han, F. X., A. Banin, Y. Su, D. L. Monts, J. M. Plodinec, W. L. Kingery, and G. E. Triplett (2002), Industrial age anthropogenic inputs of heavy metals into the pedosphere, *Naturwissenschaften*, *89*(11), 497–504, doi:10.1007/s00114-002-0373-4.

Hansom, J. D., and A. M. Hall (2009), Magnitude and frequency of extra-tropical North Atlantic cyclones: A chronology from cliff-top storm deposits, *Quaternary International*, *195*(1–2), 42–52, doi:10.1016/j.quaint.2007.11.010.

Haug, G. H., K. Hughen, A, D. M. Sigman, L. C. Peterson, and U. Rohl (2001), Southward Migration of the Intertrpoical Convergence Zone through the Holocene., *Science*, *293*(5533), 1304–1308.

Hawkes, A. D., and B. P. Horton (2012), Sedimentary record of storm deposits from Hurricane Ike, Galveston and San Luis Islands, Texas, *Geomorphology*, *171–172*, 180–189, doi:10.1016/j.geomorph.2012.05.017.

Heiri, O., A. F. Lotter, and G. Lemcke (2001), Loss on ignition as a method for estimating organic and carbonate content in sediments: reproducibility and comparability of results, *Journal of paleolimnology*, *25*(1), 101–110.

Henderson, G., M. Collins, I. Hall, M. Lockwood, H. Pälike, R. Rickaby, G. Schmidt, C. Turney, and E. Wolff (2009), Improving Future Climate Prediction using Palaeoclimate Data (an outcome of The Leverhulme Climate Symposium 2008-Earth's Climate: Past, Present and Future),

Hippensteel, S. (2010), Paleotempestology and the pursuit of the perfect paleostorm proxy, *GSA Today*, 52–53, doi:10.1130/GSATG80GW.1.

Hippensteel, S. P. (2008), Preservation Potential of Storm Deposits in South Carolina Back-Barrier Marshes, *Journal of Coastal Research*, *243*, 594–601, doi:10.2112/05-0624.1.

Hippensteel, S. P., and W. J. Garcia (2014), Micropaleontological Evidence of Prehistoric Hurricane Strikes from Southeastern North Carolina, *Journal of Coastal Research*, *298*, 1157–1172, doi:10.2112/JCOASTRES-D-12-00180.1.

Hippensteel, S. P., and M. E. Martin (1999), Foraminifera as an indicator of overwash deposits, Barrier Island sediment supply, and Barrier Island evolution: Folly Island, South Carolina, *Palaeogeography, Palaeoclimatology, Palaeoecology*, *149*, 115–125.

Hippensteel, S. P., M. D. Eastin, and W. J. Garcia (2013), The geological legacy of Hurricane Irene: Implications for the fidelity of the paleo-storm record, *GSA Today*, 4–10, doi:10.1130/GSATG184A.1.

Holmes, R. L. (1983), Computer-assisted quality control in tree-ring dating and measurement, *Tree-ring bulletin*, *43*, 51–67.

Hopkins, F., M. A. Gonzalez-Meler, C. E. Flower, D. J. Lynch, C. Czimczik, J. Tang, and J.-A. Subke (2013), Ecosystem-level controls on root-rhizosphere respiration, *New Phytologist*, *199*(2), 339–351, doi:10.1111/nph.12271.

Horton, B. P., V. Rossi, and A. D. Hawkes (2009), The sedimentary record of the 2005 hurricane season from the Mississippi and Alabama coastlines, *Quaternary International*, *195*(1–2), 15–30, doi:10.1016/j.quaint.2008.03.004.

Hurrell, J. W., Y. Kushnir, G. Ottersen, and M. Visbeck (2003), An overview of the North Atlantic Oscillation, in *Geophysical Monograph Series*, vol. 134, edited by J. W. Hurrell, Y. Kushnir, G. Ottersen, and M. Visbeck, pp. 1–35, American Geophysical Union, Washington, D. C.

Keigwin, L. D. (1996), The little ice age and medieval warm period in the Sargasso Sea, *Science*, *274*(5292), 1504.

Kiage, L. M., D. Deocampo, T. A. Mccloskey, T. A. Bianchette, and M. Hursey (2011), A 1900-year paleohurricane record from Wassaw Island, Georgia, USA, *Journal of Quaternary Science*, *26*(7), 714–722, doi:10.1002/jqs.1494.

Kilbourne, K. H., R. P. Moyer, T. M. Quinn, and A. G. Grottoli (2011), Testing coral-based tropical cyclone reconstructions: An example from Puerto Rico, *Palaeogeography, Palaeoclimatology, Palaeoecology*, *307*(1–4), 90–97, doi:10.1016/j.palaeo.2011.04.027.

Klinka, K. (2000), *The distribution and synopsis of ecological and silvical characteristics of tree species of British Columbia's forests*, Canadian Cartographics, Coquitlam, BC.

Knowles, J. T., and M. Leitner (2007), Visual representations of the spatial relationship between Bermuda High strengths and hurricane tracks, *Cartographic Perspectives*, (56), 37–51.

Knutson, T. R., J. L. McBride, J. Chan, K. Emanuel, G. Holland, C. Landsea, I. Held, J. P. Kossin, A. K. Srivastava, and M. Sugi (2010), Tropical cyclones and climate change, *Nature Geoscience*, *3*(3), 157–163, doi:10.1038/ngeo779.

Kolodny, Y., R. Calvo, and D. Rosenfeld (2009), "Too low" δ18O of paleo-meteoric, low latitude, water; do paleo-tropical cyclones explain it?, *Palaeogeography, Palaeoclimatology, Palaeoecology*, *280*(3–4), 387–395, doi:10.1016/j.palaeo.2009.06.025.

Krishnaswamy, S., D. Lal, J. M. Martin, and M. Meybeck (1971), Geochronology of lake sediments, *Earth and Planetary Science Letters*, *11*(1–5), 407–414.

Kylander, M.A., E.M. Lind, S. Wastegård, and L. Löwemark (2011), Recommendations for using XRF core scanning as a tool in tephrochronology. *The Holocene, 22*, 371-375.

Laidler, R. B., and D.B. Scott (1996), Foraminifera and Arcellacea from Porters Lake, Nova Scotia: modern distribution and paleodistribution, *Canadian Journal of Earth Sciences*, *33*(10), 1410-1427.

Lambert, W. J., P. Aharon, and A. B. Rodriguez (2008), Catastrophic hurricane history revealed by organic geochemical proxies in coastal lake sediments: a case study of Lake Shelby, Alabama (USA), *Journal of Paleolimnology*, *39*(1), 117–131, doi:10.1007/s10933-007-9101-6.

Landsea, C.W., Anderson, C., Charles, N., Clark, G., Dunion, J., Fernandez-Partagas, J., Hungerford, P., Neumann, c., Zimmer, M. (2004), The Atlantic hurricane database re-analysis project: Documentation for the 1851–1910 alterations and additions to the HURDAT database. In:

Murname RJ and Liu K-b (eds.) *Hurricanes and Typhoons: Past, Present and Future*, 177–221, New York, Columbia University Press.

Landsea, C. W., R. A. Pielke, A. M. Mestas-Nuñez, and J. A. Knaff (1999), Atlantic Basin Hurricanes: Indices of Climate Changes, *Climate Change*, *42*, 89–129.

Lane, P., J. P. Donnelly, J. D. Woodruff, and A. D. Hawkes (2011), A decadally-resolved paleohurricane record archived in the late Holocene sediments of a Florida sinkhole, *Marine Geology*, *287*(1–4), 14–30, doi:10.1016/j.margeo.2011.07.001.

Lawrence, J. R., and S. D. Gedzelman (1996), Low stable isotope ratios of tropical cyclone rains, *Geophysical Research Letters*, *23*(5), 527–530.

Lawrence, J. R., K. Hyeong, R. F. Maddocks, and K.-S. Lee (2008), Passage of Tropical Storm Allison (2001) over southeast Texas recorded in δ18O values of Ostracoda, *Quaternary Research*, *70*(2), 339–342, doi:10.1016/j.yqres.2008.04.004.

Lehmann, A., K. Getzlaff, and J. Harlass (2011), Detailed assessment of climate variability of the Baltic Sea area for the period 1958-2009, *Climate Research,* 46, 185-196, doi: 10.3354/cr00876

Li, Z.-H., N. Labbé, S. G. Driese, and H. D. Grissino-Mayer (2011), Micro-scale analysis of tree-ring δ18O and δ13C on α-cellulose spline reveals high-resolution intra-annual climate variability and tropical cyclone activity, *Chemical Geology*, *284*(1–2), 138–147, doi:10.1016/j.chemgeo.2011.02.015.

Liu, K. (2004), Paleotempestology, in *Hurricanes and typhoons: past, present, and future*, edited by R. J. Murnane and K. Liu, pp. 13–57, Columbia University Press, New York.

Liu, K. (2013), Paleotempestology. In: Elias SA (ed) The Encyclopedia of Quaternary Science. Amsterdam: Elsevier, 209–221, in *The Encyclopedia of Quaternary Science.*, edited by S. Elias, pp. 209–221, Elsevier.

Liu, K., and M. L. Fearn (1993), Lake-sediment record of late Holocene hurricane activities from coastal Alabama, *Geology*, *21*(9), 793–796.

Liu, K., and M. L. Fearn (2000), Reconstruction of Prehistoric Landfall Frequencies of Catastrophic Hurricanes in Northwestern Florida from Lake Sediment Records, *Quaternary Research*, *54*(2), 238–245, doi:10.1006/qres.2000.2166.

Liu, K., H. Lu, and C. Shen (2008), A 1200-year proxy record of hurricanes and fires from the Gulf of Mexico coast: Testing the hypothesis of hurricane–fire interactions, *Quaternary Research*, *69*(1), 29–41, doi:10.1016/j.yqres.2007.10.011.

Liu, K., H. Lu, and C. Shen (2009), Some fundamental misconceptions about paleotempestology, *Quaternary Research*, *71*(2), 253–254, doi:10.1016/j.yqres.2008.11.001.

Liu, K. B., C. Li, T. A. Bianchette, T. A. McCloskey, Q. Yao, and E. Weeks (2011), Storm deposition in a coastal backbarrier lake in Louisiana caused by Hurricanes Gustav and Ike, *Journal of Coastal Research*, (64), 1866.

Löwemark, L., H.F. Chen, T.N. Yang, et al. (2011), Normalizing XRF-scanner data: A cautionary note on the interpretation of high-resolution records from organic-rich lakes, *Journal of Asian Earth Sciences,* 40, 1250-1256.

Malaizé, B., P. Bertran, P. Carbonel, D. Bonnissent, K. Charlier, D. Galop, D. Imbert, N. Serrand, C. Stouvenot, and C. Pujol (2011), Hurricanes and climate in the Caribbean during the past 3700 years BP, *The Holocene*, *21*(6), 911–924, doi:10.1177/0959683611400198.

Malmquist, D.L. (1997), Oxygen isotopes in cave stalagmites as a proxy record of past tropical cyclone activity. *22nd Conference on Hurricanes, American Meteorological Society*, 9(3), 393-394.

Mann, M. E., J. D. Woodruff, J. P. Donnelly, and Z. Zhang (2009), Atlantic hurricanes and climate over the past 1,500 years, *Nature*, *460*(7257), 880–883, doi:10.1038/nature08219.

Mattheus, C. R., and J. K. Fowler (2015), Paleotempestite Distribution across an Isolated Carbonate Platform, San Salvador Island, Bahamas, *Journal of Coastal Research*, *314*, 842–858, doi:10.2112/JCOASTRES-D-14-00077.1.

McAndrews, J.H. (1966), Postglacial history of prairie, savanna, and forest in northwestern Minnesota. *Torrey Botanical Club Memoir*, 22, Torrey Botanical Club, Durham, NC, 72 pp.

McAndrews, J.H. (1988), Human disturbance of North American forests and grasslands: The fossil pollen record. in: Huntly, B., Webb, T. III (eds) *Vegetation History*, Dordrecht, Kluwer Academic Publishers.

McBride, D. (1978), Geology of the Ecum Secum area, Halifax and Guysborough Counties, Nova Scotia., *Nova Scotia Department of Mines*, *78*(1).

McCarroll, D., and N. J. Loader (2004), Stable isotopes in tree rings, *Quaternary Science Reviews*, *23*(7–8), 771–801, doi:10.1016/j.quascirev.2003.06.017.

McCloskey, T., and K. Liu (2012a), A 7000 year record of paleohurricane activity from a coastal wetland in Belize, *The Holocene*, 0959683612460782.

McCloskey, T., and K. Liu (2012b), A sedimentary-based history of hurricane strikes on the southern Caribbean coast of Nicaragua, *Quaternary Research*, *78*(3), 454–464, doi:10.1016/j.yqres.2012.07.003.

McCloskey, T. A., and G. Keller (2009), 5000 year sedimentary record of hurricane strikes on the central coast of Belize, *Quaternary International*, *195*(1–2), 53–68, doi:10.1016/j.quaint.2008.03.003.

McDermott, F. (2004), Palaeo-climate reconstruction from stable isotope variations in speleothems: a review, *Quaternary Science Reviews*, *23*(7–8), 901–918, doi:10.1016/j.quascirev.2003.06.021.

McTaggart-Cowan, R., E. H. Atallah, J. R. Gyakum, and L. F. Bosart (2006), Hurricane Juan (2003). Part I: A diagnostic and compositing life cycle study, *Monthly weather review*, *134*(7), 1725–1747.

Miller, D. L., C. I. Mora, H. D. Grissino-Mayer, C. J. Mock, M. E. Uhle, and Z. Sharp (2006), Tree-ring isotope records of tropical cyclone activity, *Proceedings of the National Academy of Sciences*, *103*(39), 14294–14297.

Mock, C.J. (2004), Tropical cyclone reconstructions from documentary records: Examples for South Carolina, United State. In: Murnane RJ and Liu K-b (eds.) *Hurricanes and Typhoons: Past, Present, and Future*, 121–148, New York, Columbia University Press.

Murray, J.W., (2006), Ecology and Applications of Benthic Foraminifera, New York, Cambridge University Press.

Naquin, J. D., K. Liu, T. A. McCloskey, and T. A. Bianchette (2014), Storm deposition induced by hurricanes in a rapidly subsiding coastal zone, *Journal of Coastal Research*, *70*, 308–313, doi:10.2112/SI70-052.1.

Nikitina, D. L., A. C. Kemp, B. P. Horton, C. H. Vane, O. van de Plassche, and S. E. Engelhart (2014), Storm erosion during the past 2000years along the north shore of Delaware Bay, USA, *Geomorphology*, *208*, 160–172, doi:10.1016/j.geomorph.2013.11.022.

Oliva, F., M. Peros, and A. Viau (2017), A review of the spatial distribution of and analytical techniques used in paleotempestological studies in the western North Atlantic Basin, *Progress in Physical Geography*, 030913331668389, doi:10.1177/0309133316683899.

Otvos, E. G. (2011), Hurricane signatures and landforms—toward improved interpretations and global storm climate chronology, *Sedimentary Geology*, *239*(1–2), 10–22, doi:10.1016/j.sedgeo.2011.04.014.

Otvos, E. G. (2012), Coastal barriers — Nomenclature, processes, and classification issues, *Geomorphology*, *139–140*, 39–52, doi:10.1016/j.geomorph.2011.10.037.

Paciorek, C.J., J.S. Risbey, V. Ventura, and R.D. Rosen(2002), Multiple Indices of Northern Hemisphere Cyclone Activity, Winters 1949-99, *American Meteorological Society,* 15, 1573-1590

Peros, M., B. Gregory, F. Matos, E. Reinhardt, and J. Desloges (2015), Late-Holocene record of lagoon evolution, climate change, and hurricane activity from southeastern Cuba, *The Holocene*, *25*(9), 1483–1497, doi:10.1177/0959683615585844.

Peros, M. C., E. G. Reinhardt, and A. M. Davis (2007a), A 6000-year record of ecological and hydrological changes from Laguna de la Leche, north coastal Cuba, *Quaternary Research*, *67*(1), 69–82, doi:10.1016/j.yqres.2006.08.004.

Peros, M. C., E. G. Reinhardt, H. P. Schwarcz, and A. M. Davis (2007b), High-resolution paleosalinity reconstruction from Laguna de la Leche, north coastal Cuba, using Sr, O, and C isotopes, *Palaeogeography, Palaeoclimatology, Palaeoecology*, *245*(3–4), 535–550, doi:10.1016/j.palaeo.2006.09.006.

Ponomarenko, E. (2009), Reconstruction of Pre-historical and early Historical Forest Fires in Kejimkujik National Park and Historic Site, *Parks Canada*, 1-47.

Porter, T. J., and P. Middlestead (2012), On estimating the precision of stable isotope ratios in processed tree-rings, *Dendrochronologia*, *30*(3), 239–242, doi:10.1016/j.dendro.2012.02.001.

Porter, T. J., M. F. J. Pisaric, R. D. Field, S. V. Kokelj, T. W. D. Edwards, P. deMontigny, R. Healy, and A. N. LeGrande (2013), Spring-summer temperatures since AD 1780 reconstructed from stable oxygen isotope ratios in white spruce tree-rings from the Mackenzie Delta, northwestern Canada, *Climate Dynamics*, *42*(3–4), 771–785, doi:10.1007/s00382-013-1674-3.

Reese, C. A., T. P. Strange, W. D. Lynch, and K. Liu (2008), Geologic Evidence of Hurricane Katrina Recovered from the Pearl River Marsh, MS/LA, *Journal of Coastal Research*, *246*, 1601–1607, doi:10.2112/07-0956.1.

Reimer, P. J. et al. (2013), IntCal13 and Marine13 radiocarbon age calibration curves 0–50,000 years cal BP, *Radiocarbon*, *55*(4), 1869–1887.

Rhein, M. et al. (n.d.), Observation: Ocean, in *Climate Change 2013: The Physical Science Basis Contribution of Working Group I to the Fifth Assessment Report of the Intergovernmental Panel on Climate Change*, Cambridge University Press, Cambridge, United Kingdom and New York, NY, USA.

Romero-Lankao, P., J.B. Smith, D.J. Davidson, et al. (2015), North America. In: Barros, V.R., Field, C.B., Dokken, D.J., et al. (eds) *Climate Change 2014: Impacts, Adaptation, and Vulnerability. Part B: Regional Aspects. Contribution of Working Group II to the Fifth Assessment Report of the Intergovernmental Panel on Climate Change*. Cambridge, New York: Cambridge University Press, pp.1439-1498.

Rothwell, R. G., and I. w. Croudace (2015), Twenty Years of XRF Core Scanning Marine Sediments: What Do Geochemical Proxies Tell Us?, in *Micro-XRF Studies of Sediment Cores*, vol. 17, edited by I. W. Croudace and R. G. Rothwell, pp. 25–102, Springer Netherlands, Dordrecht.

Rothwell, R. G., and F. R. Rack (2006), New techniques in sediment core analysis: an introduction, *Geological Society, London, Special Publications*, *267*(1), 1–29.

Sabatier, P., L. Dezileau, C. Colin, L. Briqueu, F. Bouchette, P. Martinez, G. Siani, O. Raynal, and U. Von Grafenstein (2012), 7000years of paleostorm activity in the NW Mediterranean Sea in response to Holocene climate events, *Quaternary Research*, *77*(1), 1–11, doi:10.1016/j.yqres.2011.09.002.

Schott, T., Landsea, C., Hafele, G., Lorens, J., Taylor, A., Thurm, H., Ward, B., Willis, M., & W. Zaleski (2012), The Saffir-Simpson hurricane wind scale, *NOAA/National Weather Service [Internet]*, 1-4.

Scileppi, E., and J.P. Donnelly (2007), Sedimentary evidence of hurricane strikes in western Long Island, New York, *Geochemistry, Geophysics, Geosystems,* 8(6).

Scott, D. B. (1977), Physiographic and oceanographic characteristics of Chezzetcook Inlet, Nova Scotia,

Scott, D. B., and F. S. Medioli (1980), Living vs. total foraminiferal populations:their relative useflness in paleoexology, *Journal of paleontology*, 813–831.

Scott, D. B., K. Brown, E. S. Collins, and F. S. Medioli (1995), A new sea-level curve from Nova Scotia: evidence for a rapid acceleration of sea-level rise in the late mid-Holocene, *Canadian Journal of Earth Sciences*, *32*(12), 2071–2080.

Scott, D. B., F. S. Medioli, and C. T. Schafer (2001), *Monitoring in coastal environments using Foraminifera and Thecamoebian indicators*, Cambridge University Press, Cambridge ; New York.

Scott, D. B., E. S. Collins, P. T. Gayes, and E. Wright (2003), Records of prehistoric hurricanes on the South Carolina coast based on micropaleontological and sedimentological evidence, with comparison to other Atlantic Coast records, *Geological Society of America Bulletin*, *115*(9), 1027–1039.

Speer, J.H. (2010), Fundamentals of Tree Ring Research, Tuscon, The University of Arizona Press.

Toomey, M. R., W. B. Curry, J. P. Donnelly, and P. J. van Hengstum (2013), Reconstructing 7000 years of North Atlantic hurricane variability using deep-sea sediment cores from the western Great Bahama Bank: A 7000 YR RECORD OF HURRICANE ACTIVITY, *Paleoceanography*, *28*(1), 31–41, doi:10.1002/palo.20012.

Tory, K. J., and W.M. Frank (2010), Tropical cyclone formation, *Global perspectives on tropical cyclones: From science to mitigation*, *4*, 55.

Trouet, V., J. Esper, N. E. Graham, A. Baker, J. D. Scourse, and D. C. Frank (2009), Persistent positive North Atlantic Oscillation mode dominated the medieval climate anomaly, *science*, *324*(5923), 78–80.

Vaasma, T. (2008), Grain-size analysis of lacustrine sediments: a comparison of pre-treatment methods, *Estonian Journal of Ecology*, *57*(4), 231, doi:10.3176/eco.2008.4.01.

Van Hengstum, P. J., J. P. Donnelly, M. R. Toomey, N. A. Albury, P. Lane, and B. Kakuk (2014), Heightened hurricane activity on the Little Bahama Bank from 1350 to 1650 AD, *Continental Shelf Research*, *86*, 103–115, doi:10.1016/j.csr.2013.04.032.

Van Hengstum, P. J., J. P. Donnelly, P. L. Fall, M. R. Toomey, N. A. Albury, and B. Kakuk (2016), The intertropical convergence zone modulates intense hurricane strikes on the western North Atlantic margin, *Scientific Reports*, *6*, 21728, doi:10.1038/srep21728.

Vecchi, G. A., and T. R. Knutson (2008), On Estimates of Historical North Atlantic Tropical Cyclone Activity, *Journal of Climate*, *21*(14), 3580–3600, doi:10.1175/2008JCLI2178.1.

Viau, A.E., K. Gajewski, M.C. Sawada, P. Fines (2006), Millennial-scale temperature variations in North America during the Holocene, *Journal of Geophysical Research: Atmospheres,* 111(D9)

Wallace, D. J., and J. B. Anderson (2010), Evidence of similar probablility of intense hurricane strikes for the Gulf of Mexico over the late Holocene, *Geology*, *38*(6), 511–514.

Wallace, D. J., J. D. Woodruff, J. B. Anderson, and J. P. Donnelly (2014), Palaeohurricane reconstructions from sedimentary archives along the Gulf of Mexico, Caribbean Sea and western

North Atlantic Ocean margins, *Geological Society, London, Special Publications*, *388*(1), 481–501, doi:10.1144/SP388.12.

Wanamaker, A. D., K. J. Kreutz, B. R. Schöne, N. Pettigrew, H. W. Borns, D. S. Introne, D. Belknap, K. A. Maasch, and S. Feindel (2008), Coupled North Atlantic slope water forcing on Gulf of Maine temperatures over the past millennium, *Climate Dynamics*, *31*(2–3), 183–194, doi:10.1007/s00382-007-0344-8.

Weltje, G. J., and R. Tjallingii (2008), Calibration of XRF core scanners for quantitative geochemical logging of sediment cores: Theory and application, *Earth and Planetary Science Letters*, *274*(3–4), 423–438, doi:10.1016/j.epsl.2008.07.054.

Williams, H. F. L. (2009), Stratigraphy, Sedimentology, and Microfossil Content of Hurricane Rita Storm Surge Deposits in Southwest Louisiana, *Journal of Coastal Research*, *254*, 1041–1051, doi:10.2112/08-1038.1.

Williams, H. F. L. (2010), Storm surge deposition by Hurricane Ike on the McFaddin National Wildlife Refuge, Texas: implications for paleotempestology studies, *The Journal of Foraminiferal Research*, *40*(3), 210–219.

Williams, H. F. L. (2013), 600-year sedimentary archive of hurricane strikes in a prograding beach ridge plain, southwestern Louisiana, *Marine Geology*, *336*, 170–183, doi:10.1016/j.margeo.2012.12.005.

Woodruff, J. D., J. P. Donnelly, D. Mohrig, and W. R. Geyer (2008), Reconstructing relative flooding intensities responsible for hurricane-induced deposits from Laguna Playa Grande, Vieques, Puerto Rico, *Geology*, *36*(5), 391–394.

Woodruff, J. D., J. P. Donnelly, and A. Okusu (2009), Exploring typhoon variability over the mid-to-late Holocene: evidence of extreme coastal flooding from Kamikoshiki, Japan, *Quaternary Science Reviews*, *28*(17–18), 1774–1785, doi:10.1016/j.quascirev.2009.02.005.

Woodruff, J. D., J. L. Irish, and S. J. Camargo (2013), Coastal flooding by tropical cyclones and sea-level rise, *Nature*, *504*(7478), 44–52, doi:10.1038/nature12855.

Yu, S.-Y., J. Shen, S. M. Colman, and others (2007), Modeling the radiocarbon reservoir effect in lacustrine systems, *Radiocarbon*, *49*(3), 1241–1254.

Ziegler, M., T. Jilbert, G. J. de Lange, L. J. Lourens, and G.-J. Reichart (2008), Bromine counts from XRF scanning as an estimate of the marine organic carbon content of sediment cores: BROMINE AS ESTIMATOR OF SEDIMENT COMPOSITION, *Geochemistry, Geophysics, Geosystems*, *9*(5), n/a-n/a, doi:10.1029/2007GC001932.

Appendix 1: Supporting Methodology (Chapter 3).

In the literature, the reporting of past hurricane strikes from sedimentary records is generally undertaken in one of three ways:

1) The identification of individual hurricane strikes (based on the presence of a single "event bed", and an age associated with it based on the dating (usually by ^{14}C) of organic material in close association with the event bed (e.g. Adomat and Gischler, 2016). This produces an age for the hurricane event, with associated error bars based on the 2-sigma distribution of the ^{14}C date.

2) The reporting of the number events beds (either one or more) within a specific age range (but without specific ages or errors assigned to each individual event bed)(e.g., Das et al., 2014); and,

3) The reporting of an interval of enhanced hurricane activity based on the presence of coarser sediment that is presumed to represent multiple hurricane strikes over this period of time (e.g., Donnelly and Woodruff, 2007), but where individual events are not distinguished by the authors.

The reasons why some records are more likely to contain evidence of single event beds, rather than periods of enhanced hurricane activity, depend on factors which include (but are not necessarily limited to): 1) the local sedimentation rate (i.e., a lower sedimentation rate will usually mean individual events may be hard to resolve; 2) the frequency of hurricane strikes (fewer strikes mean that individual events may be easier to resolve); 3) the sampling interval at which analysis is done (i.e., higher resolution sampling will better enable more events to be discerned); and 4) sediment mixing or bioturbation (which might mix evidence of single event beds, especially if very thin).

The database of 59 records contains evidence for past hurricane activity reported in one, or two of the three of the categories described above. Seventeen of these 59 studies provide dates on individual hurricane events and 24 studies provided data in interval form but with no information concerning individual events. In addition, 21 studies did not provide information suitable for our investigation (i.e., they focused only on the identification of a single, modern hurricane event, with no analysis of older sedimentary deposits).

In order to quantitatively compare paleotempestological records made using different techniques (e.g., sediment grain size, geochemical, etc.) and reported in different ways (see above), we determined the event frequency of all data that falls into categories 1 and 2. Data that falls into category 3 was excluded from our analysis but is considered separately in the discussion section of this paper. In total, our analysis is based on 37 sites from the 59 in our original database.

Calculation of event frequency and data binning methodologies

Event Frequency

For single event data, the event frequency is calculated as either 1 event per 100 years, or less than 1 event per 100 years if the error bar range exceeds 100 years. For interval data, the frequency is given by the number of events, divided by the interval range (given in 100yrs).

Binning Methodology

Event frequencies within a range or within error bars are assigned to 100-bins. Invariably, ranges or error bars extend across 100-year bins, in which case the event frequency is applied equally to multiple bins. However, when error bars from two separate events at a single study location overlap within any given 100-yr bin, a mean event frequency is calculated to represent both events.

The overall range of data for each study location is from present (1950) to the oldest assessed event age. Within these overall ranges, 100-year periods with no recorded events are assumed to have an event frequency of zero. Qualitative assessments of frequency (e.g. Donnelly and Woodruff, 2007) were excluded from the analysis.

Data type	Data type description	Interval or error bars >100 years	Interval or error bars <=100 years
Single Event Data	Single event age, with error bars	$F_e = 1\ [event/100\ yrs] \times \left(\frac{100\ [yrs]}{range\ [yrs]}\right)$ $Therefore\ F_e < 1$	$F_e = 1$
Interval Data	There are one or more events reported within an age range, but no specific event dates provided are by the authors. Furthermore, there are no error bars provided on the estimate of the number of events, or on the extents of the age range.	$F_e = \frac{n_e}{range\ [100\ yrs]}$	$F_e = \frac{n_e}{range\ [100\ yrs]}$

Table A1. Calculation of event frequency [# events per 100 years]. F_e **= event frequency [#events/100 yrs];** n_e **= number of reported events; and range = difference between oldest age and youngest age in a range, or difference between error bars.**

Appendix 2: XRF counts by element (Chapter 4).

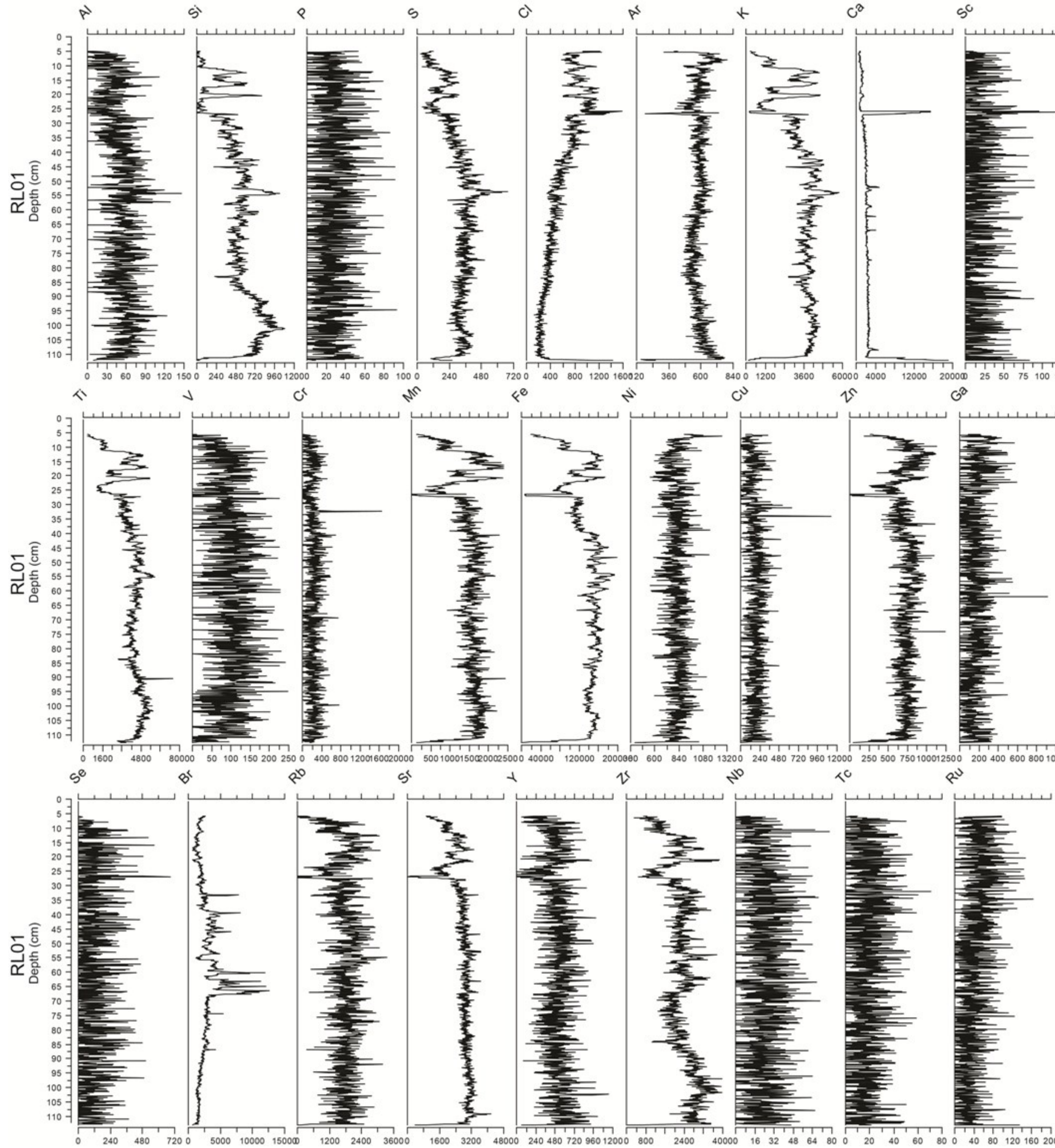

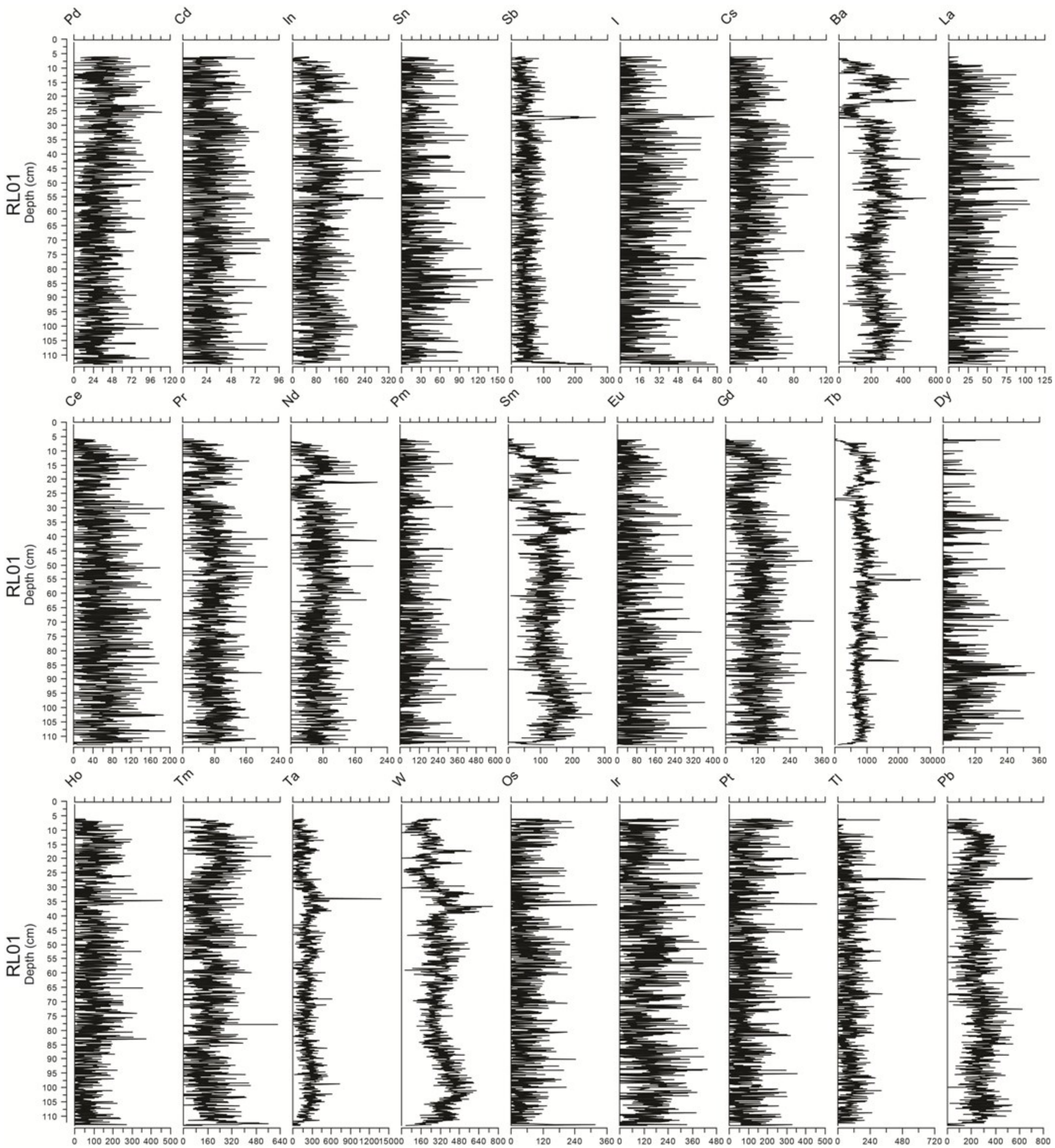

Pd
Cd
In
Sn
Sb
I
Cs
Ba
La
Ce
Pr
Nd
Pm
Sm
Eu
Gd
Tb
Dy
Ho
Tm
Ta
W
Os
Ir
Pt
Tl
Pb
RL01
Depth (cm)

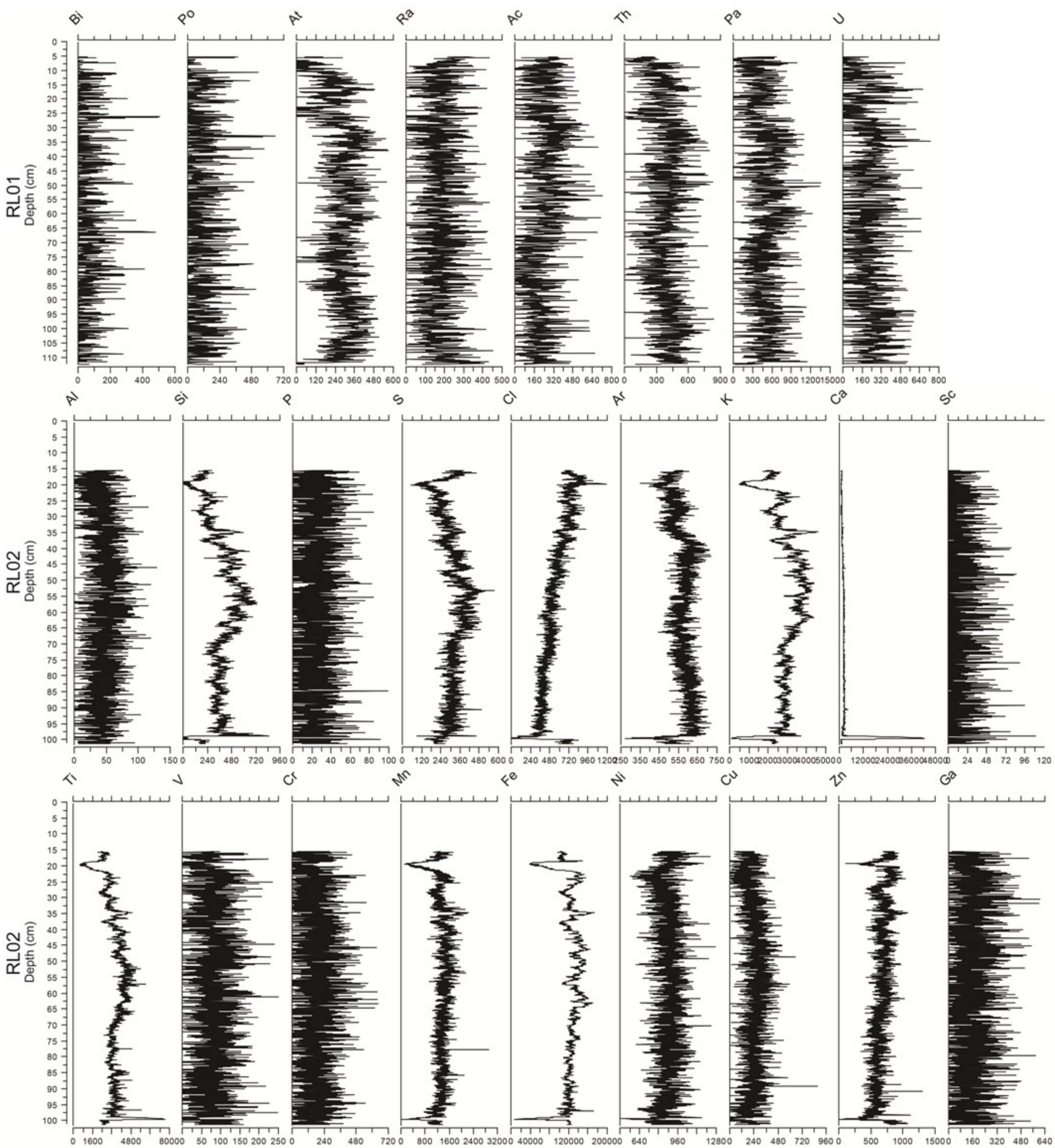
RL01
Depth (cm)
Bi
Po
At
Ra
Ac
Th
Pa
U
RL02
Depth (cm)
Al
Si
P
S
Cl
Ar
K
Ca
Sc
RL02
Depth (cm)
Ti
V
Cr
Mn
Fe
Ni
Cu
Zn
Ga

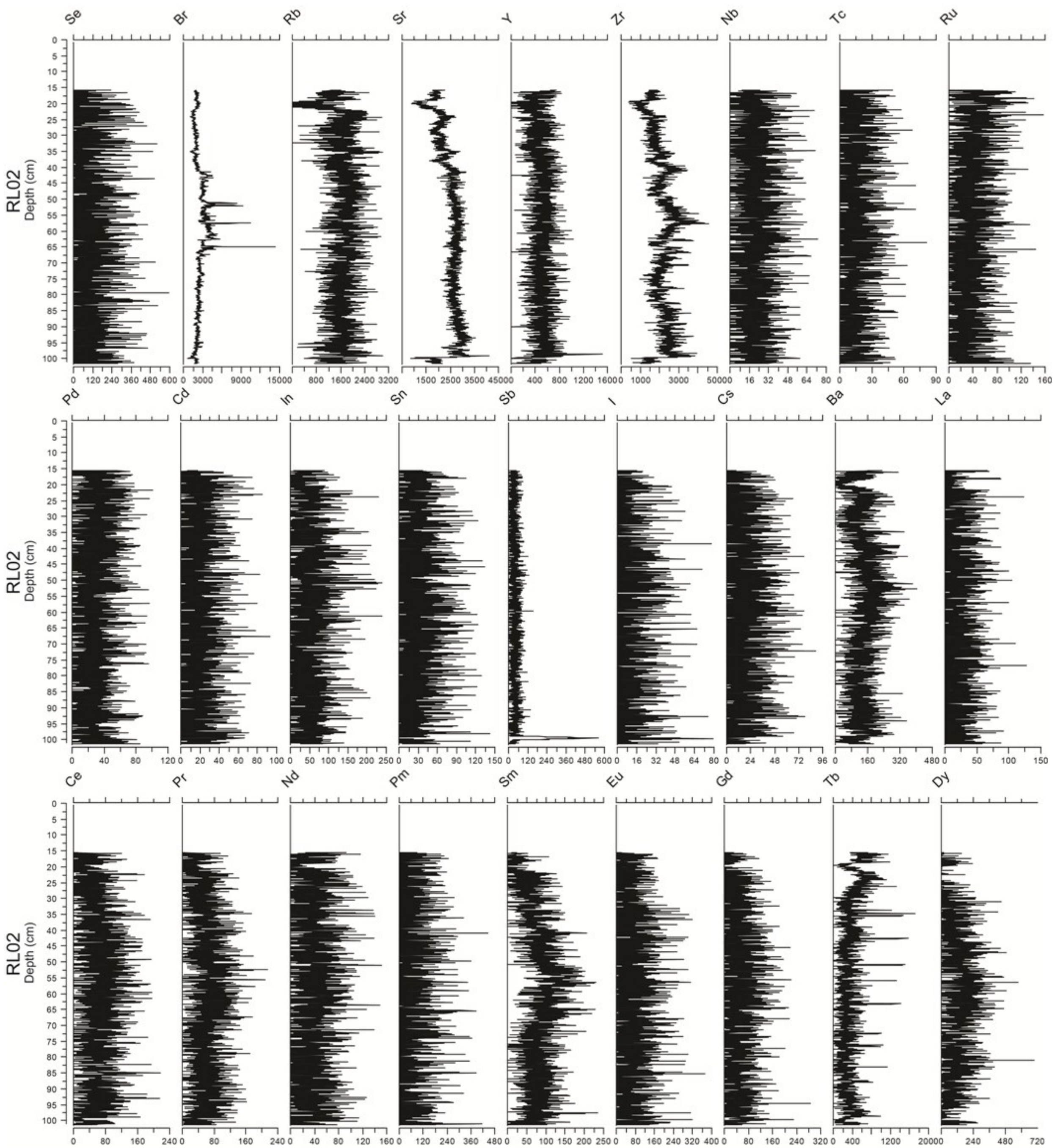
Se
Br
Rb
Sr
Y
Zr
Nb
Tc
Ru
RL02
Depth (cm)
Pd
Cd
In
Sn
Sb
I
Cs
Ba
La
RL02
Depth (cm)
Ce
Pr
Nd
Pm
Sm
Eu
Gd
Tb
Dy
RL02
Depth (cm)

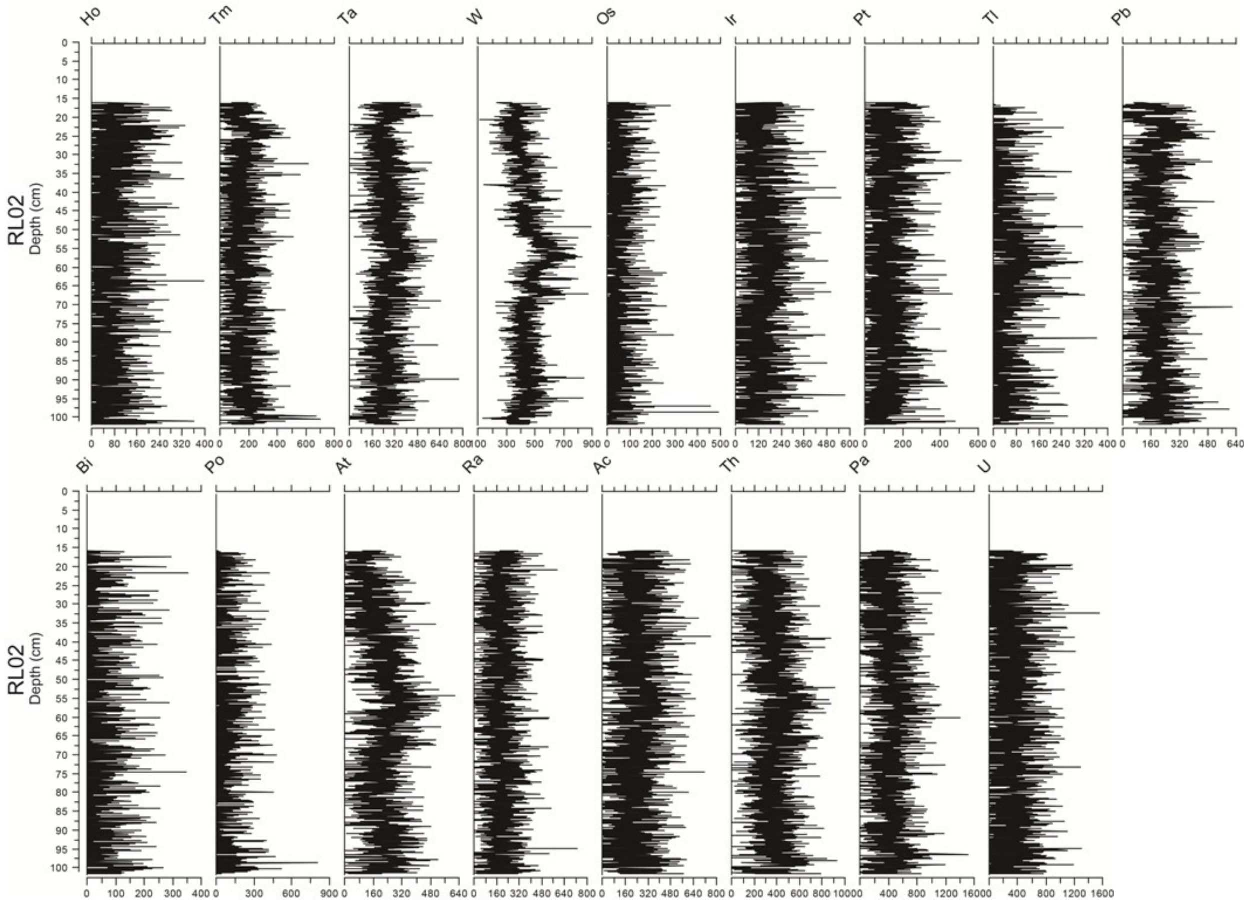

Ho
Tm
Ta
W
Os
Ir
Pt
Tl
Pb
RL02
Depth (cm)
Bi
Po
At
Ra
Ac
Th
Pa
U

Appendix 3: Raw ^{210}Pb counts (Chapter 4).

UQPo	ID	Depth (cm)	^{210}Pb dpm/g	±
		RL01		
8599	RL1DO 0-1cm	0.5	18.204	0.763
8604	RL1DO 1-2cm	1.5	21.402	0.816
8601	RL1DO 2-3cm	2.5	23.109	0.983
8602	RL1DO 3-4cm	3.5	22.219	0.962
8603	RL1DO 4-5cm	4.5	22.500	0.957
8600	RL1DO 5-6cm	5.5	23.338	0.953
8605	RL1DO 6-7cm	6.5	19.292	0.748
8606	RL1DO 7-8cm	7.5	17.366	0.693
8607	RL1DO 8-9cm	8.5	15.012	0.643
8611	RL1DO 9-10cm	9.5	11.012	0.526
8612	RL1DO 10-11cm	10.5	6.727	0.325
8613	RL1DO 11-12cm	11.5	2.809	0.168
8614	RL1DO 12-13cm	12.5	2.949	0.167
8615	RL1DO 13-14cm	13.5	2.960	0.176
8616	RL1DO 14-15cm	14.5	2.521	0.156
8617	RL1DO 15-16cm	15.5	1.951	0.118
8618	RL1DO 16-17cm	16.5	2.239	0.147
8619	RL1DO 17-18cm	17.5	2.349	0.156

8620	RL1DO 18-19cm	18.5	2.628	0.171
8621	RL1DO 19-20cm	19.5	3.304	0.187
		RL02		
8428	RL02-DO (0-1) cm	0.500	27.646	0.993
8429	RL02-DO (1-2) cm	1.500	28.642	1.044
8430	RL02-DO (2-3) cm	2.500	24.810	0.900
8431	RL02-DO (3-4) cm	3.500	28.311	1.056
8432	RL02-DO (4-5) cm	4.500	26.153	0.946
8433	RL02-DO (5-6) cm	5.500	23.320	0.862
8434	RL02-DO (6-7) cm	6.500	22.939	0.849
8435	RL02-DO (7-8) cm	7.500	20.888	0.768
8436	RL02-DO (8-9) cm	8.500	21.371	0.781
8437	RL02-DO (9-10) cm	9.500	23.017	0.851
8438	RL02-DO (10-11) cm	10.500	22.796	0.843
8439	RL02-DO (11-12) cm	11.500	21.699	0.799
8440	RL02-DO (12-13) cm	12.500	19.980	0.747
8441	RL02-DO (13-14) cm	13.500	13.286	0.513
8442	RL02-DO (14-15) cm	14.500	8.349	0.317
8510	RL2DO suite1	15.500	2.421	0.125
8511	RL2DO suite2	16.500	4.340	0.203
8512	RL2DO suite3	17.500	4.347	0.199

8513	RL2DO suite4	18.500	3.502	0.158
8514	RL2DO suite5	19.500	3.789	0.177
8515	RL2DO suite6	20.500	3.844	0.181
8516	RL2DO suite7	21.500	4.078	0.194
8517	RL2DO suite8	22.500	4.805	0.231
8518	RL2DO suite9	23.500	5.606	0.273
8519	RL2DO suite10	24.500	6.748	0.314
8520	RL2DO suite11	25.500	8.448	0.394
8521	RL2DO suite12	26.500	6.562	0.297

Appendix 4: Raw laboratory results for isotopic analysis (GG Hatch Lab, University of Ottawa) (Chapter 5)

OurLabID	Sample ID	Delta 18O (‰)	%O	Ampl 28 (mV)	Weight (mg)
G-19181	EPT1-BE-2013	26.1	50.8	4992	0.268
G-19182	EPT1-BL-2013	25.6	50.6	5266	0.285
G-19183	EPT1-BE-2012	26.7	48.8	6347	0.36
G-19184	EPT1-BL-2012	25.8	49.8	6153	0.341
G-19185	EPT1-BE-2011	25.3	50.9	5707	0.308
G-19186	EPT1-BE-2011 QCD	27.2	49.7	5552	0.306
G-19187	EPT1-BL-2011	23.3	49.3	6061	0.339
G-19188	EPT1-BE-2010	25.7	51.4	5360	0.285
G-19189	EPT1-BL-2010	26.2	49.1	5488	0.306
G-19190	EPT1-BE-2009	26.9	52.8	5421	0.281
G-19191	EPT1-BL-2009	27.1	50.0	5799	0.318
G-19192	EPT1-BE-2008	25.3	53.0	5228	0.269
G-19193	EPT1-BL-2008	25.1	51.6	5496	0.291
G-19194	EPT1-BE-2007	26.9	51.5	5347	0.283
G-19195	EPT1-BL-2007	25.8	50.8	5488	0.295
G-19196	EPT1-BE-2006	25.4	50.2	5704	0.311
G-19197	EPT1-BE-2006 QCD	25.4	53.8	5196	0.263
G-19198	EPT1-BL-2006	28.2	50.9	5634	0.303
G-19199	EPT1-BE-2005	25.8	49.3	5498	0.305
G-19200	EPT1-BL-2005	26.5	51.5	5508	0.292
G-19201	EPT1-BE-2004	26.4	51.0	5493	0.294
G-19202	EPT1-BL-2004	26.9	48.4	4837	0.271
G-19203	EPT1-BE-2003	25.4	50.6	5399	0.291
G-19204	EPT1-BL-2003	27.7	51.5	5580	0.296
G-19205	EPT1-BE-2002	24.9	49.8	5092	0.278
G-19206	EPT1-BL-2002	26.6	52.4	6007	0.315
G-19207	EPT1-BE-2001	25.9	50.5	4995	0.269
G-19208	EPT1-BE-2001 QCD	25.8	51.8	5174	0.272
G-19209	EPT1-BL-2001	26.5	51.6	6362	0.34
G-19210	EPT1-BE-2000	26.4	51.0	5471	0.293
G-19211	EPT1-BL-2000	27.5	51.0	5610	0.301
G-19212	EPT1-BE-1999	26.4	50.4	5972	0.325
G-19213	EPT1-BL-1999	26.7	50.2	5237	0.284
G-19214	EPT1-BE-1998	25.6	50.2	5538	0.301
G-19215	EPT1-BL-1998	26.8	49.1	5148	0.285
G-19216	EPT1-BE-1997	25.7	51.1	5821	0.312
G-19217	EPT1-BL-1997	28.5	52.6	5162	0.267
G-19218	EPT1-BE-1996	25.3	51.3	5494	0.292
G-19219	EPT1-BE-1996 QCD	24.6	50.0	5536	0.302
G-19220	EPT1-BL-1996	27.1	50.4	5491	0.297
G-19221	EPT1-AL-2013	27.2	48.3	4849	0.272
G-19222	EPT1-AL-2012	0.0	0.0		0
G-19223	EPT1-AE-2011	0.0	0.0		0
G-19224	EPT1-AL-2011	0.0	0.0		0

G-19225	EPT1-AE-2010	27.0	52.9	5089	0.261
G-19226	EPT1-AL-2010	26.8	52.9	5729	0.296
G-19227	EPT1-AE-2009	26.6	53.6	5648	0.288
G-19228	EPT1-AL-2009	27.6	50.1	5392	0.293
G-19229	EPT1-AE-2008	26.6	51.1	5735	0.307
G-19230	EPT1-AE-2008 QCD	26.5	51.4	5732	0.305
G-19231	EPT1-AL-2008	25.0	52.2	5888	0.309
G-19232	EPT1-AE-2007	26.0	51.5	5317	0.281
G-19233	EPT1-AL-2007	26.5	48.3	5404	0.304
G-19234	EPT1-AE-2006	26.1	47.6	5324	0.304
G-19235	EPT1-AL-2006	25.5	53.7	5539	0.281
G-19236	EPT1-AE-2005	26.4	48.0	5382	0.305
G-19237	EPT1-AL-2005	26.5	56.3	5869	0.285
G-19238	EPT1-AE-2004	26.5	46.1	5182	0.305
G-19239	EPT1-AL-2004	26.8	60.1	5944	0.271
G-19240	EPT1-AE-2003	26.2	47.7	5627	0.322
G-19241	EPT1-AE-2003 QCD	26.2	52.5	5359	0.278
G-19242	EPT1-AL-2003	27.6	50.6	5763	0.311
G-19243	EPT1-AE-2002	25.7	50.4	5495	0.297
G-19244	EPT1-AL-2002	24.2	49.6	5435	0.315
G-19245	EPT1-AE-2001	25.9	51.0	5247	0.295
G-19246	EPT1-AL-2001	26.8	50.6	5320	0.302
G-19247	EPT1-AE-2000	24.0	48.6	5146	0.303
G-19248	EPT1-AL-2000	24.2	49.5	5017	0.29
G-19249	EPT1-AE-1999	24.3	48.4	5170	0.306
G-19250	EPT1-AL-1999	26.1	48.9	5877	0.347
G-19251	EPT1-AE-1998	26.3	49.2	5101	0.297
G-19252	EPT1-AE-1998 QCD	24.7	50.8	5496	0.311
G-19253	EPT1-AL-1998	26.5	50.2	5085	0.29
G-19254	EPT1-AE-1997	26.5	49.4	5223	0.303
G-19255	EPT1-AL-1997	26.3	50.0	5933	0.343
G-19256	EPT1-AE-1996	25.3	50.4	5537	0.316
G-19257	EPT1-AL-1996	27.3	50.5	4881	0.276
G-19258	RLT8-BE-2010	28.7	53.7	5579	0.299
G-19259	RLT8-BL-2010	27.6	53.6	5429	0.291
G-19260	RLT8-BE-2009	26.6	49.8	5099	0.293
G-19261	RLT8-BL-2009	28.3	54.6	5290	0.278
G-19262	RLT8-BE-2008	26.5	52.3	5107	0.28
G-19263	RLT8-BE-2008 QCD	26.9	50.2	5152	0.294
G-19264	RLT8-BL-2008	25.5	49.7	5722	0.332
G-19265	RLT8-BE-2007	27.5	50.4	5034	0.286
G-19266	RLT8-BL-2007	26.9	51.4	4822	0.268
G-19267	RLT8-BE-2006	27.3	51.0	5407	0.305
G-19268	RLT8-BL-2006	28.6	54.0	5270	0.28
G-19269	RLT8-BE-2005	28.0	50.7	5391	0.306
G-19270	RLT8-BL-2005	26.6	48.8	5021	0.295
G-19271	RLT8-BE-2004	26.9	50.6	5237	0.297
G-19272	RLT8-BL-2004	27.4	49.0	5202	0.305

G-19273	RLT8-BE-2003	27.4	51.1	5389	0.303
G-19274	RLT8-BE-2003 QCD	27.0	50.2	5108	0.292
G-19275	RLT8-BL-2003	27.4	51.7	5323	0.296
G-19276	RLT8-BE-2002	27.2	50.6	5730	0.327
G-19277	RLT8-BL-2002	27.6	50.9	5447	0.308
G-19278	RLT8-BE-2001	26.3	48.9	4889	0.286
G-19279	RLT8-BL-2001	28.8	44.7	4627	0.296
G-19280	RLT8-BE-2000	25.8	50.0	5239	0.301
G-19281	RLT8-BL-2000	27.4	52.0	5174	0.286
G-19282	RLT8-BE-1999	27.4	49.6	5032	0.291
G-19283	RLT8-BL-1999	26.2	50.1	5440	0.313
G-19284	RLT8-BE-1998	25.1	48.9	5390	0.317
G-19285	RLT8-BE-1998 QCD	24.6	48.6	5445	0.323
G-19286	RLT8-BL-1998	27.3	49.3	4998	0.291
G-19287	RLT8-BE-1997	26.9	51.1	5508	0.311
G-19288	RLT8-BL-1997	26.5	51.2	5899	0.334
G-19289	RLT8-BE-1996	25.2	50.6	5164	0.293
G-19290	RLT8-BL-1996	25.5	49.6	4983	0.288
G-19291	RLT8-BE-1995	26.2	49.8	5281	0.305
G-19292	RLT8-BL-1995	28.3	51.1	5347	0.301
G-19293	RLT8-BE-1994	27.0	50.7	5607	0.319
G-19294	RLT8-BL-1994	26.1	49.3	5005	0.291
G-19295	RLT8-BE-1993	26.6	48.7	4791	0.281
G-19296	RLT8-BE-1993 QCD	26.2	49.2	5325	0.311
G-19297	RLT8-BL-1993	26.7	46.3	4772	0.295
G-19298	RLT8-BE-1992	26.0	50.7	5147	0.291
G-19299	RLT8-BL-1992	26.0	50.1	5337	0.306
G-19300	RLT8-BE-1991	27.9	50.1	5406	0.31
G-19301	RLT8-BL-1991	26.0	49.2	5512	0.323
G-19302	RLT8-BE-1990	25.9	54.6	5748	0.304
G-19303	RLT8-BL-1990	27.8	48.9	4695	0.274
G-19304	RLT8-BE-1989	24.4	49.2	4918	0.288
G-19305	RLT8-BL-1989	26.7	42.9	4423	0.296
G-19306	RLT8-BE-1988	25.6	50.5	4875	0.278
G-19307	RLT8-BE-1988 QCD	26.5	46.9	4520	0.277
G-19308	RLT8-BL-1988	25.9	46.1	5057	0.317
G-19309	RLT8-BE-1987	26.5	40.9	4828	0.34
G-19310	RLT8-BL-1987	27.2	49.0	4715	0.277
G-19311	RLT8-BE-1986	25.9	45.7	4458	0.28
G-19312	RLT8-BL-1986	26.4	51.7	4601	0.256
G-19313	RLT8-BE-1985	24.8	45.3	5126	0.328
G-19314	RLT8-BL-1985	25.4	47.1	5193	0.319
G-19315	RLT8-BE-1984	25.7	55.1	5806	0.307
G-19316	RLT8-BL-1984	26.1	49.8	5419	0.316
G-19317	RLT8-BE-1983	24.6	47.9	4754	0.286
G-19318	RLT8-BE-1983 QCD	24.2	47.9	4583	0.275
G-19319	RLT8-BL-1983	25.4	48.4	5165	0.309
G-19320	RLT2-AE-2005	26.0	50.0	5125	0.297

G-19321	RLT2-AL-2005	26.9	48.1	5299	0.32
G-19322	RLT2-AE-2004	27.0	48.8	5515	0.329
G-19323	RLT2-AL-2004	27.1	50.4	5200	0.299
G-19324	RLT2-AE-2003	26.7	49.6	5663	0.333
G-19325	RLT2-AL-2003	26.9	48.9	5128	0.304
G-19326	RLT2-AE-2002	26.6	44.5	4897	0.318
G-19327	RLT2-AL-2002	26.7	50.3	5396	0.312
G-19328	RLT2-AE-2001	26.8	46.8	5094	0.315
G-19329	RLT2-AE-2001 QCD	26.6	45.4	5077	0.324
G-19330	RLT2-AL-2001	27.7	54.3	5608	0.301
G-19331	RLT2-AE-2000	27.4	45.0	5429	0.351
G-19332	RLT2-AL-2000	26.8	51.5	5145	0.29
G-19333	RLT2-AE-1999	25.7	46.7	5119	0.32
G-19334	RLT2-AL-1999	28.4	49.5	5459	0.321
G-19335	RLT2-AE-1998	25.2	47.9	4913	0.297
G-19336	RLT2-AL-1998	26.4	49.5	5012	0.294
G-19337	RLT2-AE-1997	25.7	45.2	4849	0.311
G-19338	RLT2-AL-1997	26.2	49.0	5305	0.315
G-19339	RLT2-AE-1996	24.1	44.5	4456	0.289
G-19340	RLT2-AE-1996 QCD	24.0	41.3	4527	0.317
G-19341	RLT2-AL-1996	17.2	41.6	4577	0.318
G-19342	RLT2-AE-1995	24.7	46.8	4964	0.308
G-19343	RLT2-AL-1995	24.8	43.7	4520	0.299
G-19344	RLT2-AE-1994	26.3	49.2	4935	0.291
G-19345	RLT2-AL-1994	26.5	51.2	5054	0.287
G-19346	RLT2-AE-1993	23.6	40.5	4062	0.289
G-19347	RLT2-AL-1993	26.7	49.2	4851	0.287
G-19348	RLT2-AE-1992	25.3	48.0	4774	0.289
G-19349	RLT2-AL-1992	14.4	68.1	7321	0.323
G-19350	RLT2-AE-1991	25.5	46.1	4965	0.314
G-19351	RLT2-AE-1991 QCD	25.5	44.4	4577	0.299
G-19352	RLT2-AL-1991	25.0	44.7	4260	0.276
G-19353	RLT2-AE-1990	25.4	48.6	5044	0.303
G-19354	RLT2-AL-1990	0.0	0.0		0
G-19355	RLT2-AE-1989	19.3	45.9	4967	0.316
G-19356	RLT2-AL-1989	19.0	46.1	4796	0.303
G-19357	RLT2-AE-1988	0.0	0.0		0
G-19358	RLT2-AL-1988	26.1	52.3	4942	0.276
G-19359	RLT2-AE-1987	26.1	49.4	5382	0.32
G-19360	RLT2-AL-1987	0.0	0.0		0
G-19361	RLT2-AE-1986	0.0	0.0		0
G-19362	RLT2-AE-1986 QCD	0.0	0.0		0
G-19363	RLT2-AL-1986	0.0	0.0		0

Appendix 5: Sample R code for ARIMA (as scripted by F.Oliva in Notepad ++; Chapter 5)

```
#######################################################
###PLOTTING AR-1 RESIDUALS FROM ARIMA (BOX JENKINS)###
#######################################################
#Load R packages
library(forecast)
library(stats)
# Set working directory
setwd("C:\\R_TR")
######################1
## Input csv file to be used
a <- read.csv(file.choose(), header=T)
## Create stable isotope time series variable
O <- a$O
## Create year variable
Y <- (a$Year)
#ARIMA model AR-1 autoregression
TRfit <- arima(O, order=c(1,0,0), seasonal=list(order=c(1,0,0), period=1), include.mean=FALSE)
#Produce Residuals
TRres <- resid(TRfit)
######################
## Input csv file to be used
a2 <- read.csv(file.choose(), header=T)
## Create stable isotope time series variable
O2 <- a2$O
## Create year variable
Y2 <- (a2$Year)
#ARIMA model AR-1 autoregression
```

```
TRfit2 <- arima(O2, order=c(1,0,0), seasonal=list(order=c(1,0,0), period=1), include.mean=FALSE)
#Produce Residuals
TRres2 <- resid(TRfit2)
######################3
## Input csv file to be used
a3 <- read.csv(file.choose(), header=T)
## Create stable isotope time series variable
O3 <- a3$O
## Create year variable
Y3 <- (a3$Year)
#ARIMA model AR-1 autoregression
TRfit3 <- arima(O3, order=c(1,0,0), seasonal=list(order=c(1,0,0), period=1), include.mean=FALSE)
#Produce Residuals
TRres3 <- resid(TRfit3)
######################4
## Input csv file to be used
a4 <- read.csv(file.choose(), header=T)
## Create stable isotope time series variable
O4 <- a4$O
## Create year variable
Y4 <- (a4$Year)
#ARIMA model AR-1 autoregression
TRfit4 <- arima(O4, order=c(1,0,0), seasonal=list(order=c(1,0,0), period=1), include.mean=FALSE)
#Produce Residuals
TRres4 <- resid(TRfit4)
#Plot Residuals
par(mfrow = c(4,1))
#Plot 1
plot(Y, TRres, xlab="Year", ylab="Residuals-EPT1A", type="b", pch=19, las=2)
```

```
axis(side=1, at=Y, labels=Y, las=2)
abline(h="-1")
#Plot 2
plot(Y2, TRres2, xlab="Year", ylab="Residuals-EPT1B", type="b", pch=19, las=2)
axis(side=1, at=Y2, labels=Y2, las=2)
abline(h="-1")
#Plot 3
plot(Y3, TRres3, xlab="Year", ylab="Residuals-RLT2", type="b", pch=19, las=2)
axis(side=1, at=Y3, labels=Y3, las=2)
abline(h="-1")
#Plot 4
plot(Y4, TRres4, xlab="Year", ylab="Residuals-RLT8", type="b", pch=19, las=2)
axis(side=1, at=Y4, labels=Y4, las=2)
abline(h="-1")
```

Appendix 6: COFECHA cross-dating results (Chapter 5)

QUALITY CONTROL AND DATING CHECK OF TREE-RING MEASUREMENTS

File of DATED series: eptrlt.raw

CONTENTS:

Part 1: Title page, options selected, summary, absent rings by series

Part 2: Histogram of time spans

Part 3: Master series with sample depth and absent rings by year

Part 4: Bar plot of Master Dating Series

Part 5: Correlation by segment of each series with Master

Part 6: Potential problems: low correlation, divergent year-to-year changes, absent rings, outliers

Part 7: Descriptive statistics

RUN CONTROL OPTIONS SELECTED VALUE

1 Cubic smoothing spline 50% wavelength cutoff for filtering

32 years

2 Segments examined are 50 years lagged successively by 25 years

3 Autoregressive model applied A Residuals are used in master dating series and testing

4 Series transformed to logarithms Y Each series log-transformed for master dating series and testing

5 CORRELATION is Pearson (parametric, quantitative)

Critical correlation, 99% confidence level .3281

6 Master dating series saved N

7 Ring measurements listed N

8 Parts printed 1234567

9 Absent rings are omitted from master series and segment correlations (Y)

Time span of Master dating series is 1941 to 2015 75 years

Continuous time span is 1941 to 2015 75 years

Portion with two or more series is 1941 to 2015 75 years

****

C Number of dated series 18 *C*

O Master series 1941 2015 75 yrs *O*

F Total rings in all series 720 *F*

E Total dated rings checked 720 *E*

C Series intercorrelation .407 *C*

H Average mean sensitivity .278 *H*

A Segments, possible problems 9 *A*

*** Mean length of series 40.0 ***

****

ABSENT RINGS listed by SERIES: (See Master Dating Series for absent rings listed by year)

No ring measurements of zero value

PART 2: TIME PLOT OF TREE-RING SERIES: 17:09 Sun 09 Jul 2017
Page 2

1050 1100 1150 1200 1250 1300 1350 1400 1450 1500 1550 1600 1650 1700 1750 1800 1850 1900 1950 2000
2050 Ident Seq Time-span Yrs

: -------- --- ---- ---- ----

. . . . <=====> . EPT3A 1 1956 2015 60

. . . . <=> . EPT1A 2 1995 2014 20

. . . . <=> . EPT1B 3 1995 2015 21

. . . .<====> . EPT2A 4 1963 2015 53

. . . .<====> . EPT2B 5 1963 2015 53

. . . .<====> . EPT5A 6 1965 2015 51

. . . .<====> . EPT5B 7 1965 2015 51

. . . . <===> . EPT6A 8 1977 2015 39

. . . . <===> . EPT6B 9 1977 2014 38

. . . . <==> . EPT7A 10 1982 2015 34

```
 .  .  .  .  .  .  .  .  .  .  .  .  .  .  .  .  .  .  . <==>  . EPT7B    11 1982 2012   31
 .  .  .  .  .  .  .  .  .  .  .  .  .  .  .  .  .  .  . <==>  . EPT8A    12 1981 2015   35
 .  .  .  .  .  .  .  .  .  .  .  .  .  .  .  .  .  .  . <==>  . EPT8B    13 1981 2015   35
 .  .  .  .  .  .  .  .  .  .  .  .  .  .  .  .  .  .  .  <=>  . EPT9A    14 1995 2015   21
 .  .  .  .  .  .  .  .  .  .  .  .  .  .  .  .  .  .  .  <=>  . EPT9B    15 1995 2015   21
 .  .  .  .  .  .  .  .  .  .  .  .  .  .  .  .  .  .  . <==>  . RLT8B    16 1983 2015   33
 .  .  .  .  .  .  .  .  .  .  .  .  .  .  .  .  .  . <=====>  . RLT2A    17 1941 2006   66
 .  .  .  .  .  .  .  .  .  .  .  .  .  .  .  .  .  . <====>.  . RLT2B    18 1941 1998   58
 :  :  :  :  :  :  :  :  :  :  :  :  :  :  :  :  :  :  :  :  :  :
 1050 1100 1150 1200 1250 1300 1350 1400 1450 1500 1550 1600 1650 1700 1750 1800 1850 1900 1950 2000
2050
```

Year	Value	No Ab	Year	Value	No Ab	Year	Value	No Ab	Year	Value	No Ab	Year	Value	No Ab	Year	Value	No Ab
			1950	1.358	2	2000	.953	17									
			1951	-1.986	2	2001	.825	17									
			1952	1.459	2	2002	1.351	17									
			1953	-.307	2	2003	1.495	17									
			1954	.714	2	2004	.936	17									
			1955	2.022	2	2005	.403	17									
			1956	-2.226	3	2006	-.181	17									
			1957	1.220	3	2007	-1.136	16									
			1958	1.067	3	2008	.440	16									
			1959	-.152	3	2009	-.569	16									
			1960	-.019	3	2010	-.889	16									
			1961	-.710	3	2011	.550	16									
			1962	-1.349	3	2012	-1.292	16									
			1963	1.046	5	2013	.673	15									
			1964	-.111	5	2014	-1.335	15									
			1965	.057	7	2015	1.073	13									
			1966	-.026	7												
			1967	-1.554	7												
			1968	-.694	7												
			1969	-.296	7												
			1970	-.077	7												
			1971	-.029	7												
			1972	1.620	7												
			1973	.804	7												

			1974	.872	7
			1975	.462	7
			1976	.440	7
			1977	-.201	9
			1978	-.641	9
			1979	-.910	9
			1980	-.489	9
			1981	.303	11
			1982	-.706	13
			1983	.041	14
			1984	.582	14
			1985	-.143	14
			1986	.500	14
			1987	.117	14
			1988	-.838	14
			1989	-1.303	14
			1990	-.281	14
1941	-.985	2	1991	-.907	14
1942	-1.438	2	1992	-.312	14
1943	1.313	2	1993	.366	14
1944	-2.650	2	1994	-.091	14
1945	.333	2	1995	-1.267	18
1946	-1.688	2	1996	-.323	18
1947	2.167	2	1997	.113	18
1948	.942	2	1998	.176	18
1949	.760	2	1999	.562	17

Year Rel value Year Rel value Year Rel value Year Rel value Year Rel value Year Rel value Year Rel value Year Rel value

1950----------E 2000---------D

1951h 2001--------C

1952----------F 2002----------E

1953---a 2003----------F

1954--------C 2004--------D

1955----------H 2005------B

1956i 2006----a

1957---------E 2007-e

1958---------D 2008------B

1959----a 2009--b

1960-----@ 2010--d

1961--c 2011-------B

1962-e 2012-e

1963---------D 2013-------C

1964----@ 2014-e

1965-----@ 2015---------D

1966-----@

1967f

1968--c

1969---a

1970-----@

1971-----@

1972----------F

1973--------C

1974--------C

1975-------B

1976------B

1977----a

1978--c

1979--d

1980---b

1981------A

1982--c

1983-----@

1984-------B

1985----a

1986-------B

1987-----@

1988--c

1989-e

1990---a

1941--d 1991--d

1942-f 1992---a

1943---------E 1993------A

1944k 1994----@

1945------A 1995-e

1946g 1996---a

1947----------I 1997-----@

1948--------D 1998------A

1949--------C 1999-------B

PART 5: CORRELATION OF SERIES BY SEGMENTS: 17:09 Sun 09 Jul 2017 Page 5

Correlations of 50-year dated segments, lagged 25 years

Flags: A = correlation under .3281 but highest as dated; B = correlation higher at other than dated position

Seq	Series	Time_span	1925 1974	1950 1999	1975 2024
1	EPT3A	1956 2015		.42	.39
2	EPT1A	1995 2014			.12B
3	EPT1B	1995 2015			.41
4	EPT2A	1963 2015		.36	.43
5	EPT2B	1963 2015		.43	.47
6	EPT5A	1965 2015		.37	.42
7	EPT5B	1965 2015		.25A	.29A
8	EPT6A	1977 2015			.46
9	EPT6B	1977 2014			.28A
10	EPT7A	1982 2015			.26A
11	EPT7B	1982 2012			.30B
12	EPT8A	1981 2015			.67
13	EPT8B	1981 2015			.70
14	EPT9A	1995 2015			.45B
15	EPT9B	1995 2015			.50
16	RLT8B	1983 2015			.41
17	RLT2A	1941 2006	.36	.13B	-.01B
18	RLT2B	1941 1998	.54	.35	
Av segment correlation			.45	.33	.38

For each series with potential problems the following diagnostics may appear:

[A] Correlations with master dating series of flagged 50-year segments of series filtered with 32-year spline,
at every point from ten years earlier (-10) to ten years later (+10) than dated

[B] Effect of those data values which most lower or raise correlation with master series
Symbol following year indicates value in series is greater (>) or lesser (<) than master series value

[C] Year-to-year changes very different from the mean change in other series

[D] Absent rings (zero values)

[E] Values which are statistical outliers from mean for the year

==

EPT3A 1956 to 2015 60 years Series 1

[B] Entire series, effect on correlation (.466) is:

Lower 1988< -.059 1962> -.055 1989> -.020 1984< -.018 1997< -.016 2007> -.012 Higher 1956 .102 2014 .022

[E] Outliers 1 3.0 SD above or -4.5 SD below mean for year

1988 -4.5 SD

==

EPT1A 1995 to 2014 20 years Series 2

```
[A] Segment   High   -10   -9   -8   -7   -6   -5   -4   -3   -2   -1   +0   +1   +2   +3   +4   +5   +6   +7   +8   +9  +10
   --------- ----   --- --- --- --- --- --- --- --- --- --- --- --- --- --- --- --- --- --- --- --- ---
   1995 2014    1   -.11 -.40 -.18  .00  .28  .23  .13 -.04 -.02 -.09  .12| .30*  -   -   -   -   -   -   -   -   -
```

[B] Entire series, effect on correlation (.116) is:

Lower   2007> -.210   2011< -.070   2014> -.066   2010> -.034   2003< -.028   2005< -.018 Higher   2012 .207   1995 .186

1995 to 2014 segment:

Lower   2007> -.210   2011< -.070   2014> -.066   2010> -.034   2003< -.028   2005< -.018 Higher   2012 .207   1995 .186

[E] Outliers   1   3.0 SD above or -4.5 SD below mean for year

2007 +3.5 SD

===

EPT1B   1995 to 2015   21 years   Series   3

[B] Entire series, effect on correlation (.406) is:

Lower   2014> -.094   2012> -.053   1996> -.023   2002< -.022   2004< -.021   2000< -.009 Higher   1995 .104   2015 .043

===

EPT2A   1963 to 2015   53 years   Series   4

[B] Entire series, effect on correlation (.384) is:

Lower   1982> -.046   1964> -.036   1978> -.035   1973< -.023   1985< -.020   1977> -.019 Higher   1995 .046   2012 .044

===

EPT2B   1963 to 2015   53 years   Series   5

[B] Entire series, effect on correlation (.463) is:

Lower 1974< -.074 1982> -.056 1978> -.034 1964> -.019 1979> -.014 1987< -.011 Higher 2012 .051 1995 .042

==

EPT5A 1965 to 2015 51 years Series 6

[B] Entire series, effect on correlation (.392) is:

Lower 1991> -.038 2012> -.032 1965> -.028 2011< -.022 1983< -.015 1978> -.013 Higher 1972 .039 2002 .031

==

EPT5B 1965 to 2015 51 years Series 7

[A] Segment	High	-10	-9	-8	-7	-6	-5	-4	-3	-2	-1	+0	+1	+2	+3	+4	+5	+6	+7	+8	+9	+10
1965 2014	0	-.16	-.18	-.09	-.19	-.01	-.19	.02	-.06	.06	.09	.25*	.01	-	-	-	-	-	-	-	-	-
1966 2015	0	-.20	-.12	-.18	-.20	.01	-.21	.06	-.08	.05	.06	.29*	-	-	-	-	-	-	-	-	-	-

[B] Entire series, effect on correlation (.270) is:

Lower 1988> -.034 2014> -.033 1968< -.031 1965> -.016 1992> -.011 1972< -.010 Higher 2003 .033 1995 .031

1965 to 2014 segment:

Lower 1988> -.035 2014> -.033 1968< -.032 1965> -.016 1992> -.010 1975< -.010 Higher 2003 .037 1995 .032

1966 to 2015 segment:

Lower 1988> -.036 2014> -.035 1968< -.031 1992> -.012 1972< -.009 1975< -.009 Higher 2003 .033 1995 .030

==

EPT6A 1977 to 2015 39 years Series 8

[B] Entire series, effect on correlation (.462) is:

Lower 1978< -.063 1982> -.056 1995> -.027 1985> -.021 1988> -.017 1998< -.016 Higher 2012 .065 2003 .034

==

EPT6B 1977 to 2014 38 years Series 9

[A] Segment High -10 -9 -8 -7 -6 -5 -4 -3 -2 -1 +0 +1 +2 +3 +4 +5 +6 +7 +8 +9 +10

--------- ---- ---

1977 2014 0 .01 .17 -.11 -.13 -.20 -.27 -.22 .26 .13 .09 .28*-.09 - - - - - - - - - -

[B] Entire series, effect on correlation (.279) is:

Lower 1982> -.050 2014> -.041 1988> -.029 1985> -.021 2013< -.020 1978< -.014 Higher 2007 .092 2011 .033

1977 to 2014 segment:

Lower 1982> -.050 2014> -.041 1988> -.029 1985> -.021 2013< -.020 1978< -.014 Higher 2007 .092 2011 .033

==

EPT7A 1982 to 2015 34 years Series 10

[A] Segment High -10 -9 -8 -7 -6 -5 -4 -3 -2 -1 +0 +1 +2 +3 +4 +5 +6 +7 +8 +9 +10

--------- ---- ---

1982 2015   0   .04 -.13 .01 .24 -.21 -.17 .04 -.20 .25 .10 .26*   -   -   -   -   -   -   -   -   -   -

[B] Entire series, effect on correlation (.261) is:

Lower   1995> -.068   2012> -.062   2011< -.047   2002< -.043   2010> -.030   1993< -.026 Higher   2007 .136 2014 .066

1982 to 2015 segment:

Lower   1995> -.068   2012> -.062   2011< -.047   2002< -.043   2010> -.030   1993< -.026 Higher   2007 .136 2014 .066

===
==

EPT7B   1982 to 2012   31 years   Series 11

[A] Segment   High   -10   -9   -8   -7   -6   -5   -4   -3   -2   -1   +0   +1   +2   +3   +4   +5   +6   +7   +8   +9 +10

--------- ----   ---

1982 2012   2   .04 -.31 -.06 .15 -.21 .07 .20 .26 -.04 .30 .30|-.18 .57*-.11   -   -   -   -   -   -   -

[B] Entire series, effect on correlation (.299) is:

Lower   1992< -.118   1993< -.057   2009> -.047   1991> -.037   1985> -.018   1988> -.015 Higher   2012 .093 2000 .041

1982 to 2012 segment:

Lower   1992< -.118   1993< -.057   2009> -.047   1991> -.037   1985> -.018   1988> -.015 Higher   2012 .093 2000 .041

===
==

EPT8A   1981 to 2015   35 years   Series 12

[B] Entire series, effect on correlation (.666) is:

Lower   1988> -.045   1985> -.036   1995> -.025   1992< -.013   2005> -.011   1990< -.011 Higher   2012 .047 2007 .045

==
===

EPT8B 1981 to 2015 35 years Series 13

[B] Entire series, effect on correlation (.695) is:

Lower 1985> -.038 1988> -.028 2005> -.024 1995> -.020 1999< -.012 2015< -.011 Higher 2007 .031 2012 .025

==
===

EPT9A 1995 to 2015 21 years Series 14

[A] Segment High -10 -9 -8 -7 -6 -5 -4 -3 -2 -1 +0 +1 +2 +3 +4 +5 +6 +7 +8 +9 +10

--------- ---- ---

1995 2015 -2 -.20 .03 .21 .51 -.11 .34 .06 -.01 .52*-.20 .45| - - - - - - - - - -

[B] Entire series, effect on correlation (.451) is:

Lower 2007> -.110 2015< -.048 2010> -.026 2005> -.012 2014< -.008 2003< -.007 Higher 2012 .036 2002 .026

1995 to 2015 segment:

Lower 2007> -.110 2015< -.048 2010> -.026 2005> -.012 2014< -.008 2003< -.007 Higher 2012 .036 2002 .026

==
===

EPT9B 1995 to 2015 21 years Series 15

[B] Entire series, effect on correlation (.500) is:

Lower 1996< -.129 2007> -.118 2005> -.009 2009< -.003 2012> -.002 1997> -.001 Higher 1995 .075 2002 .025

==

RLT8B 1983 to 2015 33 years Series 16

[B] Entire series, effect on correlation (.415) is:

Lower 1983< -.146 1990> -.028 1987> -.024 2013< -.023 2001< -.018 2004< -.016 Higher 2007 .066 2002 .042

==

RLT2A 1941 to 2006 66 years Series 17

```
[A] Segment   High  -10  -9  -8  -7  -6  -5  -4  -3  -2  -1  +0  +1  +2  +3  +4  +5  +6  +7  +8  +9 +10
  --------- ----   --- --- --- --- --- --- --- --- --- --- --- --- --- --- --- --- --- --- --- --- ---
  1950 1999   -3      -  .15 -.06  .11  .00  .06 -.32  .29*-.01 -.07  .13|-.21  .09  .12 -.19  .27 -.28 -.06  .21  .15  .20
  1957 2006   -3   -.09  .08  .11 -.14  .18 -.09 -.13  .34* .11 -.09 -.01|-.03 -.05  .18 -.14 -.14 -.06  .04  .09  .17    -
```

[B] Entire series, effect on correlation (.307) is:

Lower 1961> -.040 1981< -.031 1995> -.016 1996< -.013 1942> -.013 2001< -.012 Higher 1944 .124 1947 .024

1950 to 1999 segment:

Lower 1961> -.053 1981< -.042 1995> -.021 1970< -.016 1996< -.014 1958< -.012 Higher 1955 .038 1956 .035

1957 to 2006 segment:

Lower 1961> -.074 1981< -.047 1995> -.027 2001< -.021 1970< -.015 1958< -.014 Higher 1972 .054 1957 .040

[E] Outliers 1 3.0 SD above or -4.5 SD below mean for year

1961 +3.3 SD

===

RLT2B 1941 to 1998 58 years Series 18

[B] Entire series, effect on correlation (.475) is:

Lower 1951> -.055 1995> -.038 1982> -.026 1998< -.016 1942< -.016 1961< -.012 Higher 1944 .078 1956 .061

[E] Outliers 1 3.0 SD above or -4.5 SD below mean for year

1995 +3.2 SD

===

PART 7: DESCRIPTIVE STATISTICS: 17:09 Sun 09 Jul 2017 Page 6

						Corr	//-------- Unfiltered	--------	\\\\		//---- Filtered	-----	\\\\	
			No.	No.	No.	with	Mean	Max	Std	Auto	Mean	Max	Std	Auto	AR
Seq	Series	Interval	Years	Segmt	Flags	Master	msmt	msmt	dev	corr	sens	value	dev	corr	()
1	EPT3A	1956 2015	60	2	0	.466	3.15	9.69	2.673	.944	.245	2.51	.443	-.136	1
2	EPT1A	1995 2014	20	1	1	.116	4.88	8.61	2.131	.506	.232	2.82	.730	.105	1
3	EPT1B	1995 2015	21	1	0	.406	4.67	11.82	3.328	.686	.363	2.50	.534	-.184	1
4	EPT2A	1963 2015	53	2	0	.384	1.51	5.08	1.101	.918	.229	2.90	.699	-.062	1
5	EPT2B	1963 2015	53	2	0	.463	1.70	4.43	1.134	.859	.291	2.68	.588	-.024	1
6	EPT5A	1965 2015	51	2	0	.392	1.75	5.11	.841	.530	.272	2.77	.499	.036	1
7	EPT5B	1965 2015	51	2	2	.270	1.79	5.27	1.084	.858	.252	2.50	.397	-.038	1
8	EPT6A	1977 2015	39	1	0	.462	2.36	4.07	.836	.754	.252	2.69	.568	-.007	1
9	EPT6B	1977 2014	38	1	1	.279	2.47	6.56	1.217	.629	.282	2.96	.643	.140	1
10	EPT7A	1982 2015	34	1	1	.261	2.20	3.58	.688	.242	.291	2.46	.523	-.105	1
11	EPT7B	1982 2012	31	1	1	.299	2.55	4.17	.833	.615	.238	2.82	.628	-.040	1

12	EPT8A	1981	2015	35	1	0	.666	2.22	4.51	1.145	.710	.402	2.62	.608	-.086	2
13	EPT8B	1981	2015	35	1	0	.695	2.66	6.62	1.587	.706	.464	2.64	.594	-.099	2
14	EPT9A	1995	2015	21	1	1	.451	3.79	5.79	1.498	.762	.260	2.44	.498	-.012	1
15	EPT9B	1995	2015	21	1	0	.500	4.00	5.91	1.632	.852	.220	2.40	.715	.161	2
16	RLT8B	1983	2015	33	1	0	.415	2.54	5.79	1.418	.563	.355	2.90	.605	.060	1
17	RLT2A	1941	2006	66	3	2	.307	1.28	2.97	.970	.934	.224	2.62	.517	-.053	2
18	RLT2B	1941	1998	58	2	0	.475	1.11	2.92	.782	.898	.242	2.64	.570	-.098	1
---	--------	---------		-----	-----	-----	------	-----	-----	-----	-----	-----	-----	-----	-----	--
Total or mean:				720	26	9	.407	2.28	11.82	1.299	.754	.278	2.96	.562	-.035	

- = [COFECHA EPT5 COF] = -